SATHYABAMA
INSTITUTE OF SCIENCE AND TECHNOLOGY
(DEEMED TO BE UNIVERSITY)
Accredited "A" Grade by NAAC | 12B Status by UGC | Approved by AICTE
www.sathyabama.ac.in

SCHOOL OF MECHANICAL ENGINEERING
DEPARTMENT OF AERONAUTICAL ENGINEERING

AERODYNAMICS – II

SAE1301

UNIT – I CONCEPT OF COMPRESSIBLE FLOW – SAE1301

ALTERNATIVE FORMS OF THE ONE-DIMENSIONAL ENERGY EQUATION

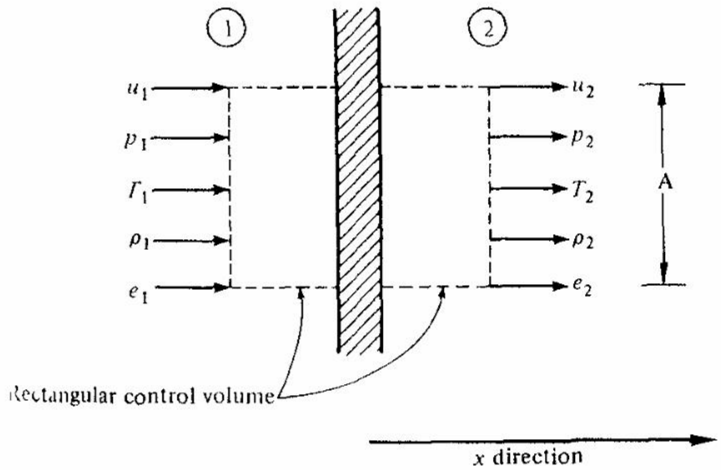

FIGURE 3 5
Rectangular control volume for one-dimensional flow

We have the energy equation for steady one-dimensional flow

$$\boxed{h_1 + \frac{u_1^2}{2} + q = h_2 + \frac{u_2^2}{2}}$$

Assuming no heat addition, this becomes

$$\boxed{h_1 + \frac{u_1^2}{2} = h_2 + \frac{u_2^2}{2}}$$

where points 1 and 2 correspond to the regions 1 and 2 identified in the above figure (Fig. 3.5).

Specializing further to a calorically perfect gas, where h = CpT, the above equation becomes,

$$\boxed{c_p T_1 + \frac{u_1^2}{2} = c_p T_2 + \frac{u_2^2}{2}}$$

$$\boxed{c_p = \frac{\gamma R}{\gamma - 1}}$$

Combining the above we get,

$$\frac{\gamma R T_1}{\gamma - 1} + \frac{u_1^2}{2} = \frac{\gamma R T_2}{\gamma - 1} + \frac{u_2^2}{2}$$

Since $a = \sqrt{\gamma R T}$

The above equation becomes,

$$\boxed{\frac{a_1^2}{\gamma - 1} + \frac{u_1^2}{2} = \frac{a_2^2}{\gamma - 1} + \frac{u_2^2}{2}}$$

When

$$\boxed{a = \sqrt{\frac{\gamma p}{\rho}}}$$

The above equation can be written as,

$$\boxed{\frac{\gamma}{\gamma - 1}\left(\frac{p_1}{\rho_1}\right) + \frac{u_1^2}{2} = \frac{\gamma}{\gamma - 1}\left(\frac{p_2}{\rho_2}\right) + \frac{u_2^2}{2}}$$

The actual speed of sound and velocity at point A are a and u, respectively. At the imagined condition of Mach 1 (point 2 in the above equations), the speed of sound is a* and the flow velocity is sonic, hence $u_2 = a^*$. Thus, the above equation yields,

$$\frac{a^2}{\gamma - 1} + \frac{u^2}{2} = \frac{a^{*2}}{\gamma - 1} + \frac{a^{*2}}{2}$$

$$\boxed{\frac{a^2}{\gamma - 1} + \frac{u^2}{2} = \frac{\gamma + 1}{2(\gamma - 1)} a^{*2}}$$

If the actual flowfield is nonadiabatic from A to B, $a^*_A \neq a^*_B$.

On the other hand, if the general flowfield is adiabatic throughout, then a* is a constant value at every point in the flow. Since many practical aerodynamic flows are reasonably adiabatic, this is an important point to remember.

Let point 1 in correspond to point A and let point 2 correspond to our imagined conditions where the fluid element is brought to rest isentropically at point A. If T and u are the actual values of static temperature and velocity, respectively, at point A, then T_1 = T and u_1 = u. Also, by definition of total conditions, u_2 = 0 and T_2 = To Hence, equation

$$\boxed{c_p T_1 + \frac{u_1^2}{2} = c_p T_2 + \frac{u_2^2}{2}}$$

becomes

$$\boxed{c_p T + \frac{u^2}{2} = c_p T_o}$$

The above equation provides a formula from which the defined total temperature, To, can be calculated for the given actual conditions of T and u at any point in a general flow field. Remember that total conditions are defined earlier as

those where the fluid element is isentropically brought to rest. However, in the derivation of the above equation, only the energy equation for an adiabatic flow is used. Isentropic conditions have not been imposed so far. Hence, the definition of To such as expressed in the above Eq is less restrictive than the definition of total conditions. Isentropic flow implies reversible and adiabatic conditions; Eq. tells us that, for the definition of To, only the "adiabatic" portion of the isentropic definition is required. That is, we can now redefine To as that temperature that would exist if the fluid element were brought to rest adiabatically. However, for the definition of total pressure, p_0, and total density, ρ_o, the imagined isentropic process is still necessary.

We have,

$$\boxed{c_p = \frac{\gamma R}{\gamma - 1}}$$

$$\boxed{c_p T + \frac{u^2}{2} = c_p T_o}$$

Several very useful equations for total conditions are obtained as follows from the above two equations.

$$\frac{T_o}{T} = 1 + \frac{u^2}{2c_pT} = 1 + \frac{u^2}{2\gamma RT/(\gamma - 1)} = 1 + \frac{u^2}{2a^2/(\gamma - 1)} = 1 + \frac{\gamma - 1}{2}\left(\frac{u}{a}\right)^2$$

Hence

$$\boxed{\frac{T_o}{T} = 1 + \frac{\gamma - 1}{2}M^2}$$

The above equation gives the ratio of total to static temperature at a point in a flow as a function of the Mach number M at that point Furthermore, for an isentropic process, the below equation

$$\boxed{\frac{p_2}{p_1} = \left(\frac{\rho_2}{\rho_1}\right)^{\gamma} = \left(\frac{T_2}{T_1}\right)^{\gamma/(\gamma-1)}}$$

holds, such that

$$\frac{p_o}{p} = \left(\frac{\rho_o}{\rho}\right)^{\gamma} = \left(\frac{T_o}{T}\right)^{\gamma/(\gamma-1)}$$

Combining the above two equations, we find

$$\boxed{\frac{p_o}{p} = \left(1 + \frac{\gamma - 1}{2} M^2\right)^{\gamma/(\gamma-1)}}$$

$$\boxed{\frac{\rho_o}{\rho} = \left(1 + \frac{\gamma - 1}{2} M^2\right)^{1/(\gamma-1)}}$$

The above two equations give the ratios of total to static pressure and density, respectively, at a point in the flow as a function of Mach number M at that point. Along with the following Eq.,

$$\boxed{\frac{p_2}{p_1} = \left(\frac{\rho_2}{\rho_1}\right)^{\gamma} = \left(\frac{T_2}{T_1}\right)^{\gamma/(\gamma-1)}}$$

they represent important relations for total properties—so important that their values are tabulated in Table (see Gas table) as a function of M for γ = 1.4 (which corresponds to air at standard conditions).

Example 3.1.

At a point in the flow over an F-15 high-performance fighter airplane, the pressure, temperature, and Mach number are 1890 lb/ft^2, 450°R, and 1 5, respectively. At this point, calculate To, p_0, T*, p*, and the flow velocity.

Rankine temperature conversion formulae

	from Rankine	to Rankine
Celsius	[°C] = ([R] − 491.67) × 5⁄9	[R] = ([°C] + 273.15) × 9⁄5
Fahrenheit	[°F] = [R] − 459.67	[R] = [°F] + 459.67
Kelvin	[K] = [R] × 5⁄9	[R] = [K] × 9⁄5

Consider the flow through a rocket engine nozzle Assume that the gas flow through the nozzle is an isentropic expansion of a calorically perfect gas In the combustion chamber, the gas which results from the combustion of the rocket fuel and oxidizer is at a pressure and temperature of 15 atm and 2500 K, respectively, the molecular weight and specific heat at constant pressure of the combustion gas are 12 and 4157 J/kg K, respectively The gas expands to supersonic speed through the nozzle, with a temperature' of 1350 K at the nozzle exit Calculate the pressure at the exit.

Solution. From our earlier discussion on the equation of state,

$$R = \frac{\mathcal{R}}{\mathcal{M}} = \frac{8314}{12} = 692\ 8\ \mathrm{J/kg}\quad \mathrm{K}$$

From Eq. (1 20)

$$c_v = c_p - R = 4157 - 692\ 8 = 3464\ \mathrm{J/kg \cdot K}$$

Thus

$$\gamma = \frac{c_p}{c_v} = \frac{4157}{3464} = 1\ 2$$

From Eq. (1.43), we have

$$\frac{p_2}{p_1} = \left(\frac{T_2}{T_1}\right)^{\gamma/(\gamma-1)} = \left(\frac{1350}{2500}\right)^{1\ 2/(1\ 2-1)} = 0\ 0248$$

$$p_2 = 0\ 025 p_1 = (0.0248)(15\ \mathrm{atm}) = \boxed{0.372\ \mathrm{atm}}$$

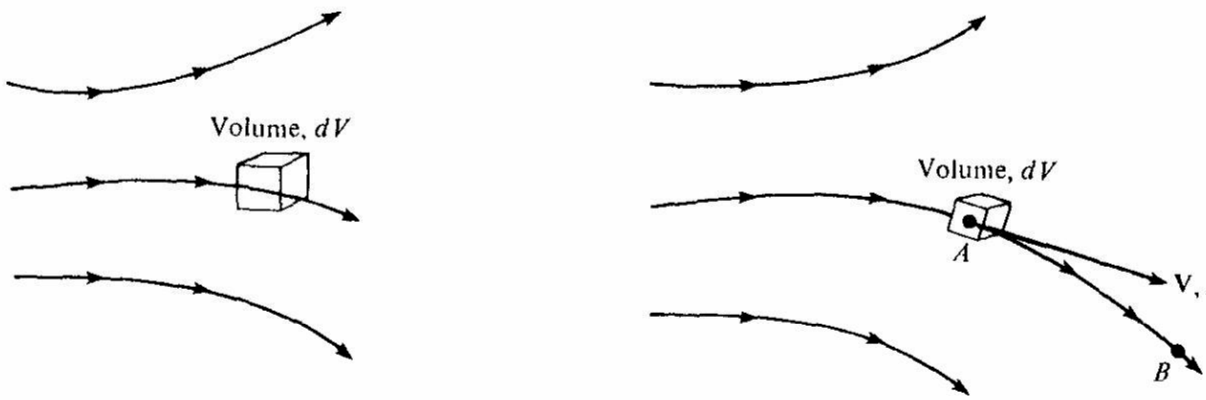

Infinitesimal fluid element fixed in space with the fluid moving through it

Infinitesimal fluid element moving along a streamline with the velocity V equal to the flow velocity at each point

FIGURE 2.2
Infinitesimal fluid element approach

It should be emphasized again that the below four equations provide formulas from which the defined quantities T_o, p_o, and ρ_0 can be calculated from the actual conditions of M, u, T, p, and ρ at a given point in a general flowfield, as sketched in Fig 2.2 (see above). Again, the actual flowfield itself does not have to be adiabatic or isentropic from one point to the next. In these equations, the isentropic process is just in our minds as part of the definition of total conditions at a point.

$$\boxed{c_p T + \frac{u^2}{2} = c_p T_o}$$

$$\boxed{\frac{T_o}{T} = 1 + \frac{\gamma - 1}{2} M^2}$$

$$\boxed{\frac{p_o}{p} = \left(1 + \frac{\gamma - 1}{2} M^2\right)^{\gamma/(\gamma - 1)}}$$

$$\boxed{\frac{\rho_o}{\rho} = \left(1 + \frac{\gamma - 1}{2} M^2\right)^{1/(\gamma - 1)}}$$

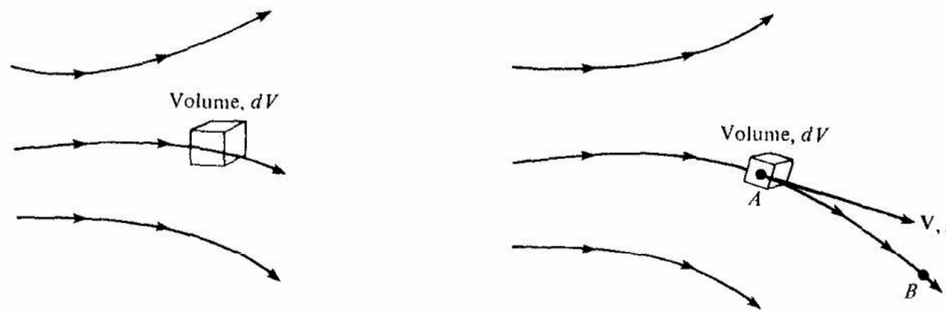

Infinitesimal fluid element fixed in space with the fluid moving through it

Infinitesimal fluid element moving along a streamline with the velocity V equal to the flow velocity at each point

FIGURE 2.2
Infinitesimal fluid element approach

Applied at point A in the above Fig 2.2, the above equations give us the values of T_o, p_o, and ρ_0 associated with point A.

Similarly, applied at point B, the above equations give us the values of T_0, p_0, and ρ_0 associated with point B. If the actual flow between A and B is nonadiabatic and irreversible, then

$$T_{o_A} \neq T_{o_B}, \; p_{o_A} \neq p_{o_B}, \text{ and } \rho_{o_A} \neq \rho_{o_B}.$$

On the other hand, if the general flowfield is isentropic throughout, then T_o, p_o, and ρ_0 are constant values at every point in the flow. The idea of constant total (stagnation) conditions in an isentropic flow will be very useful in our later discussions of various practical applications in compressible flow — keep it in mind'

We have

$$\boxed{\frac{a_1^2}{\gamma - 1} + \frac{u_1^2}{2} = \frac{a_2^2}{\gamma - 1} + \frac{u_2^2}{2}}$$

A few additional equations will be useful in subsequent sections. For example, from the above equation,

$$\boxed{\frac{a^2}{\gamma - 1} + \frac{u^2}{2} = \frac{a_o^2}{\gamma - 1}}$$

where a_o is the stagnation speed of sound.

Stagnation speed of sound $a_o = \sqrt{\gamma R T_o}$.

We have,

$$\boxed{\frac{a^2}{\gamma - 1} + \frac{u^2}{2} = \frac{\gamma + 1}{2(\gamma - 1)} a^{*2}}$$

$$\boxed{\frac{a^2}{\gamma - 1} + \frac{u^2}{2} = \frac{a_o^2}{\gamma - 1}}$$

Equating the R.H.S of the above two equations,

$$\frac{\gamma + 1}{2(\gamma - 1)} a^{*2} = \frac{a_o^2}{\gamma - 1}$$

Solving the above equation for a^*/a_o, and invoking

$$\boxed{a = \sqrt{\gamma R T}}$$

We get,

$$\boxed{\left(\frac{a^*}{a_o}\right)^2 = \frac{T^*}{T_o} = \frac{2}{\gamma + 1}}$$

$$\boxed{\frac{p_o}{p} = \left(1 + \frac{\gamma - 1}{2} M^2\right)^{\gamma/(\gamma-1)}}$$

$$\boxed{\frac{\rho_o}{\rho} = \left(1 + \frac{\gamma - 1}{2} M^2\right)^{1/(\gamma-1)}}$$

Recall that p^* and ρ^* are defined for conditions at Mach 1; hence, the above two equations with $M = 1$ lead to

$$\boxed{\frac{p^*}{p_o} = \left(\frac{2}{\gamma + 1}\right)^{\gamma/(\gamma-1)}}$$

$$\boxed{\frac{\rho^*}{\rho_o} = \left(\frac{2}{\gamma + 1}\right)^{1/(\gamma-1)}}$$

For air at standard conditions, where $\gamma = 1.4$, these ratios are

$$\frac{T^*}{T_o} = 0.833$$

$$\frac{p^*}{p_o} = 0.528$$

$$\frac{\rho^*}{\rho_o} = 0.634$$

which will be useful numbers to keep in mind for subsequent discussions.

$$\boxed{\frac{a^2}{\gamma - 1} + \frac{u^2}{2} = \frac{\gamma + 1}{2(\gamma - 1)} a^{*2}}$$

Dividing the above equation by u^2 , we have

$$\frac{(a/u)^2}{\gamma - 1} + \frac{1}{2} = \frac{\gamma + 1}{2(\gamma - 1)} \left(\frac{a^*}{u} \right)^2$$

$$\frac{(1/M)^2}{\gamma - 1} = \frac{\gamma + 1}{2(\gamma - 1)} \left(\frac{1}{M^*} \right)^2 - \frac{1}{2}$$

$$\boxed{M^2 = \frac{2}{[(\gamma + 1)/M^{*2}] - (\gamma - 1)}}$$

The above equation provides a direct relation between the actual Mach number M and the characteristic Mach number M*.

Characteristic Mach number $M^* = V/a^*$. (Note that the real Mach number is $M = V/a$.)

$$\boxed{M^2 = \frac{2}{[(\gamma + 1)/M^{*2}] - (\gamma - 1)}}$$

Using the above relation find the value of M when,

$$M^* = 1$$
$$M^* < 1$$
$$M^* > 1$$
$$M^* \to \sqrt{\frac{\gamma + 1}{\gamma - 1}}$$

$$M^* = 1 \qquad \text{if } M = 1$$
$$M^* < 1 \qquad \text{if } M < 1$$
$$M^* > 1 \qquad \text{if } M > 1$$
$$M^* \to \sqrt{\frac{\gamma + 1}{\gamma - 1}} \qquad \text{if } M \to \infty$$

Hence, qualitatively, M* acts in the same fashion as M, except when M goes to infinity.

In future discussions involving shock and expansion waves, M* will be a useful parameter because it approaches a finite number as M approaches infinity.

All the equations in this section, either directly or indirectly, are alternative forms of the original, fundamental energy equation for one-dimensional, adiabatic flow (see below Eq.).

$$\boxed{h_1 + \frac{u_1^2}{2} = h_2 + \frac{u_2^2}{2}}$$

Make certain that you examine these equations and their derivations closely. It is important at this stage that you feel comfortable with these equations, especially those with a box around them for emphasis.

Problem:

An aircraft flies at 800km/hr at an altitude of 10,000 meters (T=223.15 K, p = 0.264 bar). The air is reversibly compressed in an inlet diffuser (γ = 1.4, R = 287 J/kg K). The Mach number at the exit of the diffuser is 0.36 determine (a) entry Mach number and (b) velocity, pressure and temperature of air at the diffuser exit. (Hint: Use gas table)

Solution:

Let subscripts i and e refer to conditions at entry and exit of the diffuser respectively.

(a) P_i = 0.264 bar, T_i = 223.15 K
u_i = 800 x 1000 / 3600 = 222.22 m/s
We have

$$\boxed{c_p T + \frac{u^2}{2} = c_p T_o}$$

Using the above equation, we will get $\underline{T_0}$ = 247.84 K

= 0.74 Ans.

(b) From isentropic flow table for $\gamma = 1.4$ at
$M_i = 0.74$ (calculated) find P_i/P_0
$M_e = 0.36$ (given) find P_e/P_0 and T_e/T_0

From the isentropic flow table we have,

$P_i/P_0 = 0.695$

$P_0 = P_i / 0.695 = 0.264 / 0.695$
$= 0.379$

$P_e/P_0 = 0.914$

$P_e = P_0 \times 0.914$
$= 0.379 \times 0.914$
$=$ <u>0.346 Ans.</u>

Again from table: $T_e/T_0 = 0.975$
$T_e = T_0$ (calculated) $\times 0.975$
$= 247.84 \times 0.975$
$=$ <u>241.6 K Ans.</u>

$$a_e = \sqrt{\gamma R T_e} = \sqrt{1.4 \times 287 \times 241.6}$$

$= 311.57$ m/s

$u_e = M_e a_e = 0.36 \times 311.57$

= 112.17 m/s Ans

Physical Properties of Standard Atmosphere in SI Units				
Altitude (meters)	**Temperature (K)**	**Pressure (Pa)**	**Density (kg/m^3)**	**Viscosity (N-s/m^2)**
-5,000	320.7	1.778E+5	1.931	1.942E-5
-4,000	314.2	1.596E+5	1.770	1.912E-5
-3,000	307.7	1.430E+5	1.619	1.882E-5
-2,000	301.2	1.278E+5	1.478	1.852E-5
-1,000	294.7	1.139E+5	1.347	1.821E-5
0	288.2	1.013E+5	1.225	1.789E-5
1,000	281.7	8.988E+4	1.112	1.758E-5
2,000	275.2	7.950E+4	1.007	1.726E-5
3,000	268.7	7.012E+4	9.093E-1	1.694E-5
4,00	26	6.1	8.1	1.6

0	2.2	66E+4	94E-1	61E-5
5,000	255.7	5.405E+4	7.364E-1	1.628E-5
6,000	249.2	4.722E+4	6.601E-1	1.595E-5
7,000	242.7	4.111E+4	5.900E-1	1.561E-5
8,000	236.2	3.565E+4	5.258E-1	1.527E-5
9,000	229.7	3.080E+4	4.671E-1	1.493E-5
10,000	223.3	2.650E+4	4.135E-1	1.458E-5
15,000	216.7	1.211E+4	1.948E-1	1.422E-5
20,000	216.7	5.529E+3	8.891E-2	1.422E-5
30,000	226.5	1.197E+3	1.841E-2	1.475E-5
40,000	250.4	2.871E+2	3.996E-3	1.601E-5
50,000	270.7	7.978E+1	1.027E-3	1.704E-5
60,000	255.8	2.246E+1	3.059E-4	1.629E-5
70,000	219.7	5.520	8.754E	1.438E

			-5	-5
80, 000	18 0.7	1.0 37	1.9 99E -5	1.2 16E -5
90, 000	18 0.7	1.6 44 E-1	3.1 70E -6	1.2 16E -5

Problem-2

Air (Cp = 1.03 kJ/kg K, γ = 1.38) at P_1 = 3 x 10^5 N/m^2 and T_1
= 500 K flows with a velocity of 200 m/s in a 30 cm diameter duct.
Calculate:
(a) Mass flow rate

(b) Stagnation temperature © Mach number, and

(d) Stagnation pressure values assuming the flow as compressible and incompressible.

Solution:
R = Cp – Cv = 0.289 kJ/kg K
$\rho_1 = P_1/RT_1$ = 2.076 kg/m^3

(a) Mass flow rate = 29.348 kg/s
(b) Stagnation temperature, T_0 = 519.047 K
(c) Mach number = 0.4478
(d) Stagnation pressure
For compressible flow

$$\frac{p_0}{p_1} = \left(\frac{T_0}{T_1}\right)^{\gamma/(\gamma-1)}$$

1.145 (T_0 = 519.047 (calculated) and T_i = 500 K (given)) P_0 = 1.145 x 3 x 10^5 N/m^2

$= 3.435 \times 10^5$ N/m^2

For incompressible flow

$P_0 = P_1 + \frac{1}{2}\rho_1 u_1^2$

$= 3 \times 10^5 + \frac{1}{2} \times 2.076 \times 200^2$

$= 3.415 \times 10^5$ N/m^2

SATHYABAMA
INSTITUTE OF SCIENCE AND TECHNOLOGY
(DEEMED TO BE UNIVERSITY)
Accredited "A" Grade by NAAC | 12B Status by UGC | Approved by AICTE
www.sathyabama.ac.in

SCHOOL OF MECHANICAL ENGINEERING
DEPARTMENT OF AERONAUTICAL ENGINEERING

AERODYNAMICS – II

SAE1301

UNIT – II – COMPRESSION AND EXPANSION WAVE – SAE1301

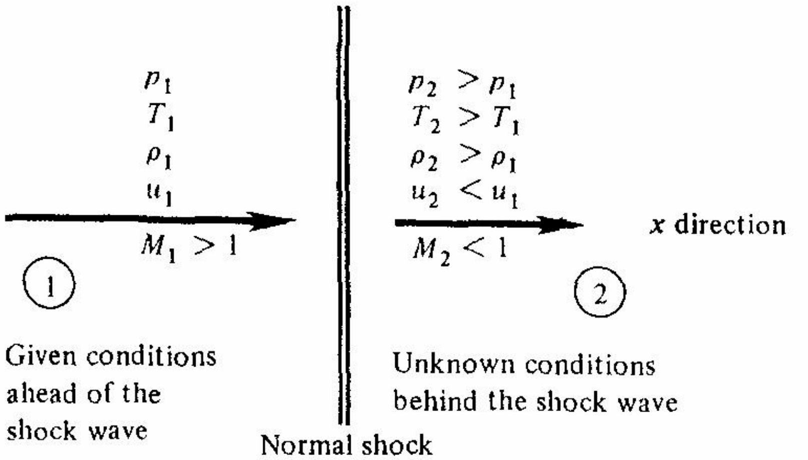

FIGURE 3.3
Diagram of a normal shock

NORMAL SHOCK RELATIONS

Let us now apply the previous information to the practical problem of a normal shock wave. As discussed earlier normal shocks occur frequently as part of many supersonic flowfields. By definition, a normal shock wave is perpendicular to the flow, as sketched in Fig. 3.3 (see above). The shock is a very thin region (the shock thickness is usually on the order of a few molecular mean free paths, typically 10^{-5} cm for air at standard conditions). The flow is supersonic ahead of the wave, and subsonic behind it, as noted in Fig 3.3. Furthermore, the static pressure, temperature, and density increase across the shock, whereas the velocity decreases, all of which we will demonstrate shortly. Nature establishes shock waves in a supersonic flow as a solution to a perplexing problem having to do with the propagation of disturbances in the flow.

To obtain some preliminary physical feel for the creation of such shock waves, consider a flat-faced cylinder mounted in a flow, as sketched in Fig. 3.7 (see below).

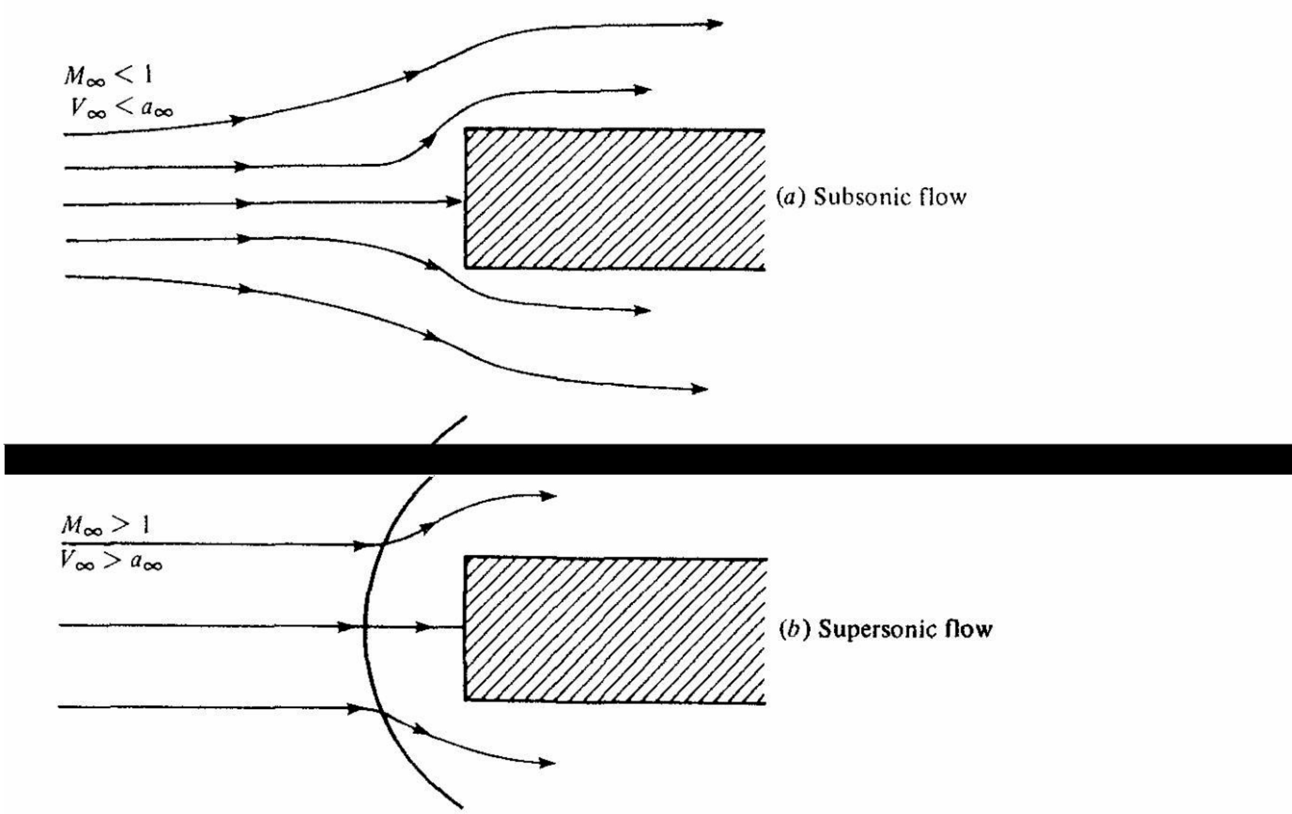

FIGURE 3.7
Comparison between subsonic and supersonic streamlines for flow over a flat-faced cylinder or slab.

Recall that the flow consists of individual molecules, some of which impact on the face of the cylinder. There is in general a change in molecular energy and momentum due to impact with the cylinder, which is seen as an obstruction by the molecules. Therefore, just as in our example of the creation of a sound wave, as discussed earlier, the random motion of the molecules communicates this change in energy and

momentum to other regions of the flow. The presence of the body tries to be propagated everywhere, including directly upstream, by sound waves.

In Fig. 3.7a, the incoming stream is subsonic, $V_\infty < a_\infty$, and the sound waves can work their way upstream and forewarn the flow about the presence of the body. In this fashion, as shown in Fig. 3.7a, the flow streamlines begin to change and the flow properties begin to compensate for the body far upstream (theoretically, an infinite distance upstream). In contrast, if the flow is supersonic, then $V_\infty > a_\infty$, and the sound waves can no longer propagate upstream. Instead, they tend to coalesce a short distance ahead of the body. In so doing, their coalescence forms a thin shock wave, as shown in Fig. 3.1b. Ahead of the shock wave, the flow has no idea of the presence of the body. Immediately behind the normal shock, however, the flow is subsonic, and hence the streamlines quickly compensate for

the obstruction. Although the picture shown in Fig. 3 1b is only one of many situations in which nature creates shock waves, the physical mechanism discussed above is quite general.

To begin a quantitative analysis of changes across a normal shock wave, consider again Fig. 3.3. Here, the normal shock is assumed to be a discontinuity across which the flow properties suddenly change. For purposes of discussion, assume that all conditions are known ahead of the shock (region 1), and that we want to solve for all conditions behind the shock (region 2). There is no heat added or taken away from the flow as it traverses the shock wave (for example, we are not putting the shock in a refrigerator, nor are we irradiating it with a laser); hence the flow across the shock wave is adiabatic. Therefore, the basic normal shock equations are obtained directly from the below equations (formulated earlier with q = 0) as,

$$\rho_1 u_1 = \rho_2 u_2 \qquad \text{(continuity)}$$

$$p_1 + \rho_1 u_1^2 = p_2 + \rho_2 u_2^2 \qquad \text{(momentum)}$$

$$h_1 + \frac{u_1^2}{2} = h_2 + \frac{u_2^2}{2} \qquad \text{(energy)}$$

The above equations are general—they apply no matter what type of gas is being considered. Also, in general they must be solved numerically for the properties behind the shock wave, as will be discussed later for the cases of thermally perfect and chemically reacting gases. However, for a calorically perfect gas, we can immediately add the thermodynamic relations

$$\rho_1 u_1 = \rho_2 u_2 \qquad \text{(continuity)}$$

$$p_1 + \rho_1 u_1^2 = p_2 + \rho_2 u_2^2 \qquad \text{(momentum)}$$

$$h_1 + \frac{u_1^2}{2} = h_2 + \frac{u_2^2}{2} \qquad \text{(energy)}$$

$$p = \rho R T$$

and

$$h = c_p T$$

The above five equations with five unknowns, ρ_2, u_2, p_2, h_2, and T_2 can be solved algebraically, as follows.

First divide the momentum equation by the continuity equation,

$$\frac{p_1}{\rho_1 u_1} - \frac{p_2}{\rho_2 u_2} = u_2 - u_1$$

Recalling that $a = \sqrt{\gamma p/\rho}$,

the above equation becomes,

$$\frac{a_1^2}{\gamma u_1} - \frac{a_2^2}{\gamma u_2} = u_2 - u_1 \qquad (1)$$

The above equation is a combination of the continuity and momentum equations. The energy equation can be utilized in one of its alternative forms,

$$\boxed{\frac{a^2}{\gamma - 1} + \frac{u^2}{2} = \frac{\gamma + 1}{2(\gamma - 1)} a^{*2}}$$

which yields,

$$a_1^2 = \frac{\gamma + 1}{2} a^{*2} - \frac{\gamma - 1}{2} u_1^2 \qquad (2)$$

and

$$a_2^2 = \frac{\gamma + 1}{2} a^{*2} - \frac{\gamma - 1}{2} u_2^2 \qquad (3)$$

Since the flow is adiabatic across the shock wave, a* in Eqs (2) and (3) is the same constant value. Substituting Eqs. (2) and (3) into (1), we obtain

$$\frac{\gamma+1}{2}\frac{a^{*2}}{\gamma u_1} - \frac{\gamma-1}{2\gamma}u_1 - \frac{\gamma+1}{2}\frac{a^{*2}}{\gamma u_2} + \frac{\gamma-1}{2\gamma}u_2 = u_2 - u_1$$

or

$$\frac{\gamma+1}{2\gamma u_1 u_2}(u_2 - u_1)a^{*2} + \frac{\gamma-1}{2\gamma}(u_2 - u_1) = u_2 - u_1$$

Dividing by $(u_2 - u_1)$,

$$\frac{\gamma+1}{2\gamma u_1 u_2}a^{*2} + \frac{\gamma-1}{2\gamma} = 1$$

Solving for a^*, this gives

$$\boxed{a^{*2} = u_1 u_2}$$

The above equation is called the Prandtl relation, and is a useful intermediate relation for normal shocks. For example, from this simple equation we obtain directly

$$1 = \frac{u_1}{a^*}\frac{u_2}{a^*} = M_1^* M_2^*$$

or

$$\boxed{M_2^* = \frac{1}{M_1^*}}$$

Based on our previous physical discussion, the flow ahead of a shock wave must be supersonic, i.e, $M_1 > 1$. It implies $M_1^* > 1$. Thus, from the above Eq. $M_2^* < 1$ and thus $M_2 < 1$. Hence, the Mach number behind the normal shock is always subsonic. This is a general result, not just limited to a calorically perfect gas.

We have

$$\boxed{M^2 = \frac{2}{[(\gamma + 1)/M^{*2}] - (\gamma - 1)}}$$

, Which solved for M^* , gives

$$M^{*2} = \frac{(\gamma + 1) M^2}{2 + (\gamma - 1) M^2}$$

Substitute the above equation into

$$\boxed{M_2^* = \frac{1}{M_1^*}}$$

We get,

$$\frac{(\gamma+1)M_2^2}{2+(\gamma-1)M_2^2} = \left[\frac{(\gamma+1)M_1^2}{2+(\gamma-1)M_1^2}\right]^{-1}$$

Solving the above Eq. for M_2^2

$$\boxed{M_2^2 = \frac{1+[(\gamma-1)/2]M_1^2}{\gamma M_1^2-(\gamma-1)/2}}$$

The above equation demonstrates that, for a calorically perfect gas with a constant value of γ, the Mach number behind the shock is a function of only the Mach number ahead of the shock. It also shows that when M_1=1, then M_2 =1 This is the case of an infinitely weak normal shock, which is defined as a Mach wave. In contrast, as M_1 increases above 1, the normal shock becomes stronger and M_2
becomes progressively less than 1. However, in the limit, as $M_1 \rightarrow \infty$, M_2 approaches a finite minimum value, $M_2 \rightarrow \sqrt{(\gamma-1)/2\gamma}$, which for air is 0 378

The upstream Mach number M_1 is a powerful parameter which dictates shock wave properties. This is already seen in the above Eq. Ratios of other properties across the shock can also be found in terms of M_1. For example, from Eq.

$$\rho_1 u_1 = \rho_2 u_2 \qquad \text{(continuity)}$$

combined with

$$\boxed{a^{*2} = u_1 u_2}$$

$$\frac{\rho_2}{\rho_1} = \frac{u_1}{u_2} = \frac{u_1^2}{u_2 u_1} = \frac{u_1^2}{a^{*2}} = M_1^{*2}$$

Substituting (we have)

$$M^{*2} = \frac{(\gamma + 1)M^2}{2 + (\gamma - 1)M^2}$$

into the above equation,

$$\boxed{\frac{\rho_2}{\rho_1} = \frac{u_1}{u_2} = \frac{(\gamma + 1)M_1^2}{2 + (\gamma - 1)M_1^2}}$$

To obtain the pressure ratio, return to the momentum equation

$$p_2 - p_1 = \rho_1 u_1^2 - \rho_2 u_2^2$$

which, combined with the continuity equation, yields

$$p_2 - p_1 = \rho_1 u_1 (u_1 - u_2) = \rho_1 u_1^2 \left(1 - \frac{u_2}{u_1}\right)$$

Dividing the above Eq. by p_1,

and recalling that $a_1^2 = \gamma p_1/\rho_1$, we obtain

$$\frac{p_2 - p_1}{p_1} = \gamma M_1^2 \left(1 - \frac{u_2}{u_1}\right)$$

We have

$$\frac{u_1}{u_2} = \frac{(\gamma + 1) M_1^2}{2 + (\gamma - 1) M_1^2}$$

Substitute it in the above Eq., we get,

$$\frac{p_2 - p_1}{p_1} = \gamma M_1^2 \left[1 - \frac{2 + (\gamma - 1) M_1^2}{(\gamma + 1) M_1^2}\right]$$

It simplifies to,

$$\boxed{\frac{p_2}{p_1} = 1 + \frac{2\gamma}{\gamma + 1}\left(M_1^2 - 1\right)}$$

To obtain the temperature ratio, recall the equation of state, $p = \rho RT$. Hence

$$\frac{T_2}{T_1} = \left(\frac{p_2}{p_1}\right)\left(\frac{\rho_1}{\rho_2}\right)$$

We have

$$\boxed{\frac{\rho_2}{\rho_1} = \frac{u_1}{u_2} = \frac{(\gamma + 1)M_1^2}{2 + (\gamma - 1)M_1^2}}$$

Combining the above three equations,

$$\boxed{\frac{T_2}{T_1} = \frac{h_2}{h_1} = \left[1 + \frac{2\gamma}{\gamma + 1}\left(M_1^2 - 1\right)\right]\left[\frac{2 + (\gamma - 1)M_1^2}{(\gamma + 1)M_1^2}\right]}$$

Examine the following equations.

$$\boxed{M_2^2 = \frac{1 + [(\gamma - 1)/2]\, M_1^2}{\gamma M_1^2 - (\gamma - 1)/2}}$$

$$\boxed{\frac{\rho_2}{\rho_1} = \frac{u_1}{u_2} = \frac{(\gamma + 1) M_1^2}{2 + (\gamma - 1) M_1^2}}$$

$$= 1 + \frac{2\gamma}{\gamma + 1}\left(M_1^2 - 1\right)$$

$$\boxed{\frac{T_2}{T_1} = \frac{h_2}{h_1} = \left[1 + \frac{2\gamma}{\gamma + 1}\left(M_1^2 - 1\right)\right]\left[\frac{2 + (\gamma - 1) M_1^2}{(\gamma + 1) M_1^2}\right]}$$

For a calorically perfect gas with a given γ, they give M_2, ρ_2/ρ_1, P_2/P_1, and T_2/T_1 as functions of M_1 only. This is our first major demonstration of the importance of Mach number in the quantitative governance of compressible fiowfields.

In contrast, as will be shown later for an equilibrium thermally perfect gas, the changes across a normal shock depend on both M_1 and T_1, whereas for an equilibrium chemically reacting gas they depend on M_1, T_1 and p_1. Moreover, for such high-temperature cases, closed-form expressions such as the above derived equations are generally not possible, and the normal shock properties must be calculated numerically. Hence, the simplicity brought about by the calorically perfect gas assumption in this section is clearly evident. Fortunately, the results of this section hold reasonably accurately up to approximately M_1 = 5 in air at standard conditions. Beyond Mach 5, the temperature behind the normal shock becomes high enough that γ is no longer constant. However, the flow regime M_1 < 5 contains a large number of everyday practical problems, and therefore the results of this section are extremely useful.

Problem-3

A normal shock wave is standing in the test section of a supersonic wind tunnel. Upstream of the wave, M_1 = 3,

p_1= 0.5 atm, and T_1 = 200 K. Find M_2, p_2, T_2, and u_2 downstream of the wave.

Solution. From Table A 2, for $M_1 = 3\cdot$ $p_2/p_1 = 10\ 33$, $T_2/T_1 = 2\ 679$, and $M_2 = \boxed{0\ 4752}$ Hence

$$p_2 = \frac{p_2}{p_1} p_1 = 10\ 33(0\ 5) = \boxed{5\ 165 \text{ atm}}$$

$$T_2 = \frac{T_2}{T_1} T_1 = 2\ 679(200) = \boxed{535\ 8 \text{ K}}$$

$$a_2 = \sqrt{\gamma R T_2} = \sqrt{(1\ 4)(287)(535\ 8)} = 464 \text{ m/s}$$

$$u_2 = M_2 a_2 = (0.4752)(464) = \boxed{220 \text{ m/s}}$$

The limiting case of $M_1 \rightarrow \infty$ can be visualized as $u_1 \rightarrow \infty$, where the calorically perfect gas assumption is invalidated by high temperatures, or as $a_1 \rightarrow \infty$, where the perfect gas equation of state is invalidated by extremely low temperatures. Nevertheless, it is interesting to examine the variation of properties across the normal shock as $M_1 \rightarrow \infty$ in the following equations (derived earlier).

$$\boxed{M_2^2 = \frac{1 + [(\gamma - 1)/2] M_1^2}{\gamma M_1^2 - (\gamma - 1)/2}}$$

$$\boxed{\frac{\rho_2}{\rho_1} = \frac{u_1}{u_2} = \frac{(\gamma + 1) M_1^2}{2 + (\gamma - 1) M_1^2}}$$

$$\boxed{\frac{p_2}{p_1} = 1 + \frac{2\gamma}{\gamma + 1}\left(M_1^2 - 1\right)}$$

$$\boxed{\frac{T_2}{T_1} = \frac{h_2}{h_1} = \left[1 + \frac{2\gamma}{\gamma + 1}\left(M_1^2 - 1\right)\right]\left[\frac{2 + (\gamma - 1) M_1^2}{(\gamma + 1) M_1^2}\right]}$$

We find, when $M_1 \to \infty$ for $\gamma = 1.4$

$$\lim_{M_1 \to \infty} M_2 = \sqrt{\frac{\gamma - 1}{2\gamma}} = 0.378 \qquad \text{(as discussed previously)}$$

$$\lim_{M_1 \to \infty} \frac{\rho_2}{\rho_1} = \frac{\gamma + 1}{\gamma - 1} = 6$$

$$\lim_{M_1 \to \infty} \frac{p_2}{p_1} = \infty$$

$$\lim_{M_1 \to \infty} \frac{T_2}{T_1} = \infty$$

At the other extreme, we also find when $M_1 = 1$ for $\gamma = 1.4$

$M_2 = 1$

$$\rho_2/\rho_1 = p_2/p_1 = T_2/T_1 = 1.$$

This is the case of an infinitely weak normal shock degenerating into a Mach wave, where no finite changes occur across the wave. This is the same as the sound wave discussed earlier.

$$M_2^2 = \frac{1 + [(\gamma - 1)/2] M_1^2}{\gamma M_1^2 - (\gamma - 1)/2}$$

$$\frac{\rho_2}{\rho_1} = \frac{u_1}{u_2} = \frac{(\gamma + 1) M_1^2}{2 + (\gamma - 1) M_1^2}$$

$$\frac{p_2}{p_1} = 1 + \frac{2\gamma}{\gamma + 1}\left(M_1^2 - 1\right)$$

$$\frac{T_2}{T_1} = \frac{h_2}{h_1} = \left[1 + \frac{2\gamma}{\gamma + 1}\left(M_1^2 - 1\right)\right]\left[\frac{2 + (\gamma - 1) M_1^2}{(\gamma + 1) M_1^2}\right]$$

To prove that the above equations have physical meaning only when $M_1 > 1$, we must invoke the second law of thermodynamics.

We have,

$$s_2 - s_1 = c_p \ln \frac{T_2}{T_1} - R \ln \frac{p_2}{p_1}$$

Substitute for T_2/T_1 and P_2/P_1 , we get

$$s_2 - s_1 = c_p \ln\left\{\left[1 + \frac{2\gamma}{\gamma+1}\left(M_1^2 - 1\right)\right]\left[\frac{2 + (\gamma-1)M_1^2}{(\gamma+1)M_1^2}\right]\right\} - R \ln\left[1 + \frac{2\gamma}{\gamma+1}\left(M_1^2 - 1\right)\right]$$

The above equation demonstrates that the entropy change across the normal shock is also a function of upstream mach number, M_1 only.

Moreover, it shows that,

if $M_1 = 1$ then $s_2 - s_1 = 0$,

if $M_l < 1$ then $s_2 - s_1 < 0$,

and if $M_1 > 1$ then $s_2 - s_1 > 0$.

Therefore, since it is necessary that $s_2 - s_1 \geq 0$ from the second law of thermodynamics, the upstream Mach number M_l must be greater than or equal to 1.

Here is another example of how the second law tells us the direction in which a physical process will proceed. If M_1 is subsonic, then the above equation says that the entropy decreases across the normal shock — an impossible situation. The only physically possible case is $M_1 > 1$, which in turn dictates from the above four equations that

$$p_2/p_1 \ge 1, \text{ and } T_2/T_1 \ge 1$$ [redacted]

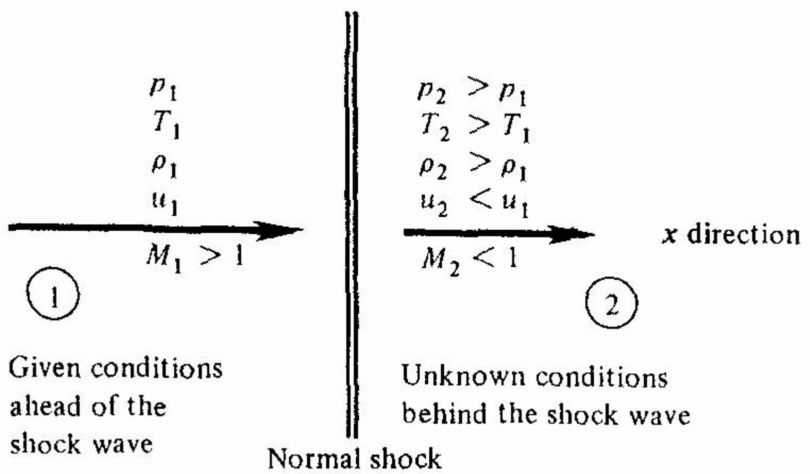

FIGURE 3.3
Diagram of a normal shock

Thus, we have now established the phenomena sketched in Fig. 3.3, namely, that across a normal shock wave the pressure, density, and temperature increase, whereas the velocity decreases and the Mach number decreases to a subsonic value.

What really causes the entropy increase across a shock wave?

To answer this, recall that the changes across the shock occur over a very short distance, on the order of 10^{-5} cm Hence, the velocity and temperature gradients inside the shock structure itself are very large. In regions of large gradients, the viscous effects of viscosity and thermal conduction become important In turn, these are dissipative, irreversible phenomena which generate entropy. Therefore, the net entropy increase predicted by the normal shock relations in conjunction with the second law of thermodynamics is appropriately provided by nature in the form of friction and thermal conduction inside the shock wave structure itself.

Finally, we need to resolve one more question!

How do the total (stagnation) conditions vary across a normal shock wave?

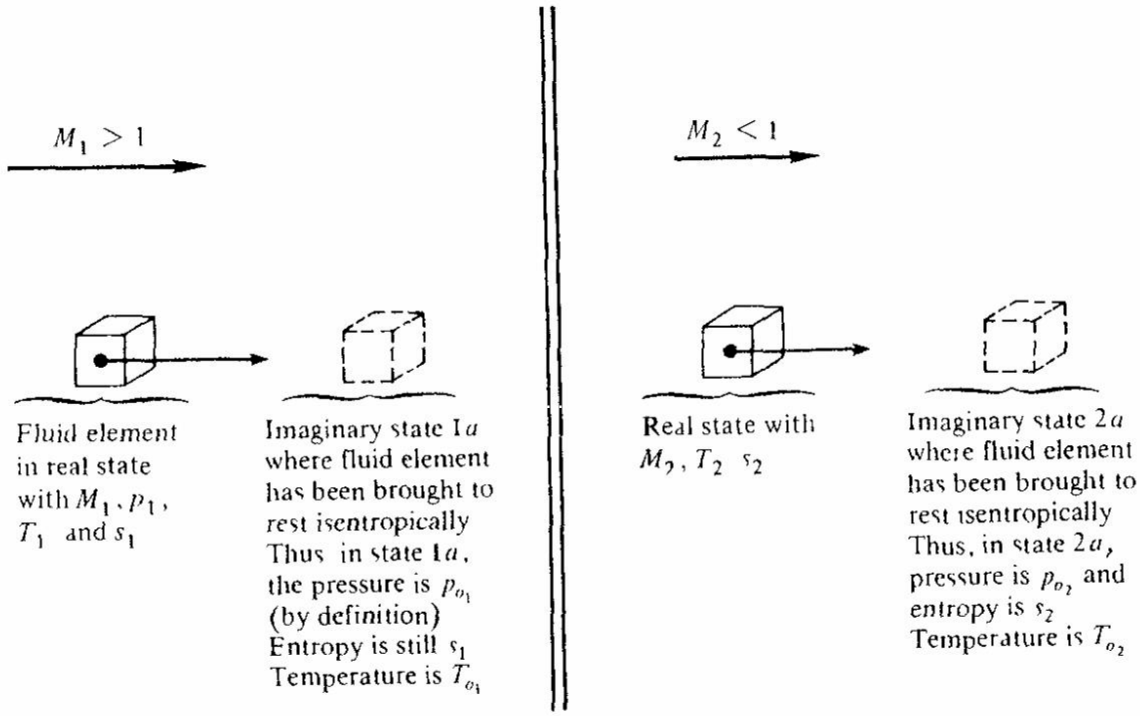

FIGURE 3.8
Illustration of total (stagnation) conditions ahead of and behind a normal shock wave

Consider Fig. 3.8, which illustrates the definition of total conditions before and after the shock. In region 1 ahead of the shock, a fluid element is moving with actual conditions of M_1, p_1, T_1 and s_1. Consider in this region the imaginary state l*a* where the fluid element has been brought to rest isentropically. Thus, by definition, the pressure and temperature in state l*a* are the total values p_{01}, and T_{01}, respectively. The entropy at state l*a* is still s_1 because the

stagnating of the fluid element has been done isentropically. In region 2 behind the shock, a fluid element is moving with actual conditions of M_2, p_2, T_2, and s_2. Consider in this region the imaginary state 2*a* where the fluid element has been brought to rest isentropically. Here, by definition, the pressure and temperature in state 2a are the total values of p_{02} and T_{02}, respectively. The entropy at state 2*a* is still s_2, by definition. The question is now raised how p_{02} and T_{02} behind the shock compare with p_{01} and T_{01}, respectively, ahead of the shock. To answer this question, we use the following equation for calorically perfect gas,

$$\boxed{c_p T_1 + \frac{u_1^2}{2} = c_p T_2 + \frac{u_2^2}{2}}$$

The total temperature is given by

$$c_p T_o = c_p T + \frac{u^2}{2}$$

Hence

$$c_p T_{o_1} = c_p T_{o_2}$$

and thus

$$\boxed{T_{o_1} = T_{o_2}}$$

From the above equation, we see that the total temperature is constant across a stationary normal shock wave, which holds for a calorically perfect gas, is a special case of the more general result that the total enthalpy is constant across the shock, as demonstrated earlier using the following equation,

$$h_1 + \frac{u_1^2}{2} = h_2 + \frac{u_2^2}{2} \qquad \text{(energy)}$$

For a stationary normal shock, the total enthalpy is always constant across the shock wave, which for calorically or thermally perfect gases translates into a constant total temperature across the shock. However, for a chemically reacting gas, the total temperature is not constant across the shock (will be discussed later). Also, if the shock wave is not stationary — if it is moving through space — neither the total enthalpy nor total temperature are constant across the wave. This becomes a matter of reference systems (will discuss later).

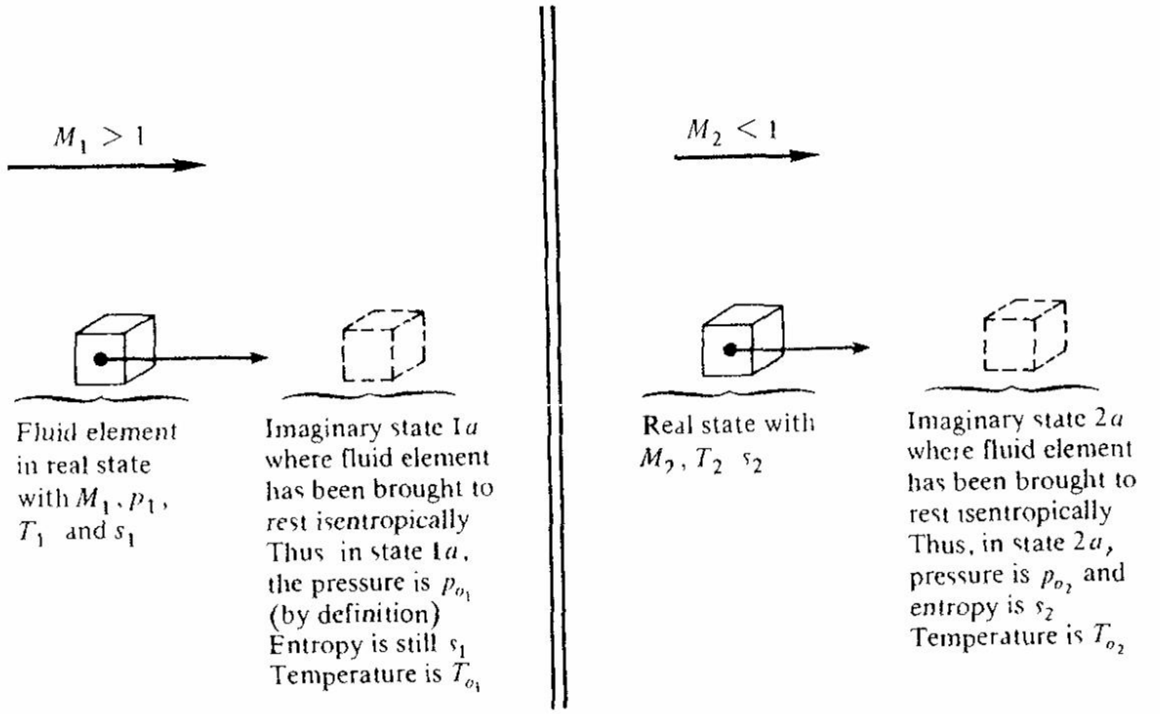

FIGURE 3.8
Illustration of total (stagnation) conditions **ahead of and behind** a normal shock wave

We have,

$$\boxed{s_2 - s_1 = c_p \ln \frac{T_2}{T_1} - R \ln \frac{p_2}{p_1}}$$

Considering the above figure again, rewrite the above equation between the imaginary states l*a* and 2*a*:

$$s_{2a} - s_{1a} = c_p \ln \frac{T_{2a}}{T_{1a}} - R \ln \frac{p_{2a}}{p_{1a}}$$

However, $s_{2a} = s_2$, $s_{1a} = s_1$, $T_{2a} = T_o = T_{1a}$, $p_{2a} = p_{o_2}$, and $p_{1a} = p_{o_1}$

Hence the above equation becomes,

$$\boxed{s_2 - s_1 = -R \ln \frac{p_{o_2}}{p_{o_1}}}$$

OR

$$\frac{p_{o_2}}{p_{o_1}} = e^{-(s_2 - s_1)/R}$$

Where,

$$s_2 - s_1 = c_p \ln\left\{\left[1 + \frac{2\gamma}{\gamma + 1}\left(M_1^2 - 1\right)\right]\left[\frac{2 + (\gamma - 1)M_1^2}{(\gamma + 1)M_1^2}\right]\right\} - R \ln\left[1 + \frac{2\gamma}{\gamma + 1}\left(M_1^2 - 1\right)\right]$$

From the above two equations we see that the ratio of total pressures across the normal shock depends on M_1 only. Also, because $s_2 > s_1$, the following equations (derived above) show that $p_{o2} < p_{o1}$. **The total pressure decreases across a shock wave.**

$$\boxed{s_2 - s_1 = -R \ln \frac{p_{o_2}}{p_{o_1}}}$$

$$\frac{p_{o_2}}{p_{o_1}} = e^{-(s_2 - s_1)/R}$$

The variations of p_2/p_1, ρ_2/ρ_1, T_2/T_1, p_{o_2}/p_{o_1}, and M_2 with M_1 as [redacted] **obtained from the above equations are tabulated in the gas table for various values of γ.**

To provide more physical feel, these variations are plotted in the below figure for $\gamma = 1.4$. Note that (as stated earlier) these curves show how, as M_1 becomes very large, T_2/T_1 and p_2/p_1 also become very large, whereas ρ_2/ρ_1 and M_2 approach finite limits.

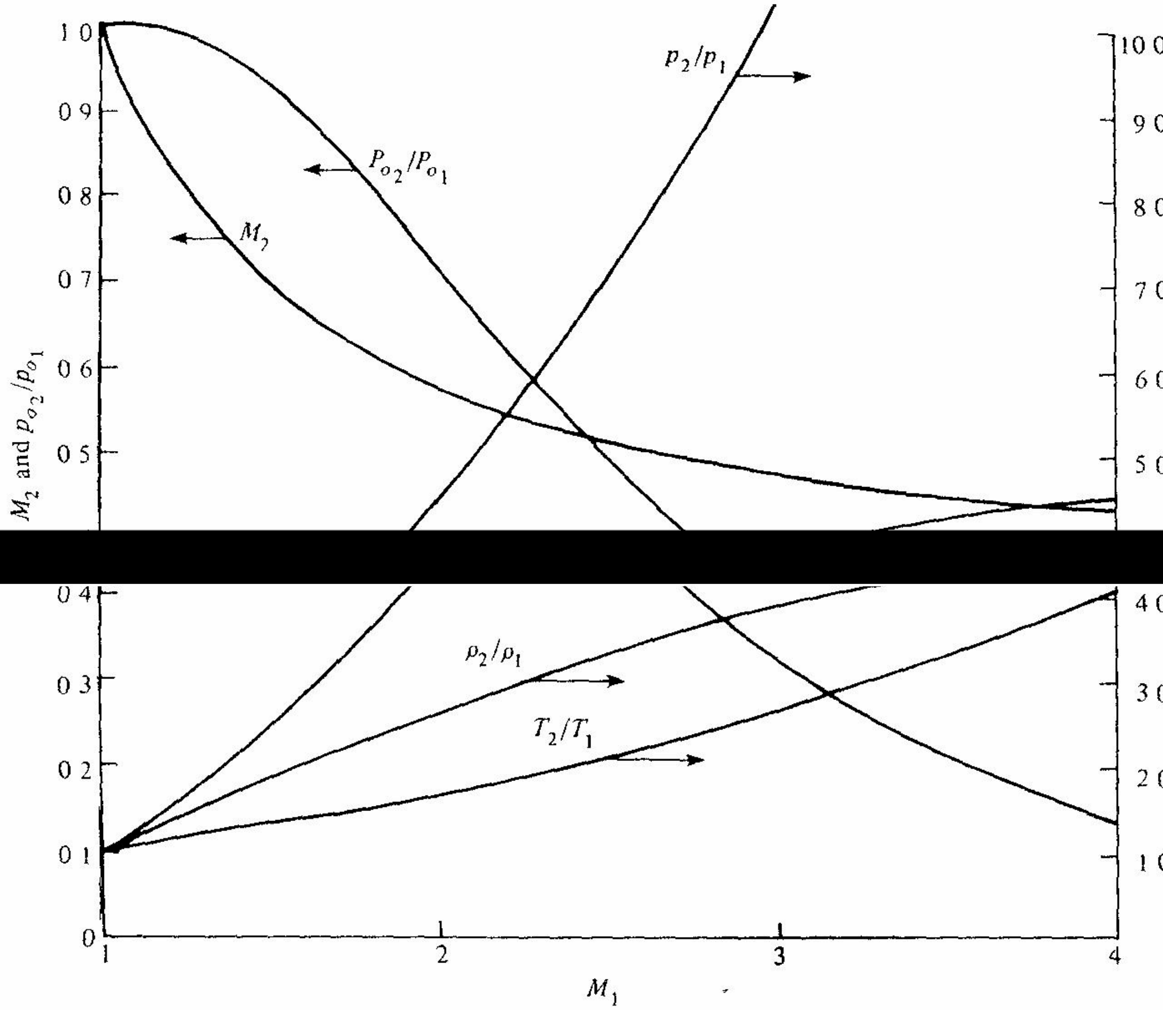

FIGURE 3 9
Properties behind a normal shock wave as a function of upstream Mach number

Example-4

A blunt-nosed missile is flying at Mach 2 at standard sea level. Calculate the temperature and pressure at the nose of the missile.

Solution. The nose of the missile is a stagnation point, and the streamline through the stagnation point has also passed through the normal portion of the bow shock wave Hence, the temperature and pressure at the nose are equal to the total temperature and pressure behind a normal shock Also, at standard sea level, $T_1 = 519°\text{R}$ and $p_1 = 2116\ \text{lb/ft}^2$

From Table A 1, for $M_1 = 2$: $T_{o_1}/T_1 = 1\ 8$ and $p_{o_1}/p_1 = 7\ 824$ Also, for adiabatic flow through a normal shock, $T_{o_2} = T_{o_1}$ Hence

$$T_{o_2} = T_{o_1} = \frac{T_{o_1}}{T_1} T_1 = 1\ 8(519) = \boxed{934\ 2°\text{R}}$$

From Table A 2, for $M_1 = 2$: $p_{o_2}/p_{o_1} = 0\ 7209$ Hence

$$p_{o_2} = \frac{p_{o_2}}{p_{o_1}} \frac{p_{o_1}}{p_1} p_1 = (0\ 7209)(7\ 824)(2116) = \boxed{11{,}935\ \text{lb/ft}^2}$$

Analytical Exercises

Prove that the change in internal energy equals the mean pressure across the shock times the change in specific volume. i.e.,

$$\boxed{e_2 - e_1 = \frac{p_1 + p_2}{2}(v_1 - v_2)}$$

Hint:

Eliminate the velocity term from the following energy equation.

$$h_1 + \frac{u_1^2}{2} = h_2 + \frac{u_2^2}{2}$$

Where,

$$h = e + p/\rho$$

Use the following continuity and momentum equation for getting the desired solution.

$$\rho_1 u_1 = \rho_2 u_2 \qquad \text{(continuity)}$$

$$p_1 + \rho_1 u_1^2 = p_2 + \rho_2 u_2^2 \qquad \text{(momentum)}$$

HUGONIOT EQUATION

The results obtained in the previous section for the normal shock wave were couched in terms of velocities and Mach numbers—quantities which quite properly emphasize the fluid dynamic nature of shock waves. However, because the static pressure always increases across a shock wave, the wave itself can also be visualized as a thermodynamic device which compresses the gas. Indeed, the changes across a normal shock wave can be expressed in terms of purely thermodynamic variables without explicit reference to a velocity or Mach number, as follows From the continuity equation

$$u_2 = u_1\left(\frac{\rho_1}{\rho_2}\right)$$

Substitute the above equation into the momentum equation,

$$p_1 + \rho_1 u_1^2 = p_2 + \rho_2\left(\frac{\rho_1}{\rho_2}u_1\right)^2$$

Solve the above equation for u_1^2

$$u_1^2 = \frac{p_2 - p_1}{\rho_2 - \rho_1}\left(\frac{\rho_2}{\rho_1}\right)$$

Alternatively, writing the continuity equation as

$$u_1 = u_2\left(\frac{\rho_2}{\rho_1}\right)$$

and again substituting into the momentum equation, this time solving for u_2, we obtain

$$u_2^2 = \frac{p_2 - p_1}{\rho_2 - \rho_1}\left(\frac{\rho_1}{\rho_2}\right)$$

From the energy equation, we have

$$h_1 + \frac{u_1^2}{2} = h_2 + \frac{u_2^2}{2}$$

and recalling that by definition h = e + p/ρ, we have

$$e_1 + \frac{p_1}{\rho_1} + \frac{u_1^2}{2} = e_2 + \frac{p_2}{\rho_2} + \frac{u_2^2}{2}$$

Substituting the values of u_1^2 and u_2^2 into the above equation, the velocities are eliminated, yielding

$$e_1 + \frac{p_1}{\rho_1} + \frac{1}{2}\left[\frac{p_2 - p_1}{\rho_2 - \rho_1}\left(\frac{\rho_2}{\rho_1}\right)\right] = e_2 + \frac{p_2}{\rho_2} + \frac{1}{2}\left[\frac{p_2 - p_1}{\rho_2 - \rho_1}\left(\frac{\rho_1}{\rho_2}\right)\right]$$

This simplifies to

$$e_2 - e_1 = \frac{(p_1 + p_2)}{2}\left(\frac{1}{\rho_1} - \frac{1}{\rho_2}\right)$$

$$\boxed{e_2 - e_1 = \frac{p_1 + p_2}{2}(v_1 - v_2)}$$

The above equation is called the Hugoniot equation. It has certain advantages because it relates only thermodynamic quantities across the shock. Also, we have made no assumption about the type of gas; the above is a general relation that holds for a perfect gas, chemically reacting gas, real gas, etc.

In addition, note that the above Hugoniot equation has the form of

$$\Delta e = -p_{\text{ave}} \, \Delta v;$$

i.e., the change in internal energy equals the mean pressure across the shock times the change in specific volume. This strongly reminds us of the first law of thermodynamics in the form of

$$\delta q - p \, dv = de$$

,

with

$$\delta q = 0$$

for the adiabatic process across the shock

In general, in equilibrium thermodynamics any state variable can be expressed as a function of any other two state variables, for example $e = e(p, v)$ This relation could be substituted into Eq (3 72), resulting in a functional relation

$$p_2 = f(p_1, v_1, v_2) \qquad (3\ 73)$$

For given conditions of p_1 and v_1 upstream of the normal shock, Eq (3 73) represents p_2 as a function of v_2. A plot of this relation on a *pv* graph is called the *Hugoniot curve*, which is sketched in Fig 3.10. This curve is the locus of all possible pressure-volume conditions behind normal shocks of various strengths for one specific set of upstream values for p_1 and v_1 (point 1 in Fig 3 10) Each point on the Hugoniot curve in Fig. 3 10 therefore represents a different shock with a different upstream velocity u_1.

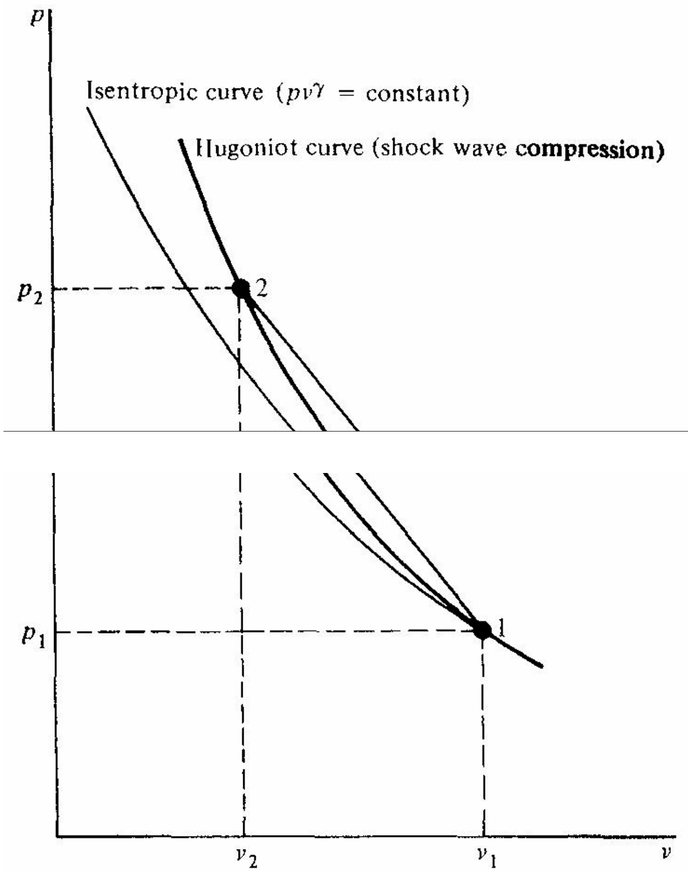

FIGURE 3.10
Hugoniot curve, comparison with isentropic compression

OBLIQUE SHOCK WAVES


1904

A Boeing F/A-18 with afterburners on. Note shock/expansion patterns int he supersonic nozzle exhaust.

http://images.google.co.in/imgres?imgurl=http://www.ae.gatech.edu/labs/windtunl/classes/Propulsion/mig25mm.jpg&imgrefurl=http://www.ae.gatech.edu/labs/windtunl/classes/Propulsion/ae42512.html&usg=__2oZgbPgFEdoyr-GAsJ3FDrzlf9w=&h=391&w=638&sz=27&hl=en&start=8&um=1&tbnid=u37vEw2l3IOESM:&tbnh=84&tbnw=137&prev=/images%3Fq%3Doblique%2Bshock%26hl%3Den%26sa%3DX%26um%3D1

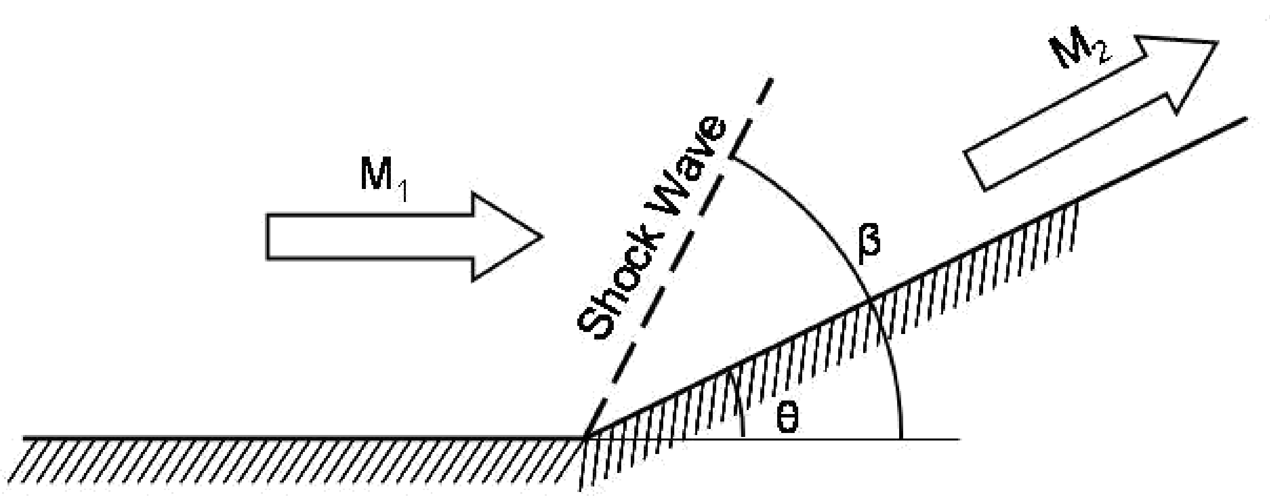

M_1
Shock Wave
M_2
β
θ

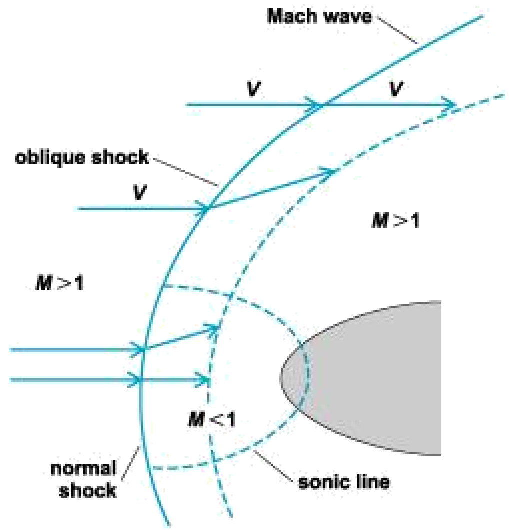

Mach wave
V
V
oblique shock
V
M > 1
M > 1
M < 1
normal shock
sonic line

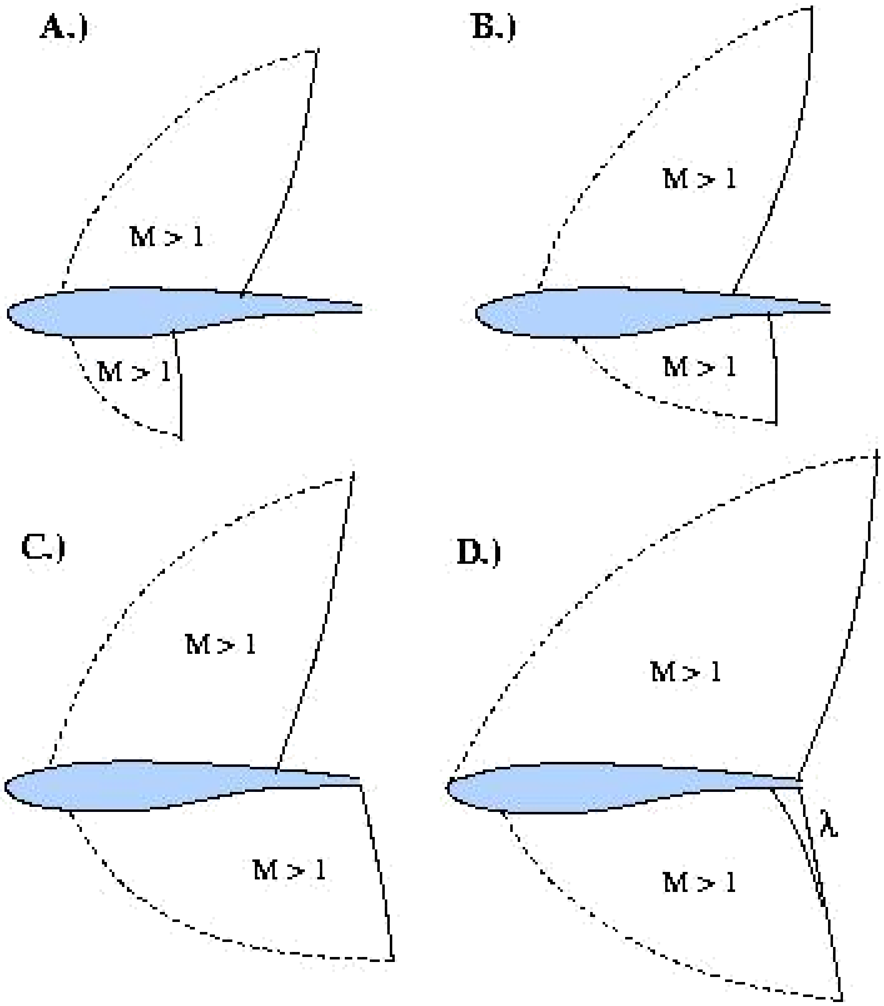

Shock Progression on Airfoil

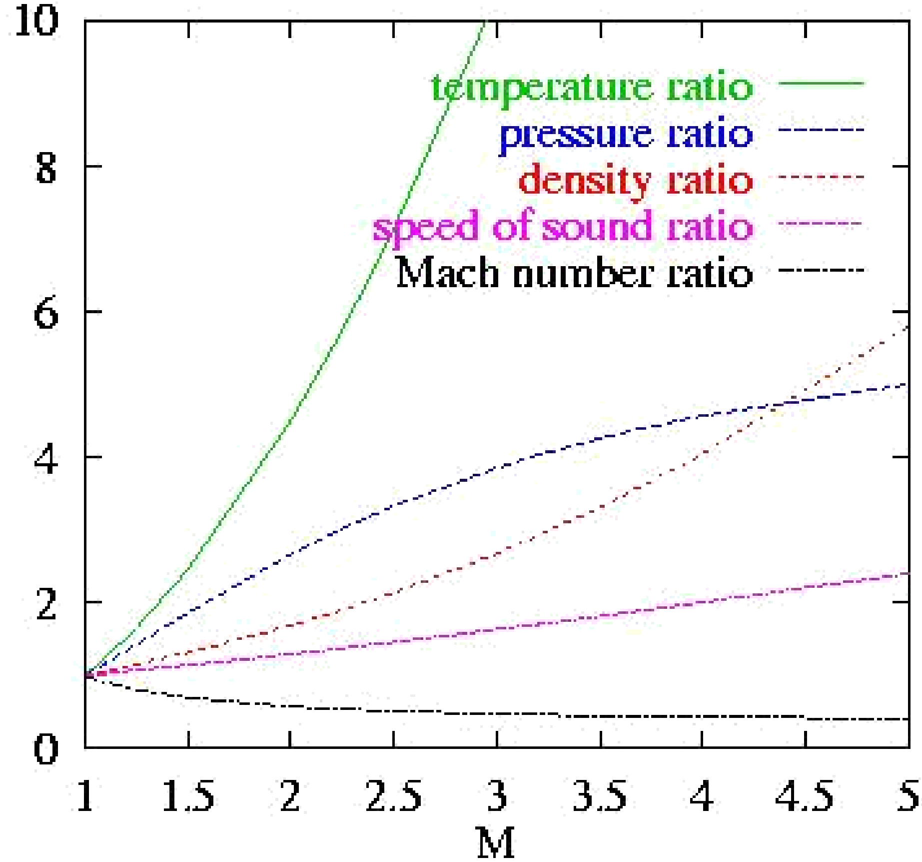

Normal shock ratios at supersonic speeds

EXTERNAL FLOW APPLIED TO AIRCRAFT / SPACECRAFT

Viscosity.- There are basically three states of matter - solid, liquid, and gas. H_2O is commonly called "ice" in the solid state, "water" in the liquid state, and "water vapor" in the gaseous state. Assume one has a piece of ice and side forces are applied to it (called shearing forces). Very large forces are needed to deform or break it. The solid has a very high internal friction or resistance to shearing. The word for internal friction is viscosity and for a solid its value is generally very large.

Liquids and gases are considered to be fluids since they behave differently from a solid. Imagine two layers of water or air. If shear forces are applied to these layers, one discovers a substantial and sustained relative motion of the layers with the air layers sliding faster over one another than the water layers. However, the fact that a

shear force must be applied to deform the fluids indicates that they also possess internal friction.

Water, under normal temperatures, is about fifty times more viscous than air. Ice is 5 x 10^{16} times more viscous than air. One concludes that, in general, solids have extremely high viscosities whereas fluids have low viscosities. Under the category of fluids, liquids generally possess higher viscosities than gases. Air, of primary interest in aerodynamics, has a relatively small viscosity, and in some theories, it is described as a perfect fluid-one that has zero viscosity or is "inviscid." But it will be shown that even this small viscosity of air (or internal friction) has important effects on an airplane in terms of lift and drag.

Oblique Shock

- The discontinuities in supersonic flows do not always exist as normal to the flow direction. There are oblique shocks which are inclined with respect to the flow direction. Refer to the shock structure on an obstacle, as depicted qualitatively in the below Fig.
- The segment of the shock immediately in front of the body behaves like a normal shock.
- Oblique shock can be observed in following cases-
  1. **Oblique shock formed as a consequence of the bending of the shock in the free-stream direction** (shown in the below Fig.)
  2. **In a supersonic flow through a duct, viscous effects cause the shock to be oblique near the walls, the shock being normal only in the core region.**
  3. **The shock is also oblique when a supersonic flow is made to change direction near a sharp corner**

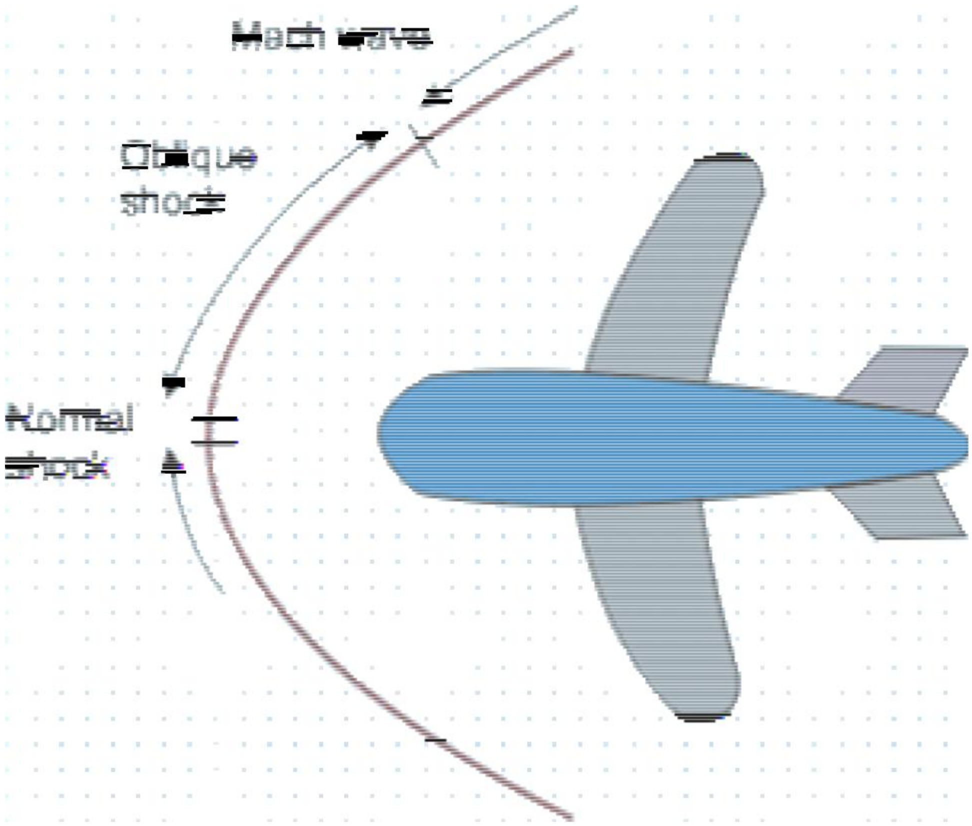

Normal and oblique Shock in front of an Obstacle

- The relationships derived earlier for the normal shock are valid for the velocity components normal to the oblique shock. The oblique shock continues to bend in the downstream direction until the Mach number of the velocity component normal to the wave is unity. At that instant, **the oblique shock degenerates into a so called Mach wave across which changes in flow properties are infinitesimal.**

Tutorial:

A pitot tube mounted on the nose of a supersonic aircraft shows that the ratio of stagnation to static pressure is 27. Find out the aircraft speed in terms of Mach number.

$$\frac{p_{\text{stagnation}}}{p_{\text{static}}} = \frac{\left[\dfrac{\gamma+1}{2}M^2\right]^{\left(\gamma/_{\gamma-1}\right)}}{\left[\dfrac{2\gamma}{\gamma+1}M^2 - \dfrac{\gamma-1}{\gamma+1}\right]^{\left(1/_{\gamma-1}\right)}}$$

$$= \frac{\gamma+1}{2}M^2\left[\frac{(\gamma+1)^2 M^2}{4\gamma M^2 - 2(\gamma-1)}\right]^{\left(1/_{\gamma-1}\right)}$$

Therefore, the Mach angle is simply determined by the local Mach number as

$$\boxed{\mu = \sin^{-1}\frac{1}{M}} \qquad (4.1)$$

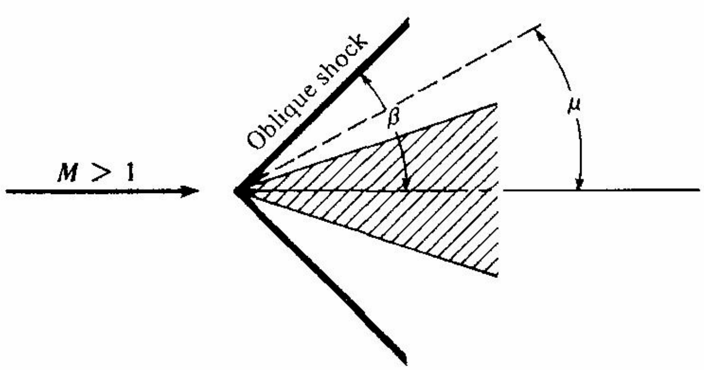

FIGURE 4 3
Comparison between the wave angle and the Mach angle

SUMMARY

Whenever a supersonic flow is turned into itself, shock waves can occur; when the flow is turned away from itself, expansion waves can occur. In either case, if the wave is infinitely weak, it becomes a Mach wave, which makes an angle μ with respect to the upstream flow direction; μ is called the Mach angle, defined as

$$\mu = \sin^{-1}\frac{1}{M} \tag{4.1}$$

Across an oblique shock wave, the tangential components of velocity in front of and behind the wave are equal (However, the tangential components of Mach number are *not* the same.) The thermodynamic properties across the oblique shock are dictated by the normal component of the upstream Mach number M_{n_1}. The values of p_2/p_1, ρ_2/ρ_1, T_2/T_1, $s_2 - s_1$, and p_{o_2}/p_{o_1} across the oblique shock are the same as for a normal shock wave with an upstream Mach number of M_{n_1}. In this fashion, the normal shock tables in Appendix A.2 can be used for oblique shocks. The value of M_{n_1} depends on both M_1 and the wave angle, β, via

$$M_{n_1} = M_1 \sin\beta \tag{4.7}$$

In turn, β is related to M_1 and the flow deflection angle θ through the θ-β-M relation

$$\tan\theta = 2\cot\beta\left[\frac{M_1^2\sin^2\beta - 1}{M_1^2(\gamma + \cos 2\beta) + 2}\right] \tag{4.17}$$

In light of the above, we can make the following comparison (1) In Chapter 3, we noted that the changes across a normal shock depended *only* on one flow parameter, namely the upstream Mach number M_1 (2) In the present chapter, we note that *two* flow parameters are needed to uniquely define the changes across an oblique shock. Any combination of two parameters will do For example, an oblique shock is uniquely defined by any one of the following pairs of parameters: M_1 and β, M_1 and θ, θ and β, M_1 and p_2/p_1, β and p_2/p_1 etc.

For the solution of shock wave problems, especially cases involving shock intersections and reflections, the graphical constructions associated with the shock polar and the pressure-deflection diagrams are instructional.

For the curved, detached bow shock wave in front of a supersonic blunt body, the properties at any point immediately behind the shock are given by the oblique shock relations studied in this chapter, for the values of M_1 and the local β. Indeed, the oblique shock relations studied here apply in general to points immediately behind *any* curved, three-dimensional shock wave, so long as the component of the upstream Mach number *normal* to the shock at a given point is used to obtain the shock properties.

The properties through and behind a Prandtl-Meyer expansion fan are dictated by the differential relation

$$d\theta = \sqrt{M^2 - 1}\,\frac{dV}{V} \tag{4.31}$$

When integrated across the wave, this equation becomes

$$\theta_2 = \nu(M_2) - \nu(M_1) \tag{4.41}$$

where θ_1 is assumed to be zero and ν is the Prandtl-Meyer function given by

$$\nu(M) = \sqrt{\frac{\gamma+1}{\gamma-1}}\tan^{-1}\sqrt{\frac{\gamma-1}{\gamma+1}(M^2-1)} - \tan^{-1}\sqrt{M^2-1} \tag{4.40}$$

The flow through an expansion wave is isentropic; from the local Mach numbe obtained from the above relations, all other flow properties are given by tl isentropic flow relations discussed in Section 3.5

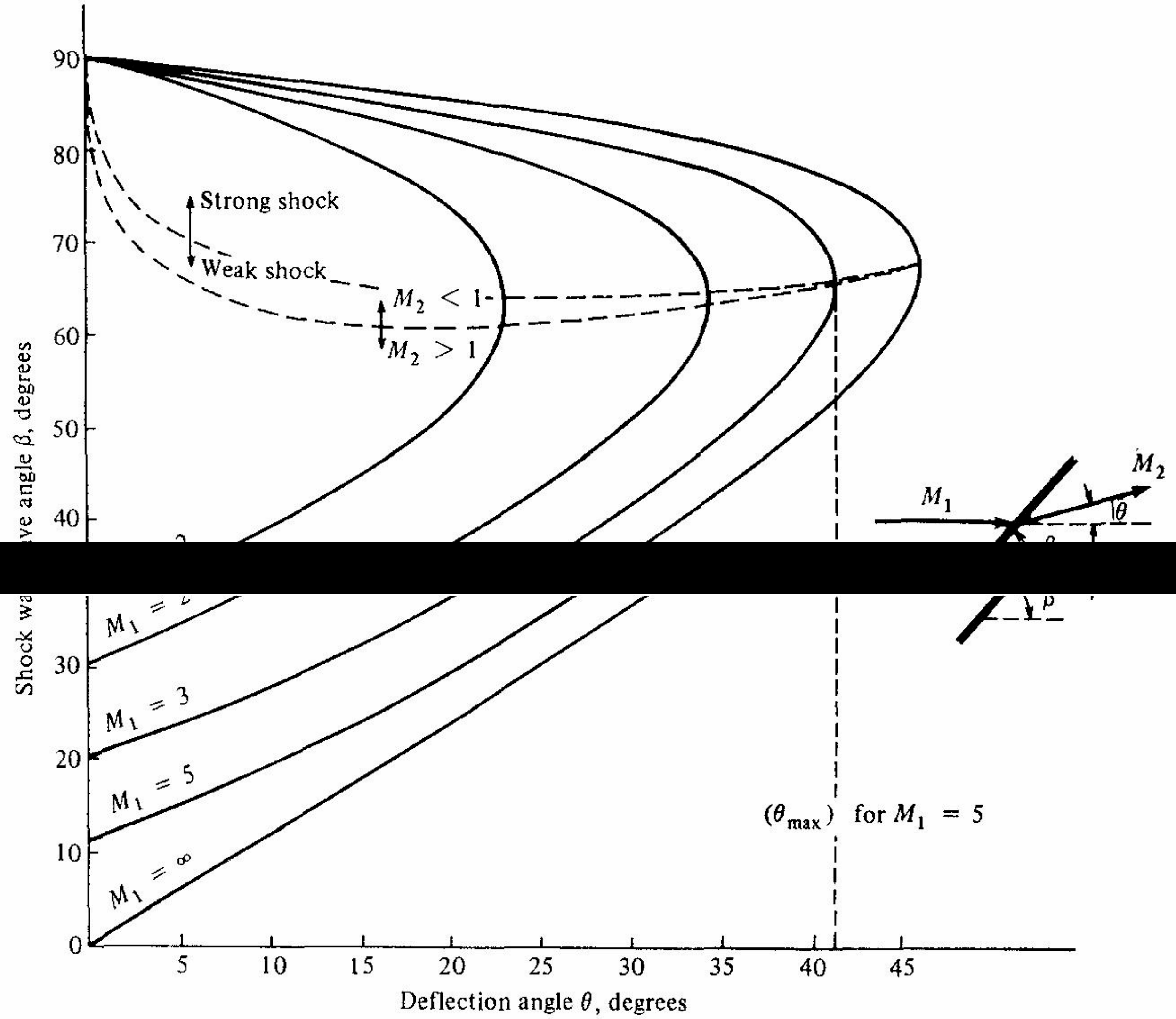

FIGURE 4.5
θ-β-M curves Oblique shock properties *Important* See end pages for a more detailed chart

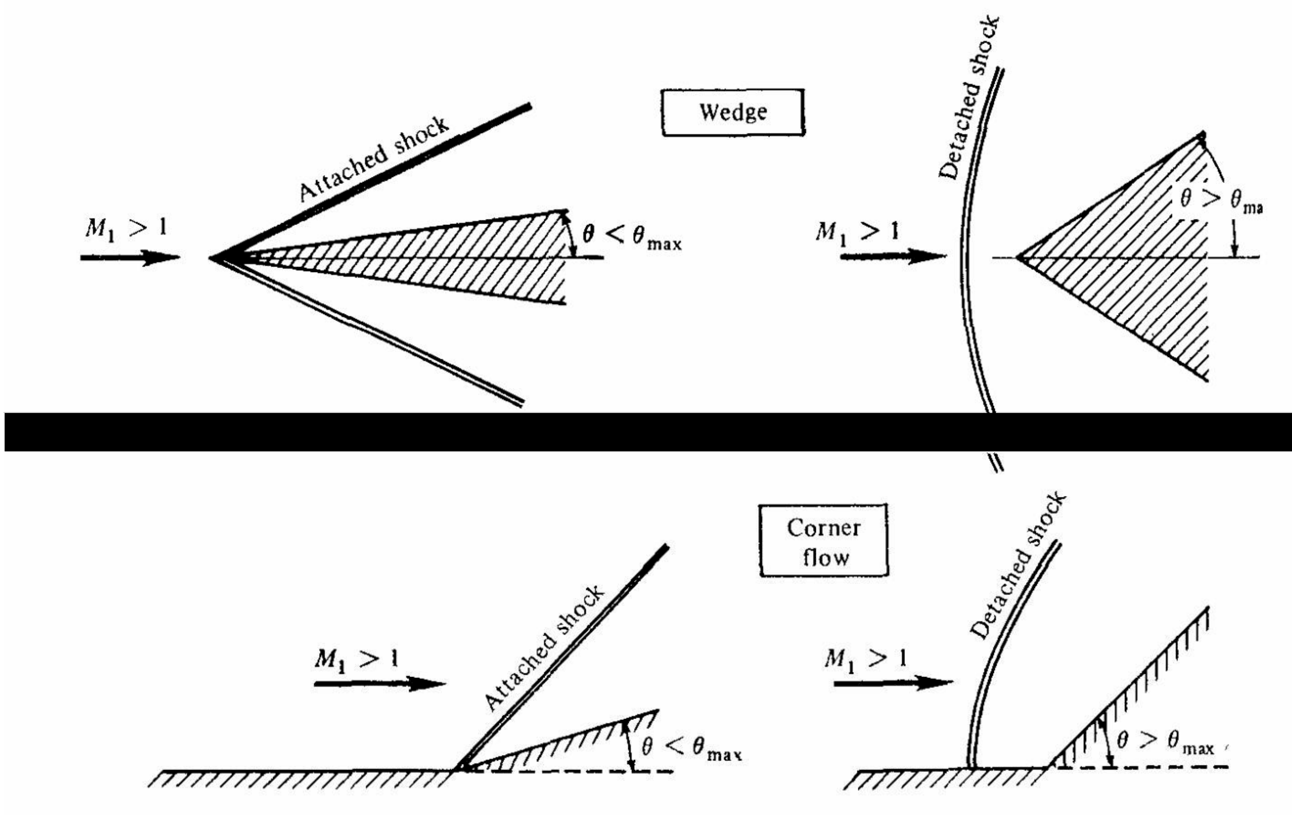

FIGURE 4 6

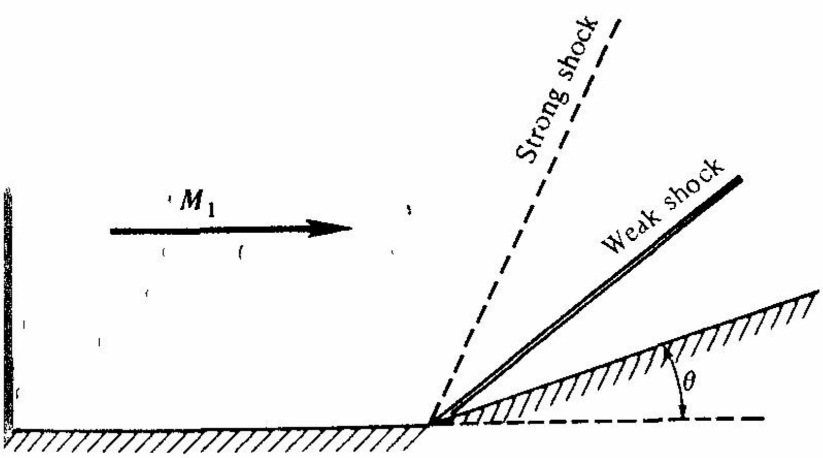

FIGURE 4.7
Weak and strong shocks

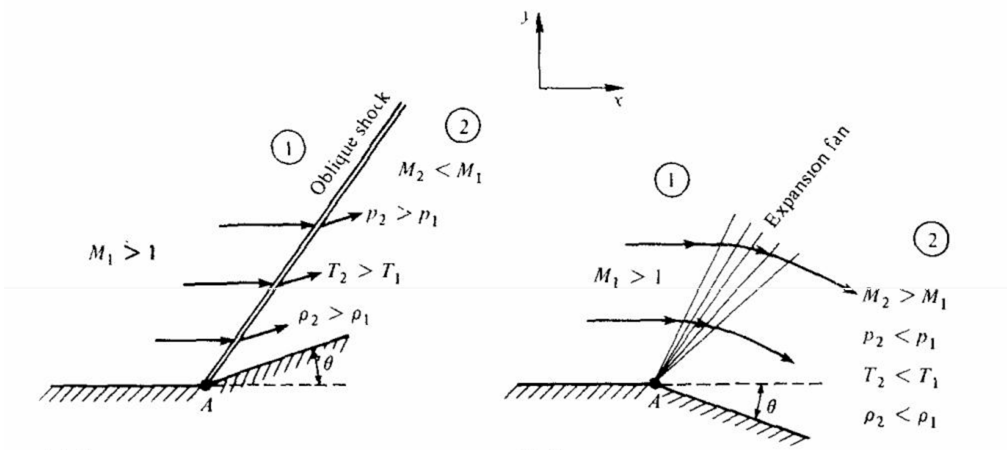

(a) Concave corner

(b) Convex corner

FIGURE 4.1
Supersonic flow over a corner

Example 4.1. A uniform supersonic stream with $M_1 = 3\ 0$, $p_1 = 1$ atm, and $T_1 = 288$ K encounters a compression corner (see Fig 4 1*a*) which deflects the stream by an angle $\theta = 20°$ Calculate the shock wave angle, and p_2, T_2, M_2, p_{o_2}, and T_{o_2} behind the shock wave

Solution. For the geometrical picture, refer to Fig 4 4 Also, from Fig 4 5, for $M_1 = 3$ and $\theta = 20°$, $\boxed{\beta = 37.5°}$. Thus

$$M_{n_1} = M_1 \sin\beta = 3 \sin 37\ 5° = 1\ 826$$

From Table A.2, for $M_{n_1} = 1.826$. $p_2/p_1 = 3\ 723$, $T_2/T_1 = 1\ 551$, $M_{n_2} = 0\ 6108$, and $p_{o_2}/p_{o_1} = 0\ 8011$ Hence,

$$p_2 = \frac{p_2}{p_1} p_1 = (3\ 723)(1) = \boxed{3.723 \text{ atm}}$$

$$T_2 = \frac{T_2}{T_1} T_1 = (1\ 551)(288) = \boxed{446\ 7 \text{ K}}$$

$$M_2 = \frac{M_{n_2}}{\sin(\beta - \theta)} = \frac{0\ 6108}{\sin 17.5°} = \boxed{2\ 03}$$

From Table A.1, for $M_1 = 3$: $p_{o_1}/p_1 = 36.73$ and $T_{o_1}/T_1 = 2\ 8$ Hence

$$p_{o_2} = \frac{p_{o_2}}{p_{o_1}} \frac{p_{o_1}}{p_1} p_1 = (0\ 8011)(36\ 73)(1) = \boxed{29\ 42 \text{ atm}}$$

$$T_{o_2} = T_{o_1} = \frac{T_{o_1}}{T_1} T_1 = (2\ 8)(288) = \boxed{806\ 4 \text{ K}}$$

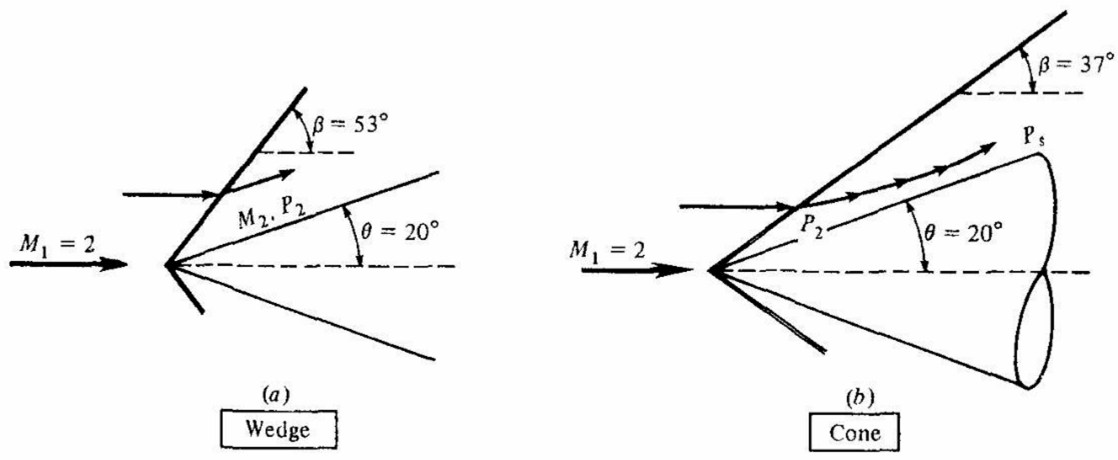

FIGURE 4 8
Comparison between wedge and cone flow; illustration of the three-dimensional relieving effect.

SHOCK POLAR

Graphical explanations go a long way towards the understanding of supersonic flow with shock waves. One such graphical representation of oblique shock properties is given by the shock polar, described below.

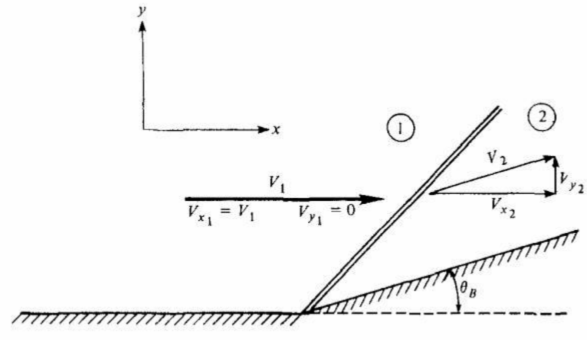

FIGURE 4.10
The physical (xy) plane

Consider an oblique shock with a given upstream velocity V_1 and deflection angle θ_B, as sketched in Fig. 4.10. Also, consider an xy cartesian coordinate system with the x axis in the direction of V_1. Figure 4.10 is called the *physical plane* Define V_{x_1}, V_{y_1}, V_{x_2}, and V_{y_2} as the x and y components of velocity ahead of and behind the shock, respectively. Now plot these velocities on a graph which uses V_x and V_y as axes, as shown in Fig. 4.11. This graph of velocity components is called the *hodograph plane*. The line OA represents V_1 ahead of the shock; the line OB represents V_2 behind the shock. In turn, *point A* in the hodograph plane of Fig. 4.11 represents the entire *flowfield* of region 1 in the physical plane of Fig 4.10. Similarly, point B in the hodograph plane represents the entire flowfield of region 2 in the physical plane. If now the deflection angle in Fig. 4.10 is increased to a larger value, say θ_C, then the velocity V_2 is inclined further to angle θ_C, and its magnitude is decreased because the shock wave becomes stronger. This condition is shown as point C in the hodograph diagram of Fig. 4.12. Indeed, if

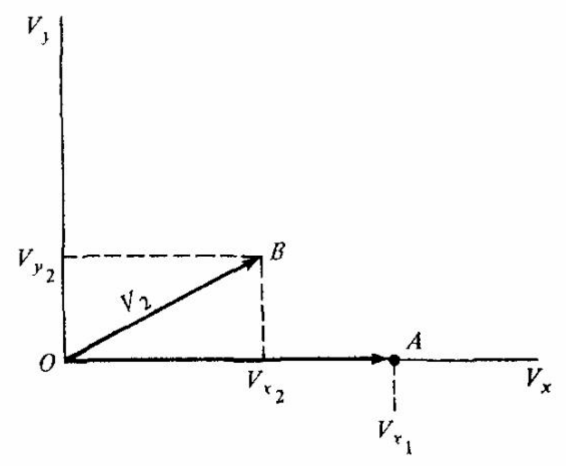

FIGURE 4 11
The hodograph plane

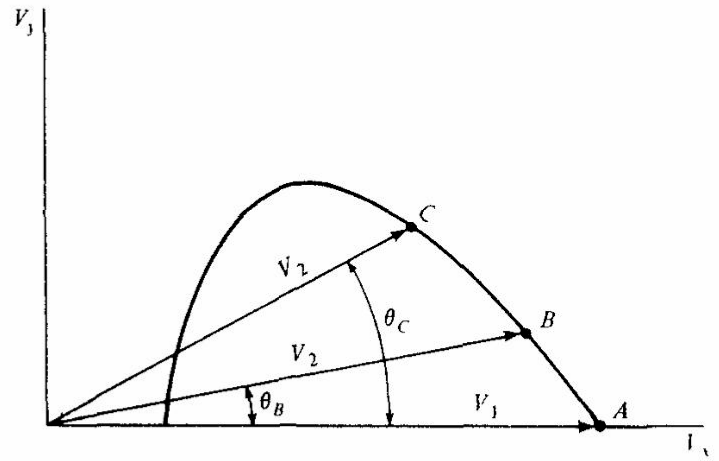

FIGURE 4.12
Shock polar for a given V_1

the deflection angle θ in Fig. 4.9 is carried through all possible values for which there is an oblique shock solution ($\theta < \theta_{max}$), then the locus of all possible velocities behind the shock is given in Fig. 4.12. This locus is defined as a *shock polar*. Points A, B, and C in Figs. 4.11 and 4.12 are just three points on the shock polar for a given V_1.

For convenience, let us now nondimensionalize the velocities in Fig. 4.12 by a^*, defined in Sec. 3.4. Recall that the flow across a shock is adiabatic, hence a^* is the same ahead of and behind the shock Consequently, we obtain a shock polar which is the locus of all possible M_2^* values for a given M_1^*, as sketched in Fig. 4.13. The convenience of using M^* instead of M or V to plot the shock polar is that, as $M \rightarrow \infty$, $M^* \rightarrow 2.45$ (see Sec. 3.5). Hence, the shock polars for a wide range of Mach numbers fit compactly on the same page when plotted in terms of M^*. Also note that a circle with radius $M^* = 1$ defines the *sonic circle* shown in Fig. 4.13. Inside this circle, all velocities are subsonic; outside it, all velocities are supersonic.

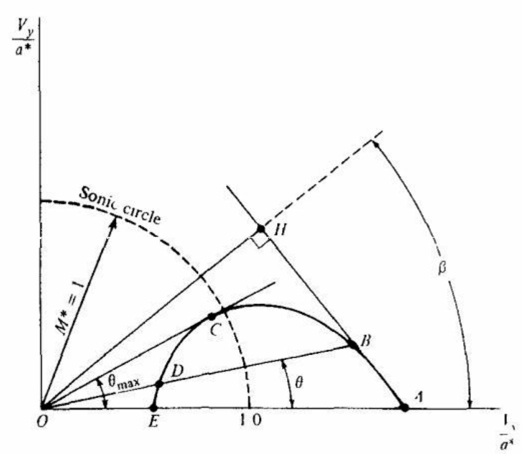

FIGURE 4.13
Geometric constructions using the shock polar

Several important properties of the shock polar are illustrated in Fig. 4.13 as follows:

1. For a given deflection angle θ, the shock polar is cut at two points B and D Points B and D represent the weak and strong shock solutions, respectively Note that D is inside the sonic circle, as would be expected.
2. The line OC drawn tangent to the shock polar represents the maximum deflection angle θ_{max} for the given $\mathscr{M}_1^*$ (hence also for the given M_1). For $\theta > \theta_{max}$, there is no oblique shock solution
3. Points E and A represent flow with no deflection. Point E is the normal shock solution; point A corresponds to a Mach line.
4. If a line is drawn through A and B, and line OH is drawn perpendicular to AB, then the angle HOA is the wave angle β corresponding to the shock solution at point B. This can be proved by simple geometric argument, recalling that the tangential component of velocity is preserved across the shock wave. Try it yourself.
5. The shock polars for different Mach numbers form a family of curves, as drawn in Fig. 4.14. Note that the shock polar for $M_1^* = 2\,45(M_1 \to \infty)$ is a circle.

The analytic equation for the shock polar (V_y/a^* versus V_x/a^*) can be obtained from the oblique shock equations given in Sec. 4.3. The derivation is given in such classic texts as those by Ferri (Ref. 5) or Shapiro (Ref. 16). The

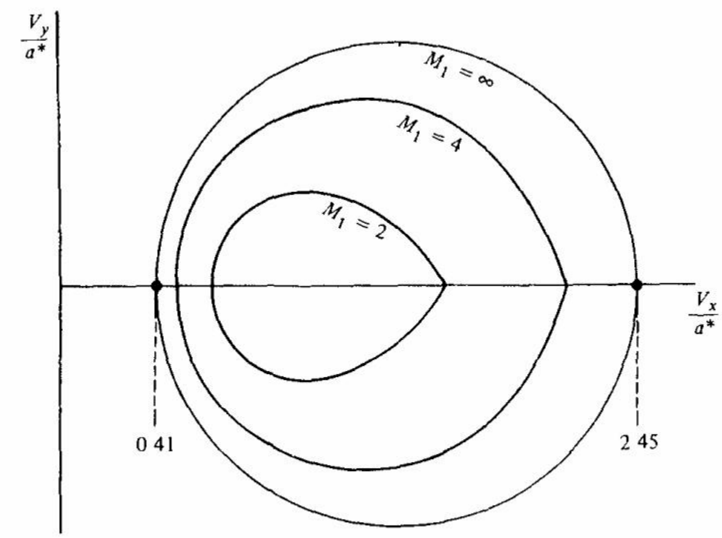

FIGURE 4.14
Shock polars for different Mach numbers

INTERSECTION OF SHOCKS OF THE SAME FAMILY

Consider the compression corner sketched in Fig. 4.20, where the supersonic flow in region 1 is deflected through an angle θ, with the consequent oblique shock wave emanating from point B. Now consider a Mach wave generated at point A ahead of the shock. Will this Mach wave interest the shock, or will it simply diverge, i.e., is μ_1 greater than or less than β? To find out, consider Eq. (4.7), which written in terms of velocities is

$$u_1 = V_1 \sin \beta$$

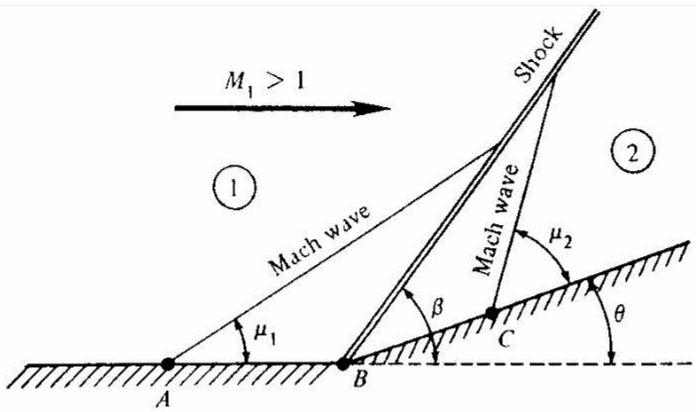

FIGURE 4.20
Mach waves ahead of and behind a shock wave

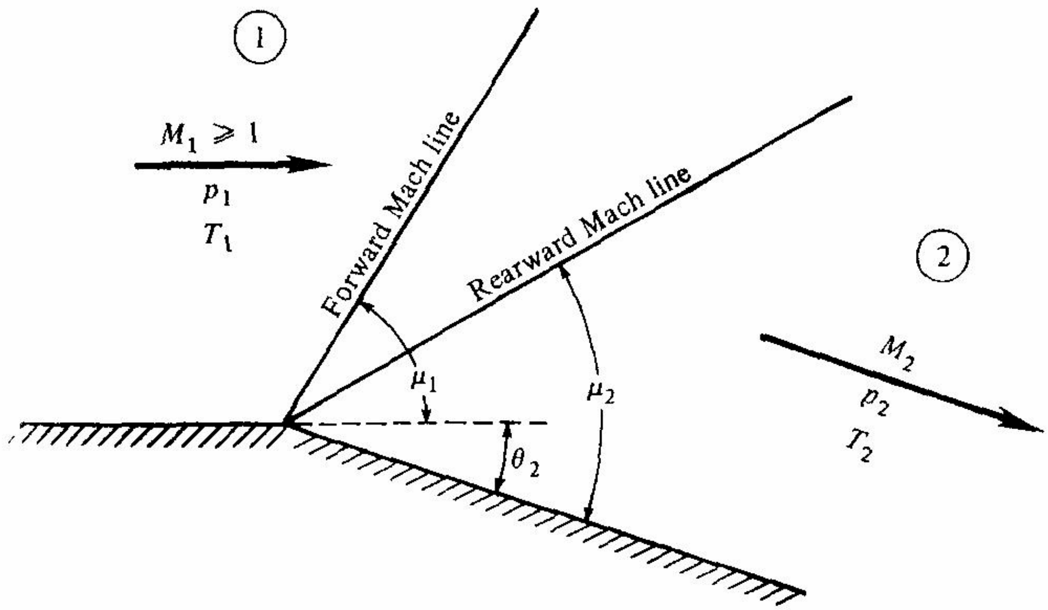

FIGURE 4.27
Prandtl-Meyer **expansion**

An expansion wave emanating from a sharp convex corner such as sketched in Figs. 4.1*b* and 4.27 is called a *centered* expansion fan. Moreover, because Prandtl in 1907, followed by Meyer in 1908, first worked out the theory for such a supersonic flow, it is denoted as a *Prandtl-Meyer expansion wave*.

The quantitative problem of a Prandtl-Meyer expansion wave can be stated as follows (referring to Fig. 4.27): For a given M_1, p_1, T_1, and θ_2, calculate M_2, p_2, and T_2. The analysis can be started by considering the infinitesimal changes across a very weak wave (essentially a Mach wave) produced by an infinitesimally small flow deflection, $d\theta$, as illustrated in Fig. 4 28 From the law of sines,

$$\frac{V + dV}{V} = \frac{\sin(\pi/2 + \mu)}{\sin(\pi/2 - \mu - d\theta)} \tag{4.24}$$

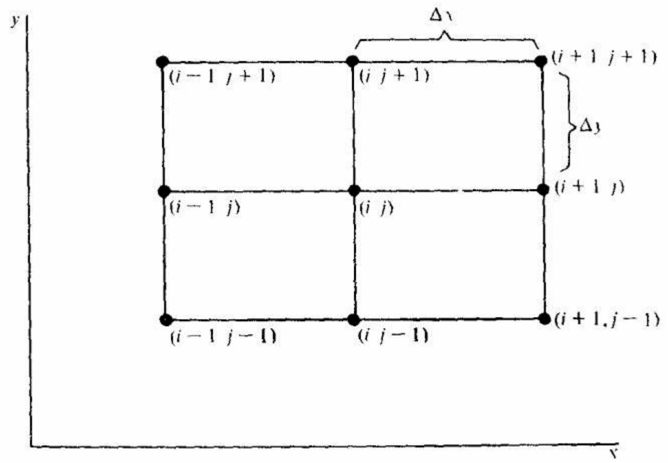

FIGURE 11.1
Rectangular finite-difference grid

SATHYABAMA
INSTITUTE OF SCIENCE AND TECHNOLOGY
(DEEMED TO BE UNIVERSITY)
Accredited "A" Grade by NAAC | 12B Status by UGC | Approved by AICTE
www.sathyabama.ac.in

SCHOOL OF MECHANICAL ENGINEERING
DEPARTMENT OF AERONAUTICAL ENGINEERING

AERODYNAMICS – II

SAE1301

UNIT – III FLOW THROUGH DUCTS – SAE1301

ONE-DIMENSIONAL FLOW WITH HEAT ADDITION

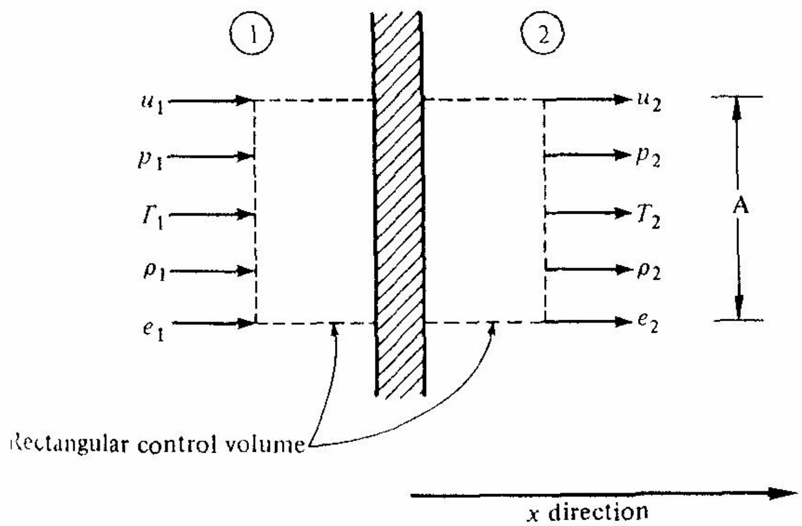

FIGURE 3 5
Rectangular control volume for one-dimensional flow

Consider again Fig 3 5, which illustrates a control volume for one-dimensional flow Inside this control volume some action is occurring which causes the flow properties in region 2 to be different than in region 1. In the previous sections, this action has been due to a normal shock wave, where the large gradients inside the shock structure ultimately result in an increase in entropy via the effects of viscosity and thermal conduction. However, these effects are taking place inside the control volume in Fig. 3.5 and therefore the governing normal shock equations relating conditions in regions 1 and 2 did not require explicit terms accounting for friction and thermal conduction.

The action occurring inside the control volume in Fig. 3.5 can be caused by effects other than a shock wave For example, if the flow is through a duct, friction between the moving fluid and the stationary walls of the duct causes changes between regions 1 and 2. This can be particularly important in long pipelines transferring gases over miles of land, for example. Another source of change in a one-dimensional flow is heat addition If heat is added to or taken away from the gas inside the control volume in Fig 3.5, the properties in region 2 will be different than those in region 1. This is a governing phenomenon in turbojet and ramjet engine burners, where heat is added in the form of fuel-air combustion. It also has an important effect on the supersonic flow in the cavities of modern gas dynamic and chemical lasers, where heat is effectively added by chemical reactions and molecular vibrational energy deactivation. Another examble would be the heat added to an absorbing gas by an intense beam of radiation; such an idea has been suggested for laser-heated wind tunnels. In general, therefore, changes in a one-dimensional flow can be created by both friction and heat addition without the presence of a shock wave.

Consider the one-dimensional flow in Fig. 3.5, with heat addition (or extraction) taking place between regions 1 and 2. The governing equations are repeated here for convenience,

$$\rho_1 u_1 = \rho_2 u_2$$

$$p_1 + \rho_1 u_1^2 = p_2 + \rho_2 u_2^2$$

$$h_1 + \frac{u_1^2}{2} + q = h_2 + \frac{u_2^2}{2}$$

If conditions in region 1 are known, then for a specified amount of heat added per unit mass, q, these equations along with the appropriate equations of state can be solved for conditions in region 2 In general, a numerical solution is required. However, for the specific case of a calorically perfect gas, closed-form analytical expressions can be obtained—just as in the normal shock problem. Therefore, the remainder of this section will deal with a calorically perfect gas.

$$h_1 + \frac{u_1^2}{2} + q = h_2 + \frac{u_2^2}{2}$$

Solving the above energy equation for q with h = C_pT we get,

$$q = \left(c_p T_2 + \frac{u_2^2}{2}\right) - \left(c_p T_1 + \frac{u_1^2}{2}\right)$$

From the definition of total temperature, the terms on the right-hand side of the above equation simply result in

$$\boxed{q = c_p T_{o_2} - c_p T_{o_1} = c_p\left(T_{o_2} - T_{o_1}\right)}$$

The above equation clearly indicates that the effect of heat addition is to directly change the total temperature of the flow. If heat is added, T_o increases; if heat is extracted, T_o decreases.

Let us proceed to find the ratios of properties between regions 1 and 2 in terms of the Mach numbers M_1 and M_2. We have,

$$\boxed{p_1 + \rho_1 u_1^2 = p_2 + \rho_2 u_2^2}$$

Noting that

$$\rho u^2 = \rho a^2 M^2 = \rho \frac{\gamma p}{\rho} M^2 = \gamma p M^2$$

We obtain,

$$p_2 - p_1 = \rho_1 u_1^2 - \rho_2 u_2^2 = \gamma p_1 M_1^2 - \gamma p_2 M_2^2$$

[redacted]

Hence,

$$\boxed{\frac{p_2}{p_1} = \frac{1 + \gamma M_1^2}{1 + \gamma M_2^2}}$$

Also, from the perfect gas equation of state and the below continuity equation,

$$\boxed{\rho_1 u_1 = \rho_2 u_2}$$

We get,

$$\frac{T_2}{T_1} = \frac{p_2}{p_1}\frac{\rho_1}{\rho_2} = \frac{p_2}{p_1}\frac{u_2}{u_1}$$

$$\boxed{a = \sqrt{\gamma R T}}$$

From the above equation for velocity of sound and the definition of Mach number, we get

$$\frac{u_2}{u_1} = \frac{M_2}{M_1}\frac{a_2}{a_1} = \frac{M_2}{M_1}\left(\frac{T_2}{T_1}\right)^{1/2}$$

Using the above equations and substituting the values of P_2/P_1, and u_2/u_1 in T_2/T_1 we get,

$$\boxed{\frac{T_2}{T_1} = \left(\frac{1 + \gamma M_1^2}{1 + \gamma M_2^2}\right)^2 \left(\frac{M_2}{M_1}\right)^2}$$

Since $\rho_2/\rho_1 = (p_2/p_1)(T_1/T_2)$,

We get,

$$\boxed{\frac{\rho_2}{\rho_1} = \left(\frac{1 + \gamma M_2^2}{1 + \gamma M_1^2}\right)\left(\frac{M_1}{M_2}\right)^2}$$

We have

$$\boxed{\frac{p_o}{p} = \left(1 + \frac{\gamma - 1}{2} M^2\right)^{\gamma/(\gamma-1)}}$$

$$\boxed{\frac{p_2}{p_1} = \frac{1 + \gamma M_1^2}{1 + \gamma M_2^2}}$$

The ratio of total pressures is obtained directly from the above two equations,

$$\boxed{\frac{p_{o_2}}{p_{o_1}} = \frac{1 + \gamma M_1^2}{1 + \gamma M_2^2}\left(\frac{1 + \dfrac{\gamma - 1}{2}M_2^2}{1 + \dfrac{\gamma - 1}{2}M_1^2}\right)^{\gamma/(\gamma-1)}}$$

We have,

$$\boxed{\frac{T_o}{T} = 1 + \frac{\gamma - 1}{2}M^2}$$

$$\boxed{\frac{T_2}{T_1} = \left(\frac{1 + \gamma M_1^2}{1 + \gamma M_2^2}\right)^2 \left(\frac{M_2}{M_1}\right)^2}$$

The ratio of total temperatures is obtained directly from the above equations,

$$\boxed{\frac{T_{o_2}}{T_{o_1}} = \left(\frac{1 + \gamma M_1^2}{1 + \gamma M_2^2}\right)^2 \left(\frac{M_2}{M_1}\right)^2 \left(\frac{1 + \frac{\gamma - 1}{2} M_2^2}{1 + \frac{\gamma - 1}{2} M_1^2}\right)}$$

Finally, the entropy change can be found from the below equation with the above derived equations for T_2/T_1 and P_2/P_1 .

$$\boxed{s_2 - s_1 = c_p \ln \frac{T_2}{T_1} - R \ln \frac{p_2}{p_1}}$$

$$\boxed{\frac{p_2}{p_1} = \frac{1 + \gamma M_1^2}{1 + \gamma M_2^2}} \tag{3 78}$$

$$\boxed{\frac{T_2}{T_1} = \left(\frac{1 + \gamma M_1^2}{1 + \gamma M_2^2}\right)^2 \left(\frac{M_2}{M_1}\right)^2} \tag{3.81}$$

$$\boxed{\frac{\rho_2}{\rho_1} = \left(\frac{1 + \gamma M_2^2}{1 + \gamma M_1^2}\right) \left(\frac{M_1}{M_2}\right)^2} \tag{3 82}$$

$$\boxed{\frac{p_{o_2}}{p_{o_1}} = \frac{1 + \gamma M_1^2}{1 + \gamma M_2^2} \left(\frac{1 + \frac{\gamma - 1}{2} M_2^2}{1 + \frac{\gamma - 1}{2} M_1^2}\right)^{\gamma/(\gamma - 1)}} \tag{3.83}$$

$$\boxed{\frac{T_{o_2}}{T_{o_1}} = \left(\frac{1 + \gamma M_1^2}{1 + \gamma M_2^2}\right)^2 \left(\frac{M_2}{M_1}\right)^2 \left(\frac{1 + \frac{\gamma - 1}{2} M_2^2}{1 + \frac{\gamma - 1}{2} M_1^2}\right)} \tag{3.84}$$

For convenience of calculation, we use sonic flow as a reference condition. Let $M_1 = 1$, the corresponding flow properties are denoted by $p_1 = p^*$, $T_1 = T^*$, $\rho_1 = \rho^*$, $p_{o_1} = p_o^*$, and $T_{o_1} = T_o^*$ The flow properties at any other value of M are then obtained by inserting $M_1 = 1$ and $M_2 = M$ into Eq (3.78) and Eqs (3 81) to (3.84), yielding

$$\frac{p}{p^*} = \frac{1 + \gamma}{1 + \gamma M^2}$$

$$\frac{T}{T^*} = M^2 \left(\frac{1 + \gamma}{1 + \gamma M^2} \right)^2$$

$$\frac{\rho}{\rho^*} = \frac{1}{M^2} \left(\frac{1 + \gamma M^2}{1 + \gamma} \right)$$

$$\frac{p_o}{p_o^*} = \frac{1 + \gamma}{1 + \gamma M^2} \left[\frac{2 + (\gamma - 1) M^2}{\gamma + 1} \right]^{\gamma/(\gamma - 1)}$$

$$\frac{T_o}{T_o^*} = \frac{(\gamma + 1) M^2}{(1 + \gamma M^2)^2} \left[2 + (\gamma - 1) M^2 \right]$$

Example 3.8. Air enters a constant-area duct at $M_1 = 0\ 2$, $p_1 = 1$ atm, and $T_1 = 273$ K Inside the duct, the heat added per unit mass is $q = 1\ 0 \times 10^6$ J/kg Calculate the flow properties M_2, p_2, T_2, ρ_2, T_{o_2}, and p_{o_2} at the exit of the duct

Solution. From Table A.1, for $M_1 = 0\ 2$ $T_{o_1}/T_1 = 1\ 008$ and $p_{o_1}/p_1 = 1\ 028$ Hence

$$T_{o_1} = 1\ 008 T_1 = 1\ 008(273) = 275\ 2 \text{ K}$$

$$p_{o_1} = 1\ 028 p_1 = 1\ 028(1 \text{ atm}) = 1\ 028 \text{ atm}$$

$$c_p = \frac{\gamma R}{\gamma - 1} = \frac{(1\ 4)(287)}{0\ 4} = 1005 \text{ J/kg K}$$

We have

$$\boxed{q = c_p T_{o_2} - c_p T_{o_1} = c_p\left(T_{o_2} - T_{o_1}\right)}$$

$$T_{o_2} = \frac{q}{c_p} + T_{o_1} = \frac{1\ 0 \times 10^6}{1005} + 275\ 2 = \boxed{1270 \text{ K}}$$

From Gas Table

From Table A 3, for $M_1 = 0\ 2$ $T_1/T^* = 0\ 2066$, $p_1/p^* = 2\ 273$, $p_{o_1}/p_o^* = 1\ 235$, and $T_{o_1}/T_o^* = 0\ 1736$ Hence

$$\frac{T_{o_2}}{T_o^*} = \frac{T_{o_2}}{T_{o_1}}\frac{T_{o_1}}{T_o^*} = \frac{1270}{275\ 2}(0\ 1736) = 0\ 8013$$

From **Table A.3**, this corresponds to $\boxed{M_2 = 0\ 58}$

Also from Table A3, **for** $M_2 = 0\ 58$· $T_2/T^* = 0.8955$, $p_2/p^* = 1\ 632$, p_{o_2}/p_o^* $= 1\ 083$ Hence

$$T_2 = \frac{T_2}{T^*}\frac{T^*}{T_1}T_1 = (0\ 8955)\left(\frac{1}{0\ 2066}\right)(273) = \boxed{1183\ \text{K}}$$

$$p_2 = \frac{p_2}{p^*}\frac{p^*}{p_1}p_1 = 1\ 632\frac{1}{2\ 273}1\ \text{atm} = \boxed{0\ 718\ \text{atm}}$$

$$p_{o_2} = \frac{p_{o_2}}{p_o^*}\frac{p_o^*}{p_{o_1}}p_{o_1} = 1\ 083\frac{1}{1\ 235}1\ 028 = \boxed{0\ 902\ \text{atm}}$$

Since 1 atm $= 1\ 01 \times 10^5\ \text{N/m}^2$,

$$\rho_2 = \frac{p_2}{RT_2} = \frac{(0.718)(1\ 01 \times 10^5)}{(278)(1183)} = \boxed{0\ 214\ \text{kg/m}^3}$$

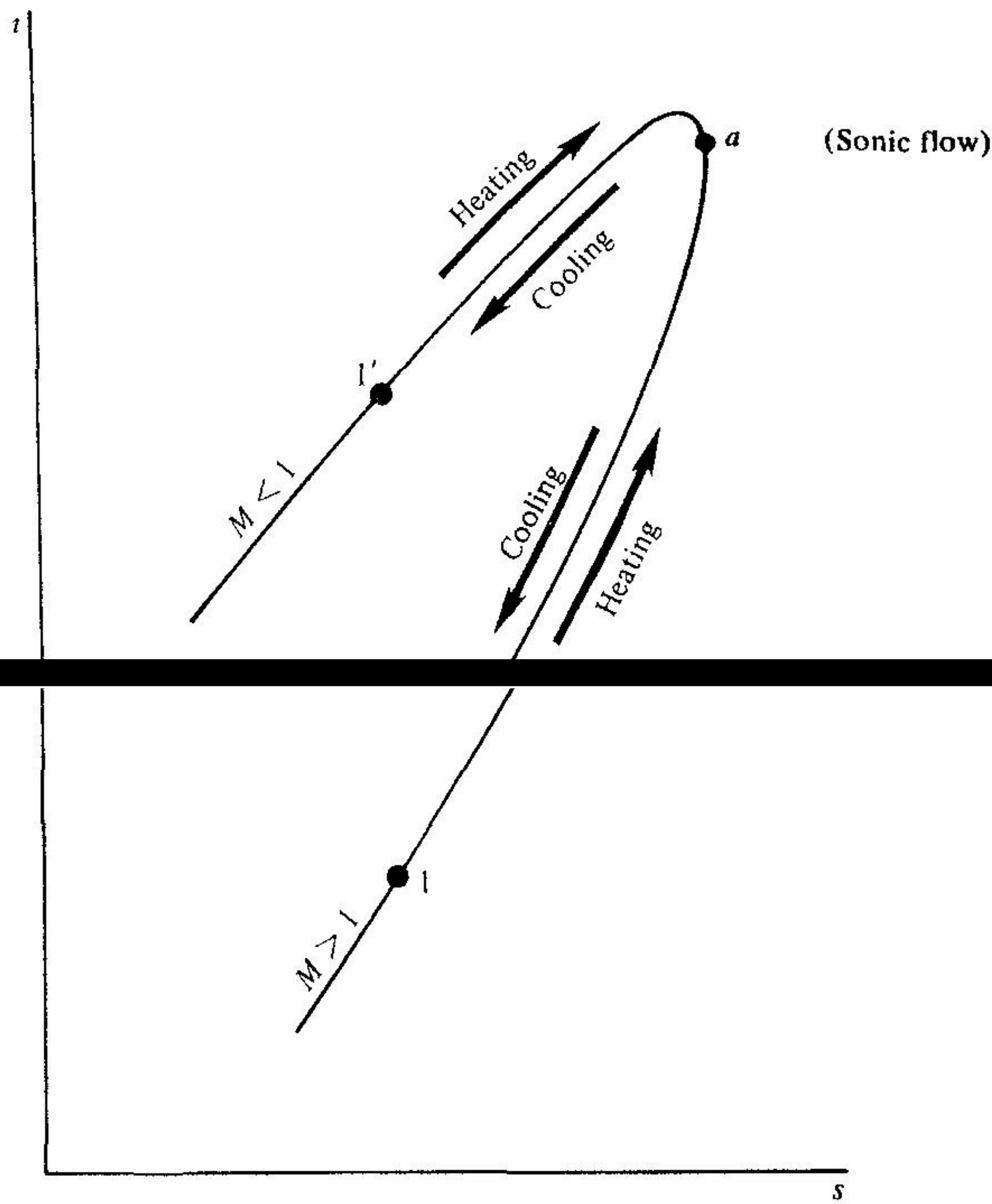

FIGURE 3.12
The Rayleigh curve

From the above, it is important to note that heat addition always drives the Mach numbers toward 1, decelerating a supersonic flow and accelerating a subsonic flow. This is emphasized in Fig. 3.12, which is a Mollier diagram (enthalpy versus entropy) of the one-dimensional heat-addition process. The curve in Fig. 3.12 is called the *Rayleigh curve*, and is drawn for a set of given initial conditions. If the conditions in region 1 are given by point 1 in Fig. 3.12, then the particular Rayleigh curve through point 1 is the locus of all possible states in region 2. Each point on the curve corresponds to a different value of q added or taken away. Point a corresponds to maximum entropy, also at point a the flow is sonic. The lower branch of the Rayleigh curve below point a corresponds to supersonic flow; the upper branch above point a corresponds to subsonic flow. If the flow in region 1 of Fig. 3.5 is supersonic and corresponds to point 1 in Fig. 3.12, then heat addition will cause conditions in region 2 to move closer to point a, with a consequent decrease of Mach number towards unity. As q is made larger, conditions in region 2 get closer and closer to point a. Finally, for a certain value of q, the flow will become sonic in region 2. For this condition, the flow is said to be *choked*, because any further increase in q is not possible without a drastic revision of the upstream conditions in region 1. For example, if the initial supersonic conditions in region 1 were obtained by expansion through a supersonic nozzle, and if a value of q is added to the flow above that allowed for attaining Mach 1 in region 2, then a normal shock will form inside the nozzle and conditions in region 1 will suddenly become subsonic

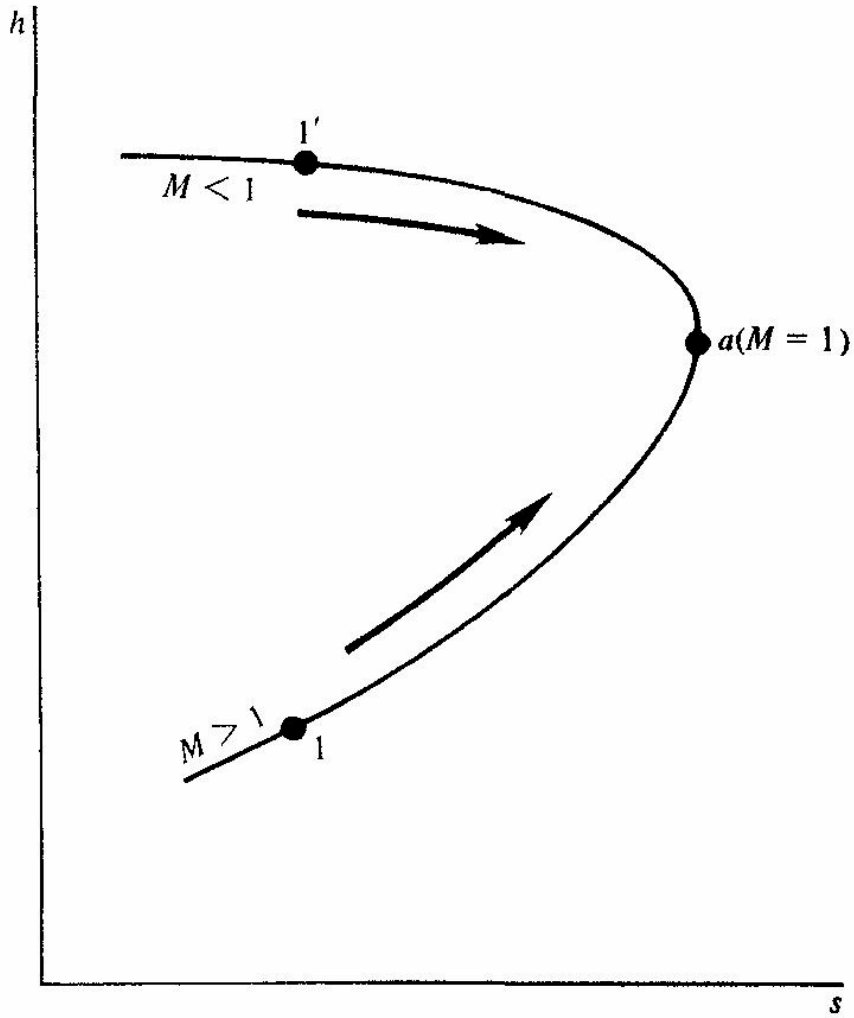

FIGURE 3.14
The Fanno curve

From the above, note that friction always drives the Mach number toward 1, decelerating a supersonic flow and accelerating a subsonic flow. This is emphasized in Fig 3 14, which is a Mollier diagram of one-dimensional flow with friction. The curve in Fig 3.14 is called the *Fanno curve*, and is drawn for a set of given initial conditions. Point a corresponds to maximum entropy, where the flow is sonic. This point splits the Fanno curve into subsonic (upper) and supersonic (lower) portions. If the inlet flow is supersonic and corresponds to point 1 in Fig 3.14, then friction causes the downstream flow to move closer to point a, with a consequent decrease of Mach number towards unity Each point on the curve between points 1 and a corresponds to a certain duct length L As L is made larger, the conditions at the exit move closer to point a Finally, for a certain value of L, the flow becomes sonic For this condition, the flow is *choked*, because any further increase in L is not possible without a drastic revision of the inlet conditions. For example, if the inlet conditions at point 1 were obtained by expansion through a supersonic nozzle, and if L were larger than that allowed for attaining Mach 1 at the exit, then a normal shock would form inside the nozzle, and the duct inlet conditions would suddenly become subsonic

Example 3.9. Air enters a constant-area duct at $M_1 = 3$, $p_1 = 1$ atm, and $T_1 = 300$ K. Inside the duct, the heat added per unit mass is $q = 3 \times 10^5$ J/kg Calculate the flow properties M_2, p_2, T_2, ρ_2, T_{o_2}, and p_{o_2} at the exit of the duct

Also find how much heat per unit mass must be added to choke the flow.

Solution. From Table A 1, for $M_1 = 3$ $T_{o_1}/T_1 = 2\ 8$ Hence

$$T_{o_1} = 2\ 8(300) = 840 \text{ K}$$

$$c_p = \frac{\gamma R}{\gamma - 1} = \frac{(1\ 4)(287)}{0\ 4} = 1004\ 5 \text{ J/kg K}$$

From **Eq.** (3.77)

$$q = c_p\left(T_{o_2} - T_{o_1}\right)$$

Thus

$$T_{o_2} = \frac{q}{c_p} + T_{o_1} = \frac{3 \times 10^5}{1004\ 5} + 840 = \boxed{1139 \text{ K}}$$

From Table A 3, for $M_1 = 3$ $p_1/p^* = 0\ 1765$, $T_1/T^* = 0\ 2803$, and $T_{o_1}/T^* = 0\ 6540$ Hence

$$\frac{T_{o_2}}{T_o^*} = \frac{T_{o_2}}{T_{o_1}}\frac{T_{o_1}}{T_o^*} = \frac{1139}{840}(0\ 6540) = 0\ 8868$$

From Table A 3, for $T_{o_2}/T_o^* = 0\ 8868$ $M_2 = \boxed{1\ 58}$ Also from Table A 3, $p_2/p^* = 0\ 5339$ and $T_2/T^* = 0\ 7117$ Thus

$$p_2 = \frac{p_2}{p^*}\frac{p^*}{p_1}p_1 = 0\ 5339\left(\frac{1}{0\ 1765}\right)(1 \text{ atm}) = \boxed{3\ 025 \text{ atm}}$$

$$T_2 = \frac{T_2}{T^*}\frac{T^*}{T_1}T_1 = 0\ 7117\left(\frac{1}{0\ 2803}\right)(300) = \boxed{761\ 7 \text{ K}}$$

$$\rho_2 = \frac{p_2}{RT_2} = \frac{(3\ 025)(1\ 01 \times 10^5)}{(287)(761\ 7)} = \boxed{1\ 398 \text{ kg/m}^3}$$

Example-5.

Consider a point in a supersonic flow where the static pressure is 0.4 atm. When a Pitot tube is inserted in the flow at this point, the pressure measured by the Pitot tube is 3 atm. Calculate the Mach number at this point. Calculate the entropy change across the shock (Hint: Normal shock occurs in front of the Pitot tube).

Solution.

The pressure measured by a Pitot tube is the total pressure However, when the tube is inserted into a supersonic flow, a normal shock is formed a short distance ahead of the mouth of the tube. In this case, the Pitot tube is sensing the total pressure behind the normal shock.

Hence

$$\frac{p_{o_2}}{p_1} = \frac{3}{0\ 4} = 7\ 5$$

From Table A 2, for $p_{o_2}/p_1 = 7\ 5 \quad M_1 = \boxed{2\ 35}$ [redacted]

From Table A 2, for $M_1 = 2\ 35 \quad p_{o_2}/p_{o_1} = 0\ 5615$

Using the following equation,

$$\boxed{\ln\frac{p_{o_2}}{p_{o_1}}}$$ [redacted]

$$\frac{s_2 - s_1}{R} = -\ln\frac{p_{o_2}}{p_{o_1}} = -\ln(0\ 5615) = 0\ 577$$

$$s_2 - s_1 = 0\ 577R$$

Example-6:

A supersonic wind tunnel settling chamber expands air or Freon-21 through a nozzle from a pressure of 10 bar to 4 bar in the test section. Calculate the stagnation temperature to be maintained in the settling chamber to obtain a velocity of 500 m/s in the test section for,

(a) Air, Cp = 1.025 kJ/kg K, Cp = 0.735 kJ/ K

(b) Freon – 21, Cp = 0.785 kJ/kg K, Cv = 0.675 kJ/K

What is the test section Mach number in each case?

Ans: M (air) = 1.225

M (Freon) = 1.296

Example-7:

A nozzle in a wind tunnel gives a test-section Mach number of 2.0. air enters the nozzle from a large reservoir at 0.69 bar and 310 K. The cross-sectional area of the throat is 1000 cm^2 . Determine the following quantities for the tunnel for one dimensional isentropic flow:

(i) pressure, temperature and velocities at the throat and test section
(ii) area of cross-section of the test section
(iii) mass flow rate
(iv) power required to drive the compressure.

Solution:

Given: P_0 = 0.69 bar, T_0 = 310 K, A^* = 1000 cm^2

Find $\rho_0 = P_0/RT_0$, and a_0

From Gas table at M =1 (throat section)
Find P^*/P_0 , T^*/To, ρ^*/ρ_0

P^* = 0.365 bar (Ans.)
T^* = 258 K (Ans.)
ρ_* = 0.49 kg/m^3 (Ans.)

$C^* = a^*$ = 323 m/s (Ans.)

From Gas table at Mt = 2.0 (test section)
P/P0 = 0.128   P = 0.0885 bar (Ans.)

T/T0 = 0.555   T = 175 K (Ans.)
A/A* = 1.687; A = 1687 cm2
Velocity at test section = M a = 2 x 264 = 528 m/s (Ans.) Mass flow rate = 15.9 kg/s

Compressor work = mass flow rate x Cp x temperature drop

= 2182 kW

NORMAL, OBLIQUE SHOCKS AND EXPANSION WAVES

Prandtl equation and Rankine – Hugonoit relation, Normal shock equations, Pitot static tube, corrections for subsonic and supersonic flows, Oblique shocks and corresponding equations, Hodograph and pressure turning angle, shock polars, flow past wedges and concave corners, strong, weak and detached shocks, Raleigh and Fanno Flow. Flow past convex corners, Expansion hodograph, Reflection and interaction of shocks and expansion, waves, Families of shocks, Methods of Characteristics, Two dimensional supersonic nozzle contours.

From **Table A.3, for** $M_1 = 3.$ $p_{o_1}/p_o^* = 3\ 424$ For $M_2 = 1\ 58$: $p_{o_2}/p_o^* = 1\ 164$
Thus

$$\frac{p_{o_2}}{p_{o_1}} = \frac{p_{o_2}/p_o^*}{p_{o_1}/p_o^*} = \frac{1\ 164}{3\ 424} = 0\ 340$$

From **Table** A 1, For $M_1 = 3$: $p_{o_1}/p_1 = 36\ 73$ Hence

$$p_{o_2} = \frac{p_{o_2}}{p_{o_1}}\frac{p_{o_1}}{p_1}p_1 = (0\ 340)(36\ 73)(1\ \text{atm}) = \boxed{12\ 49\ \text{atm}}$$

Solution. From Example 3 9, $T_{o_1} = 840$ K Also from Table A 3, for $M_1 = 3$: $T_{o_1}/T_o^* = 0.6540$ Thus

$$T_o^* = \frac{T_{o_1}}{0\ 6540} = \frac{840}{0\ 6540} = 1284\ \text{K}$$

When the flow is choked, the Mach number at the end of the duct is $M_2 = 1$ Thus

$$T_{o_2} = T_o^* = 1284\ \text{K}$$

$$q = c_p\left(T_{o_2} - T_{o_1}\right) = (1004\ 5)(1284 - 840) = \boxed{4\ 46 \times 10^5\ \text{J/kg}}$$

SCHOOL OF MECHANICAL ENGINEERING
DEPARTMENT OF AERONAUTICAL ENGINEERING

AERODYNAMICS – II

SAE1301

UNIT – IV LINEARIZED THEORY – SAE1301

Small perturbation potential theory

LINEARIZED FLOW

Transport yourself back in time to the year 1940, and imagine that you are an aerodynamicist responsible for calculating the lift on the wing of a **high-performance fighter plane. You recognize that the airspeed is high enough so that the well-established incompressible flow techniques of the day will give inaccurate results. Compressibility must be taken into account. However, you also recognize that the governing equations for compressible flow are nonlinear, and that no general solution exists for these equations. Numerical solutions are out of the question! So, what do you do? The only practical recourse is to seek assumptions regarding the physics of the flow which will allow the governing equations to become linear, but which at the same time do not totally compromise the accuracy of the real problem. In turn, these linear equations can be attacked by conventional mathematical techniques.**

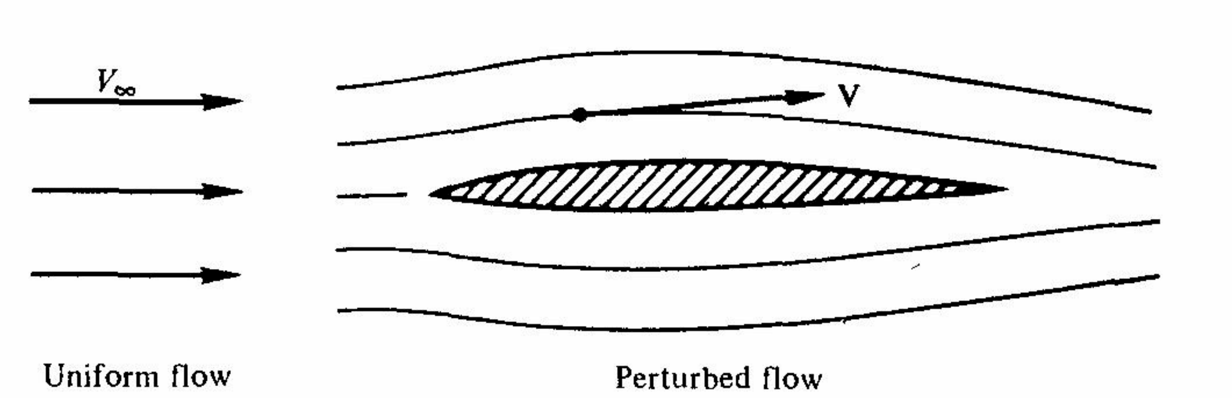

Comparison between uniform and perturbed flows

There are a number of practical aerodynamic problems where, on a physical basis, a uniform flow is changed, or perturbed, only slightly. One such example is the flow over a thin airfoil illustrated in in the above figure. The flow is characterized by only a small deviation of the flow from its original uniform state. The analyses of such flows are usually called small-perturbation theories. Small-perturbation theory is frequently (but not always) linear theory, an example is the acoustic theory, where the assumption of small perturbations allowed a linearized solution. Linearized solutions in compressible flow always contain the assumption of small perturbations, but small perturbations

do not always guarantee that the governing equations can be linearized.

LINEARIZED VELOCITY POTENTIAL EQUATION

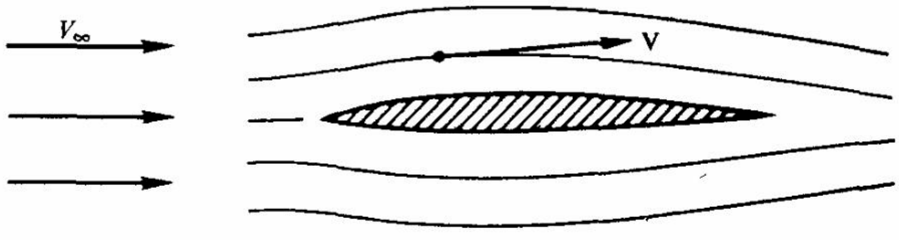

FIGURE 9.1
Comparison between uniform and perturbed flows

Consider a slender body immersed in a uniform flow, as sketched in Fig. 9.1. In the uniform flow, the velocity is V_∞, and is oriented in the x direction. In the perturbed flow, the local velocity is $\mathbf{V}$, where $\mathbf{V} = V_x\mathbf{i} + V_y\mathbf{j} + V_z\mathbf{k}$, and where

V_x, V_y, and V_z are now used to denote the x, y, and z components of velocity, respectively. In this chapter, u', v', and w' denote *perturbations* from the uniform flow, such that

$$V_x = V_\infty + u'$$

$$V_y = v'$$

$$V_z = w'$$

Here, u', v', and w' are the *perturbation velocities* in the x, y, and z directions, respectively. Also in the perturbed flow, the pressure, density, and temperature are p, ρ, and T, respectively. In the uniform stream, $V_x = V_\infty$, $V_y = 0$, and $V_z = 0$. Also in the uniform stream, the pressure, density, and temperature are p_∞, ρ_∞, and T_∞, respectively.

In terms of the velocity potential,

$$\nabla\Phi = \mathbf{V} = (V_\infty + u')\mathbf{i} + v\mathbf{j} + w\mathbf{k}$$

where Φ is now denoted as the "total velocity potential"

LINEARIZED PRESSURE COEFFICIENT

The pressure coefficient Cp is defined as

$$C_p \equiv \frac{p - p_\infty}{\frac{1}{2}\rho_\infty V_\infty^2}$$

where p is the local pressure, and p_∞, ρ_∞, and V_∞ are the pressure, density, and velocity, respectively, in the uniform free stream. The pressure coefficient is simply a non-dimensional pressure difference; it is extremely useful in fluid dynamics.

An alternative form of the pressure coefficient, convenient for compressible flow, can be obtained as follows

$$\tfrac{1}{2}\rho_\infty V_\infty^2 = \frac{1}{2}\frac{\gamma p_\infty}{\gamma p_\infty}\rho_\infty V_\infty^2 = \frac{\gamma}{2}p_\infty \frac{V_\infty^2}{a_\infty^2} = \frac{\gamma}{2}p_\infty M_\infty^2$$

Substitute it in the above equation, we get

$$C_p = \frac{p - p_\infty}{(\gamma/2)p_\infty M_\infty^2} = \frac{p_\infty(p/p_\infty - 1)}{(\gamma/2)p_\infty M_\infty^2}$$

$$\boxed{C_p = \frac{2}{\gamma M_\infty^2}\left(\frac{p}{p_\infty} - 1\right)}$$

The above equation is an alternative form of C_p expressed in terms of γ and M_∞ rather than ρ_∞, and V_∞. It is still an exact representation of C_p.

We now proceed to obtain an approximate expression for C_p which is consistent with linearized theory. Since the total enthalpy is constant,

$$h + \frac{V^2}{2} = h_\infty + \frac{V_\infty^2}{2}$$

For a calorically perfect gas, this becomes

$$T + \frac{V^2}{2c_p} = T_\infty + \frac{V_\infty^2}{2c_p}$$

$$T - T_\infty = \frac{V_\infty^2 - V^2}{2c_p} = \frac{V_\infty^2 - V^2}{2\gamma R/(\gamma - 1)}$$

$$\frac{T}{T_\infty} - 1 = \frac{\gamma - 1}{2} \frac{V_\infty^2 - V^2}{\gamma R T_\infty} = \frac{\gamma - 1}{2} \frac{V_\infty^2 - V^2}{a_\infty^2}$$

Since

$$V^2 = (V_\infty + u')^2 + v'^2 + w'^2$$

The above equation becomes,

$$\frac{T}{T_\infty} = 1 - \frac{\gamma - 1}{2a_\infty^2}\left(2u'V_\infty + u'^2 + v'^2 + w'^2\right)$$

Since the flow is isentropic, $p/p_\infty = (T/T_\infty)^{\gamma/(\gamma-1)}$,

and the above equation gives,

$$\frac{p}{p_\infty} = \left[1 - \frac{\gamma - 1}{2a_\infty^2}\left(2u'V_\infty + u'^2 + v'^2 + w'^2\right)\right]^{\gamma/(\gamma-1)}$$

or

$$\frac{p}{p_\infty} = \left[1 - \frac{\gamma - 1}{2}M_\infty^2\left(\frac{2u'}{V_\infty} + \frac{u'^2 + v'^2 + w'^2}{V_\infty^2}\right)\right]^{\gamma/(\gamma-1)}$$

The above equation is still an exact expression. However considering small perturbations:

$u'/V_\infty \ll 1$; u'^2/V_∞, v'^2/V_∞^2, and $w'^2/V_\infty^2 \lll 1$.

Hence the above equation is of the form

$$\frac{p}{p_\infty} = (1 - \varepsilon)^{\gamma/(\gamma-1)}$$

where ε is small. Hence, from the binomial expansion, neglecting higher-order terms,

$$\frac{p}{p_\infty} = 1 - \frac{\gamma}{\gamma - 1}\varepsilon + \cdots$$

Thus, the previous equation can be expressed in the form of the above equation as follows, neglecting higher-order terms:

$$\frac{p}{p_\infty} = 1 - \frac{\gamma}{2}M_\infty^2\left(\frac{2u'}{V_\infty} + \frac{u'^2 + v'^2 + w'^2}{V_\infty^2}\right) + \cdots$$

Substituting the above equation in the below equation,

$$\boxed{C_p = \frac{2}{\gamma M_\infty^2}\left(\frac{p}{p_\infty} - 1\right)}$$

We get,

$$C_p = \frac{2}{\gamma M_\infty^2}\left[1 - \frac{\gamma}{2}M_\infty^2\left(\frac{2u'}{V_\infty} + \frac{u'^2 + v'^2 + w'^2}{V_\infty^2}\right) + \cdots - 1\right]$$

$$= -\frac{2u'}{V_\infty} - \frac{u'^2 + v'^2 + w'^2}{V_\infty^2} + \cdots$$

Since u'^2/V_∞^2, v'^2/V_∞^2, and $w'^2/V_\infty^2 \lll 1$,

The above equation becomes,

$$\boxed{C_p = -\frac{2u'}{V_\infty}}$$

The above equation gives the linearized pressure coefficient, valid for small perturbations. Note its particularly simple form; the linearized pressure

coefficient depends only on the x component of the perturbation velocity.

Prandtl-Glauert rule

It is a similarity rule, which relates incompressible flow over a given two-dimensional profile to subsonic compressible flow over the same profile.

$$\boxed{C_p = \frac{C_{p_0}}{\sqrt{1 - M_\infty^2}}}$$

where C_{p0} is the incompressible pressure coefficient.

The above equation is called the Prandtl-Glauert rule.

Consider the compressible subsonic flow over a thin airfoil at small angle of attack (hence small perturbations), as sketched in the Fig 9.2 (pp.259). The usual inviscid flow boundary condition must hold at the surface, i e., the flow velocity must be

tangent to the surface. Referring to Fig. 9 2, at the surface this boundary condition is

$$\frac{df}{dx} = \frac{v'}{V_\infty + u'} = \tan\theta$$

We have the linearized perturbation-velocity potential equation.

$$\boxed{(1 - M_\infty^2)\frac{\partial^2\phi}{\partial x^2} + \frac{\partial^2\phi}{\partial y^2} + \frac{\partial^2\phi}{\partial z^2} = 0}$$

Note that this is an approximate equation and no longer represent the exact physics of the flow.

1. **The perturbations must be small.**
2. **Transonic flow 0.8 $\leq$ M_∞ $\leq$ 1.2) is excluded.**
3. **Hypersonic flow (M_∞ $\geq$ 5) is excluded.**

This equation is valid for subsonic and supersonic flow only. However, this equation has the striking advantage that it is linear.

In summary, we have demonstrated that subsonic and supersonic flows lend themselves to

approximate, linearized theory for the case of irrotational, isentropic flow with small perturbations. In contrast, transonic and hypersonic flows cannot be linearized, even with small perturbations. This is another example of the consistency of nature. Note some of the physical problems associated with transonic flow (mixed subsonic-supersonic regions with possible shocks, and extreme sensitivity to geometry changes at sonic conditions) and with hypersonic flow (strong shock waves close to the geometric boundaries, i e., thin shock layers, as well as high enthalpy, and hence high-temperature conditions in the flow). Just on an intuitive basis, we would expect such physically complicated flows to be inherently nonlinear. For the remainder of this chapter, we will consider linear flows only; thus, we will deal with subsonic and supersonic flows.

$$\boxed{C_p = \frac{C_{p_o}}{\sqrt{1 - M_\infty^2}}} \tag{9.36}$$

Equation (9.36) is called the *Prandtl-Glauert* rule; it is a similarity rule which relates *incompressible* flow over a given two-dimensional profile to *subsonic compressible* flow over the *same* profile. Moreover, consider the aerodynamic lift L and moment M on this airfoil We define the lift and moment coefficients, C_l and C_M, respectively, as

$$C_L = \frac{L}{\frac{1}{2}\rho_\infty V_\infty^2 S}$$

$$C_M = \frac{M}{\frac{1}{2}\rho_\infty V_\infty^2 Sl}$$

$$\boxed{C_L = \frac{C_{L_o}}{\sqrt{1 - M_\infty^2}}} \tag{9.37a}$$

$$\boxed{C_M = \frac{C_{M_o}}{\sqrt{1 - M_\infty^2}}} \tag{9.37b}$$

Equations 9.37*a* and 9.37*b* are also called the *Prandtl-Glauert rule*. They are exceptionally practical aerodynamic formulas for the approximate compressibility correction to low-speed lift and moments on slender two-dimensional aerodynamic shapes. Note that the effect of compressibility is to increase the magnitudes of C_l and C_M.

XXX

In an effort to obtain an improved compressibility correction, Laitone (see Ref. 23) applied Eq (9.36) locally in the flow, i.e.,

$$C_p = \frac{C_{p_o}}{\sqrt{1 - M^2}}$$

where M is the local Mach number In turn, M can be related to M_∞ and the pressure coefficient through the isentropic flow relations. The resulting compressibility correction is

$$C_p = -\frac{C_{p_o}}{\sqrt{1 - M_\infty^2} + \left[M_\infty^2\left(1 + \frac{\gamma - 1}{2}M_\infty^2\right)\Big/2\sqrt{1 - M_\infty^2}\right]C_{p_o}} \tag{9.39}$$

Note that, as C_{p_o} becomes small, Eq. (9.39) approaches the Prandtl-Glauert rule.

Another compressibility correction that has been adopted widely is that due to von Karman and Tsien (see Refs. 24 and 25). Utilizing a hodograph solution of the nonlinear equations of motion along with a simplified "tangent gas" equation of state, the following result was obtained:

$$C_p = \frac{C_{p_o}}{\sqrt{1 - M_\infty^2} + \left(\dfrac{M_\infty^2}{1 + \sqrt{1 - M_\infty^2}}\right)\dfrac{C_{p_o}}{2}} \tag{9.40}$$

Equation (9.40) is called the *Karman-Tsien rule*.

SCHOOL OF MECHANICAL ENGINEERING
DEPARTMENT OF AERONAUTICAL ENGINEERING

AERODYNAMICS – II

SAE1301

UNIT – V METHOD OF CHARACTERISTICS – SAE1301

METHOD OF CHARACTERISTICS

Method of characteristics is a numerical method for solving the full nonlinear equations of motion for inviscid, irrotational flow. If we are looking for better accuracy of results than that obtained by using the approximate linearized equations, it is necessary to work out improved solutions, by including higher-order terms in the approximate equations or by considering the exact equations. However, in the latter case, it is rarely possible to get solutions in analytical form because of the nonlinear nature of the equations. We must then resort to numerical techniques; the method of characteristics being one such technique.

11.2 PHILOSOPHY OF THE METHOD OF CHARACTERISTICS

Let us begin to obtain a feeling for the method of characteristics by considering again Fig. 11.1 and Eq (11.1). Neglect the second-order term in Eq (11 1), and write

$$u_{i+1,j} = u_{i,j} + \left(\frac{\partial u}{\partial x}\right)_{i,j} \Delta x + \cdots \tag{11 2}$$

The value of the derivative $\partial u/\partial x$ can be obtained from the general conservation equations. For example, consider a two-dimensional irrotational flow, so that Eq (8 17) yields, in terms of velocities,

$$\left(1 - \frac{u^2}{a^2}\right)\frac{\partial u}{\partial x} + \left(1 - \frac{v^2}{a^2}\right)\frac{\partial v}{\partial y} - \frac{2uv}{a^2}\frac{\partial u}{\partial y} = 0 \tag{11 3}$$

Solve Eq. (11.3) for $\partial u/\partial x$·

$$\frac{\partial u}{\partial x} = \frac{\dfrac{2uv}{a^2}\dfrac{\partial u}{\partial y} - \left(1 - \dfrac{v^2}{a^2}\right)\dfrac{\partial v}{\partial y}}{\left(1 - u^2/a^2\right)} \tag{11 4}$$

Now assume the velocity **V**, and hence u and v, is known at each point along a vertical line, $x = x_o$, as sketched in Fig 11 3· Specifically, the values of u and v are known at point (i, j), as well as above and below, at points $(i, j + 1)$ and $(i, j - 1)$ Hence, the y derivatives, $\partial u/\partial y$ and $\partial v/\partial y$, are known at point (i, j) (They can be calculated from finite-difference quotients, to be discussed later.) Consequently, the right-hand side of Eq (11.4) yields a number for $(\partial u/\partial x)_{i,j}$, which can be substituted into Eq (11.2) to calculate $u_{i+1,j}$ However, *there is one notable exception*· If the denominator of Eq (11 4) is zero, then

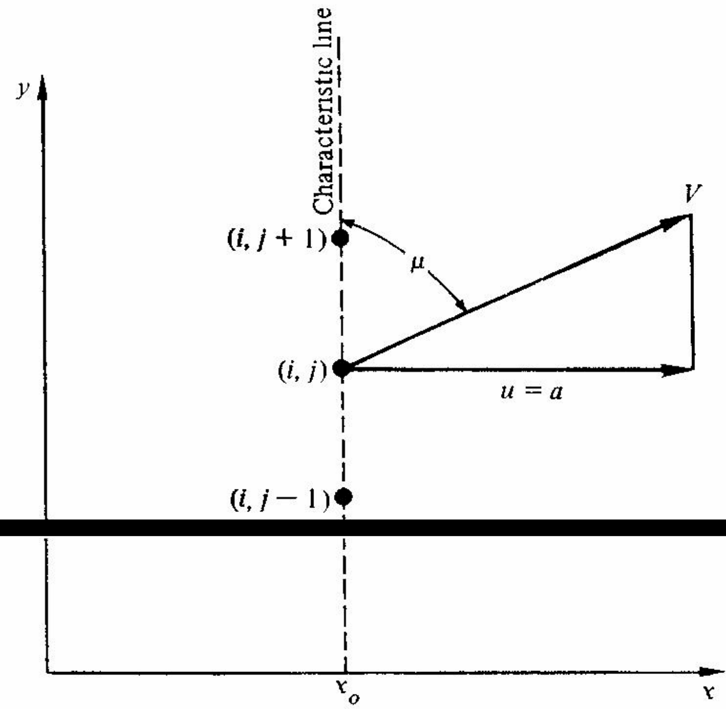

FIGURE 11 3
Illustration of the characteristic direction

$\partial u/\partial x$ is at least indeterminate, and may even be discontinuous. The denominator is zero when $u = a$, i.e., when the component of flow velocity perpendicular to $x = x_o$ is sonic, as shown in Fig. 11.3 Moreover, from the geometry of Fig 11.3, the angle μ is defined by $\sin \mu = u/V = a/V = 1/M$, i.e., μ is the *Mach angle*. The orientation of the x and y axes with respect to $\mathbf{V}$ in Fig. 11 3 is arbitrary, the germane aspect of the above discussion is that a line which makes a Mach angle with respect to the streamline direction at a point is also a line along which the derivative of u is indeterminate, and across which it may be discontinuous. We have just demonstrated that such lines exist, and that they are Mach lines. The choice of u was arbitrary in the above discussion. The derivatives of the other flow variables, p, ρ, T, v, etc., are also indeterminate along these lines Such lines are defined as *characteristic lines*

With the above in mind, we can now outline the general philosophy of the method of characteristics Consider a region of steady, supersonic flow in xy space. (For simplicity, we will initially deal with two-dimensional flow; extensions to three-dimensional flows will be discussed later.) This flowfield can be solved in three steps, as follows·

STEP 1. Find some particular lines (directions) in the xy space where *flow variables* (p, ρ, T, u, v, etc) are *continuous*, but along which the *derivatives* ($\partial p/\partial x$, $\partial u/\partial y$, etc) are *indeterminate*, and in fact across which the derivatives may even sometimes be discontinuous. As defined above, such lines in the xy space are called *characteristic lines.*

STEP 2. Combine the partial differential conservation equations in such a fashion that ordinary differential equations are obtained which hold *only along the characteristic lines* Such ordinary differential equations are called the *compatibility equations.*

STEP 3. Solve the compatibility equations step by step *along* the characteristic lines, starting from the given initial conditions at some point or region in the flow. In this manner, the complete flowfield can be mapped out along the characteristics. In general, the characteristic lines (sometimes referred to as the "characteristics net") depend on the flowfield, and the compatibility equations are a function of geometric location along the characteristic lines, hence, the characteristics and the compatibility equations must be constructed and solved simultaneously, step by step. An exception to this is two-dimensional irrotational flow, for which the compatibility equations become algebraic equations explicitly independent of geometric location This will be made clear in subsequent sections

As an analog to this discussion, the above philosophy is clearly exemplified in the unsteady, one-dimensional flow discussed in Chap. 7 Consider a centered expansion wave traveling to the left, as sketched in Fig 11 4 In Chap. 7, the governing partial differential equations were reduced to ordinary differential

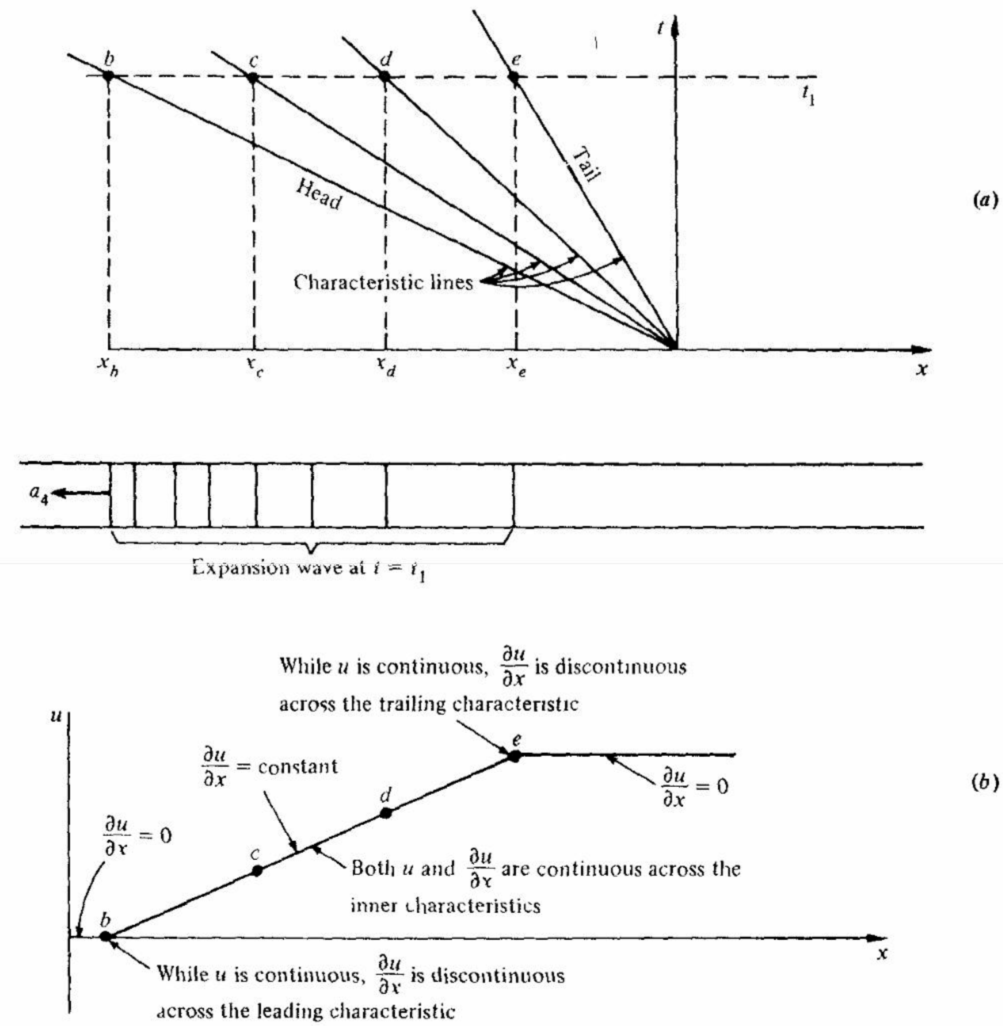

FIGURE 11 4
Relationship of characteristics in unsteady one-dimensional flow

equations (compatibility equations) which held only along certain lines in the xt plane that had slopes of $dx/dt = u \pm a$. The compatibility equations are Eqs. (7.65) and (7.66), and the lines were defined as characteristic lines in Sec. 7.6. These characteristics are sketched in Fig. 11 4a. However, in Chap. 7, we did not explicitly identify such characteristic lines with indeterminate or discontinuous derivatives. Nevertheless, this identification can be made by examining Eq (7 89), which gives $u = u(x, t)$ Consider a given time $t = t_1$, which is illustrated by the dashed horizontal line in Fig. 11.4a At time t_1, the head of the wave is located at x_b, and the tail at x_e Equation (7.89) for the mass motion u is evaluated at time t_1, as sketched in Fig. 11.4b. Note that at x_b the velocity is continuous, but $\partial u/\partial x$ is discontinuous across the leading characteristic. Similarly, at x_e, u is continuous but $\partial u/\partial x$ is discontinuous across the trailing characteristic. Hence, by examining Fig. 11 4a and b, we see that the characteristic lines identified in Chap. 7 are indeed consistent with the definition of characteristics given in the present chapter.

For more details Ref: Anderson

11.7 SUPERSONIC NOZZLE DESIGN

In order to expand an internal steady flow through a duct from subsonic to supersonic speed, we established in Chap. 5 that the duct has to be convergent-divergent in shape, as sketched in Fig 11 11a Moreover, we developed relations for the local Mach number, and hence the pressure, density, and temperature, as functions of local area ratio A/A^* However, these relations assumed quasi-one-dimensional flow, whereas, strictly speaking, the flow in Fig. 11.11a is two-dimensional. Moreover, the quasi-one-dimensional theory tells us nothing about the proper *contour* of the duct, i e , what is the proper variation of area with respect to the flow direction $A = A(x)$. If the nozzle contour is not proper, shock waves may occur inside the duct.

The method of characteristics provides a technique for properly designing the contour of a supersonic nozzle for shockfree, isentropic flow, taking into account the multidimensional flow inside the duct The purpose of this section is to illustrate such an application

The subsonic flow in the convergent portion of the duct in Fig 11.11a is accelerated to sonic speed in the throat region In general, because of the multidimensionality of the converging subsonic flow, the sonic line is gently curved. However, for most applications, we can assume the sonic line to be straight, as illustrated by the straight dashed line from a to b in Fig. 11.11a Downstream of the sonic line, the duct diverges. Let θ_w represent the angle of the duct wall with respect to the x direction. The section of the nozzle where θ_w is increasing is called the *expansion* section, here, expansion waves are generated and propagate across the flow downstream, reflecting from the opposite wall Point c is an inflection point of the contour, where $\theta_w = \theta_{w_{max}}$ Downstream of point c, θ_w decreases until the wall becomes parallel to the x direction at points d and f. The section from c to d is a "straightening" section specifically designed to cancel all the expansion waves generated by the expansion section For

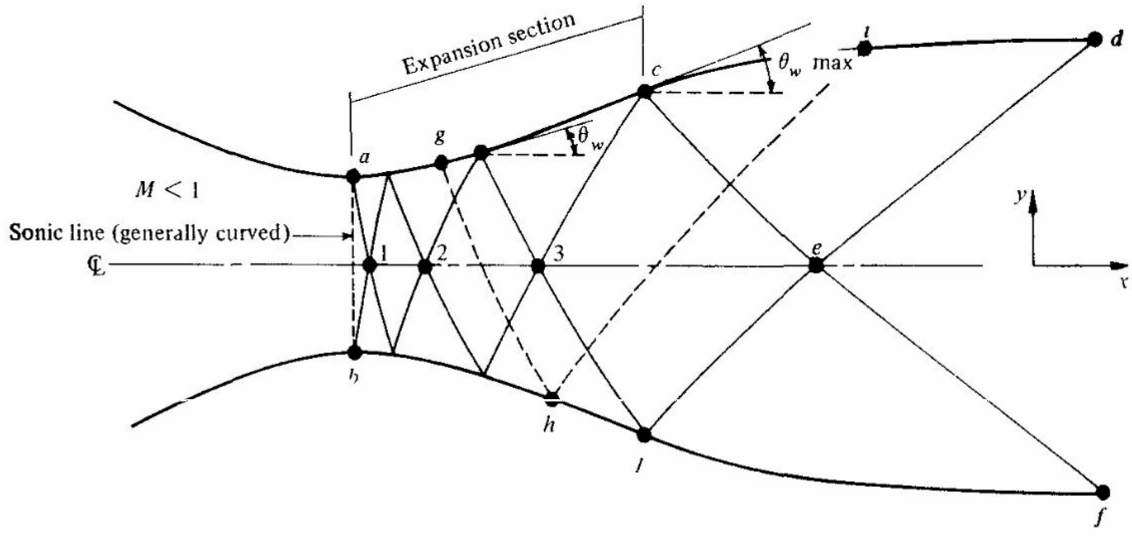

(a)

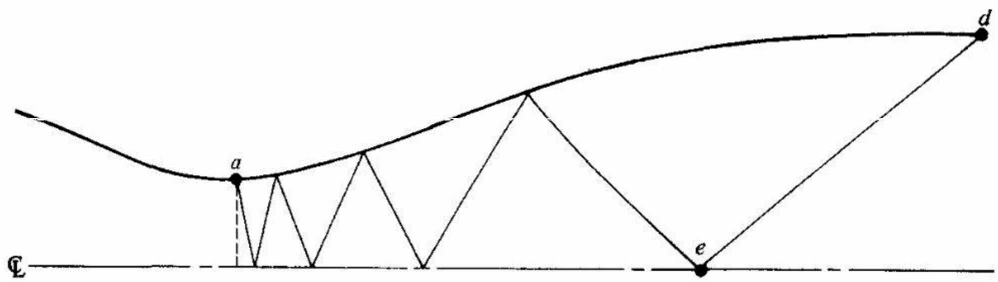

(b)

FIGURE 11.11
Schematic of supersonic nozzle design by the method of characteristics

example, as shown by the dashed line in Fig. 11.11a, the expansion wave generated at g and reflected at h is cancelled at i Also shown in Fig. 11.11a are the characteristic lines going through points d and f at the nozzle exit. These characteristics represent infinitesimal expansion waves in the nozzle, i.e., Mach waves. Tracing these two characteristics upstream, we observe multiple reflections up to the throat region. The area *acejb* is the expansion region of the nozzle, covered with both left- and right-running characteristics. Such a region with waves of both families is defined as a *nonsimple region* (analogous to the nonsimple waves described for unsteady one-dimensional flow in Sec 7.7). In this region, the characteristics are curved lines. In contrast, the regions *cde* and *jef* are covered by waves of only one family because the other family is cancelled at the wall. Hence, these are *simple regions*, where the characteristic lines are straight Downstream of *def*, the flow is uniform and parallel, at the desired Mach number Finally, due to the symmetry of the nozzle flow, the waves (characteristics) generated from the top wall act as if they are "reflected" from the centerline. This geometric ploy due to symmetry allows us to consider in our calculations only the flow above the centerline, as sketched in Fig. 11.11b.

Supersonic nozzles with gently curved expansion sections as sketched in Fig 11.11a and b are characteristic of wind tunnel nozzles where high-quality, uniform flow is desired in the test section (downstream of *def*) Hence, wind tunnel nozzles are long, with a relatively slow expansion By comparison, rocket nozzles are short in order to minimize weight Also, in cases where rapid expansions are desirable, such as the nonequilibrium flow in modern gasdynamic lasers (see Ref. 21), the nozzle length is as short as possible In such *minimum-length nozzles*, the expansion section in Fig. 11 11a is shrunk to a point, and the expansion takes place through a centered Prandtl-Meyer wave emanating from a sharp-corner throat with an angle $\theta_{w_{\max}}\ _{M_l}$, as sketched in Fig 11.12a The length of the supersonic nozzle, denoted as L in Fig 11 12a is the minimum value consistent with shockfree, isentropic flow. If the contour is made shorter than L, shocks will develop inside the nozzle.

Assume that the nozzles sketched in Figs 11.11a and 11 12a are designed for the same exit Mach numbers For the nozzle in Fig 11 11a with an arbitrary expansion contour ac, multiple reflections of the characteristics (expansion waves) occur from the wall along ac A fluid element moving along a streamline is constantly accelerated while passing through these multiple reflected waves In contrast, for the minimum-length nozzle shown in Fig 11 12a, the expansion contour is replaced by a sharp corner at point a. There are no multiple reflections and a fluid element encounters only two systems of waves—the right-running waves emanating from point a and the left-running waves emanating from point d. As a result, $\theta_{w_{\max},\ M_l}$ in Fig 11 12a must be larger than $\theta_{w_{\max}}$ in Fig 11 11a, although the exit Mach numbers are the same.

Let ν_M be the Prandtl-Meyer function associated with the design exit Mach number Hence, along the C_+ characteristic cb in Fig 11.12a, $\nu = \nu_M = \nu_c = \nu_b$. Now consider the C_- characteristic through points a and c At point c, from

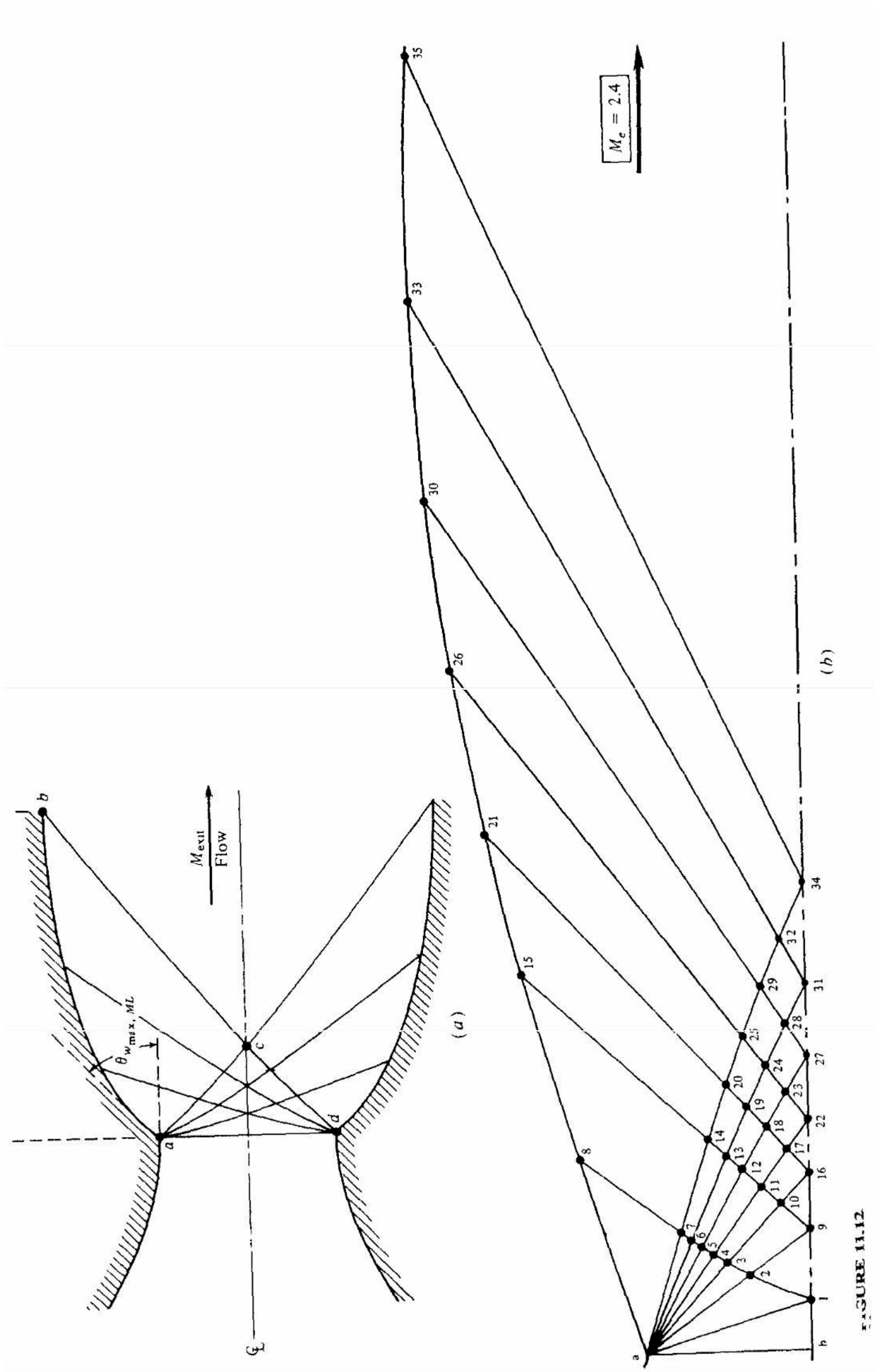

FIGURE 11.12

Eq. (11.20),

$$\theta_c + \nu_c = (K_-)_c \tag{11.28}$$

However, $\theta_c = 0$ and $\nu_c = \nu_M$. Hence, from Eq. (11.28),

$$(K_-)_c = \nu_M \tag{11.29}$$

At point a, along the same C_- characteristic ac, from Eq. (11.20),

$$\theta_{w_{\max},\, M_l} + \nu_a = (K_-)_a \tag{11.30}$$

Since the expansion at point a is a Prandtl-Meyer expansion from initially sonic conditions, we know from Sec. 4.13 that $\nu_a = \theta_{w_{\max},\, M_l}$. Hence, Eq. (11.30) becomes

$$\theta_{w_{\max},\, M_l} = \tfrac{1}{2}(K_-)_a \tag{11.31}$$

However, along the same C_- characteristic, $(K_-)_a = (K_-)_c$; hence Eq. (11.31) becomes

$$\theta_{w_{\max},\, M_l} = \tfrac{1}{2}(K_-)_c \tag{11.32}$$

Combining Eqs. (11.29) and (11.32), we have

$$\boxed{\theta_{w_{\max},\, M_l} = \frac{\nu_M}{2}} \tag{11.33}$$

Equation (11.33) demonstrates that, *for a minimum-length nozzle the expansion angle of the wall downstream of the throat is equal to one-half the Prandtl-Meyer function for the design exit Mach number*. For other nozzles such as that sketched in Fig. 11.11a, the maximum expansion angle is *less* than $\nu_M/2$

The shape of the finite-length expansion section in Fig. 11.11a can be somewhat arbitrary (within reason). It is frequently taken to be a circular arc with a diameter larger than the nozzle throat height However, once the shape of the expansion section is chosen, then its length and $\theta_{w_{\max}}$ are determined by the design exit Mach number These properties can be easily found by noting that the characteristic line from the end of the expansion section intersects the centerline at point e, where the local Mach number is the same as the design exit Mach number Hence, to find the expansion section length and $\theta_{w_{\max}}$, simply keep track of the centerline Mach number (at points 1, 2, 3, etc.) as you construct your characteristics solution starting from the throat region. When the centerline Mach number equals the design exit Mach number, this is point e. Then the expansion section is terminated at point c, which fixes both its length and the value of $\theta_{w_{\max}}$

CRITICAL MACH NUMBER

By definition, the critical Mach number M_{cr} is that free-stream Mach number at which sonic flow is first encountered on the airfoil.

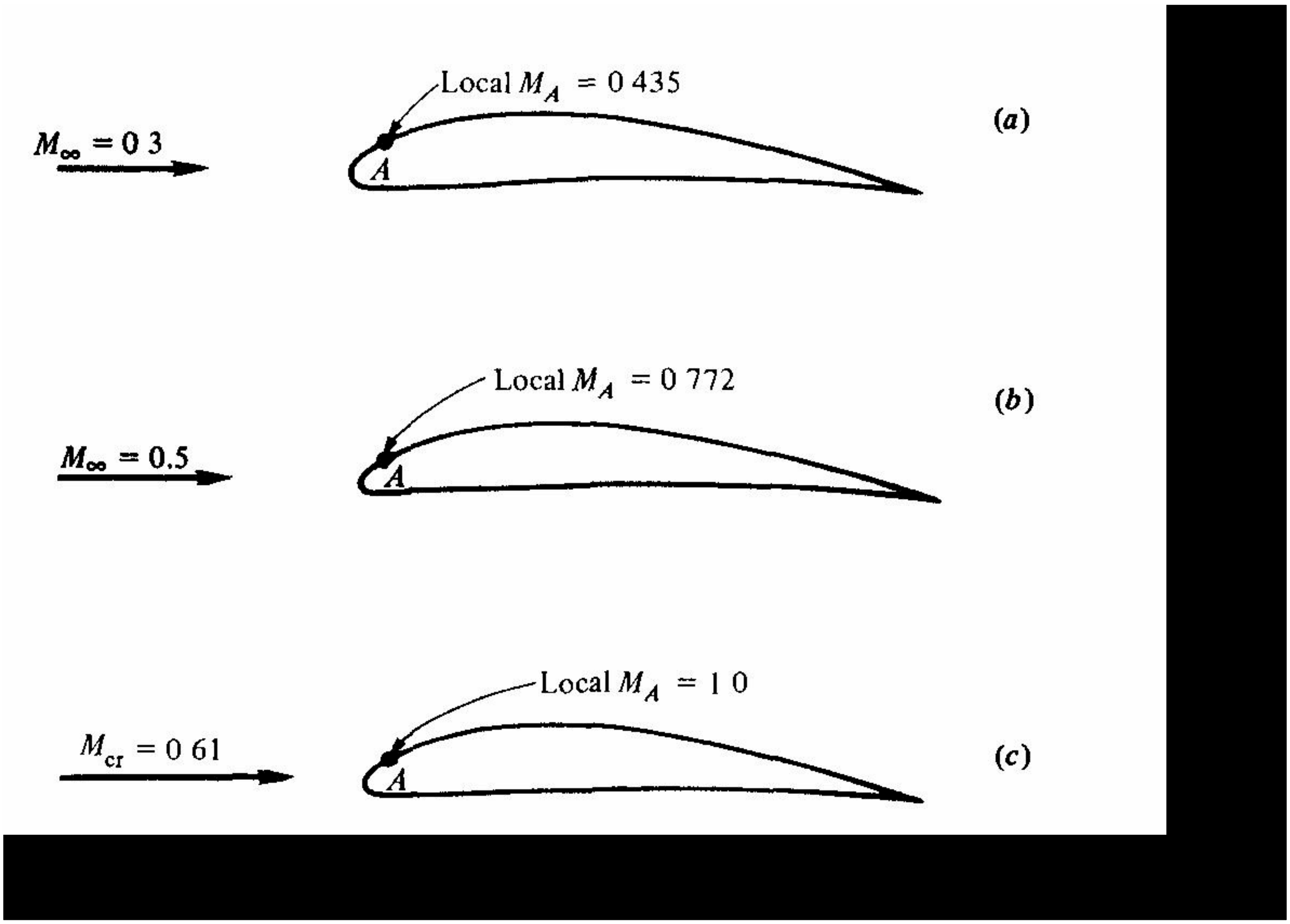

Fig. Definition of critical Mach number Point A is the location of minimum pressure on the top surface of the airfoil

The critical Mach number can be calculated as follows. Assuming isentropic flow throughout the flow field and using the following equation derived from the previous isentropic flow relationship, we get

$$\frac{p_A}{p_\infty} = \left(\frac{1 + \frac{\gamma - 1}{2} M_\infty^2}{1 + \frac{\gamma - 1}{2} M_A^2} \right)^{\gamma/(\gamma - 1)}$$

We have,

$$\boxed{C_p = \frac{2}{\gamma M_\infty^2} \left(\frac{p}{p_\infty} - 1 \right)}$$

Combining the above two equations the pressure coefficient at point A is

$$C_{pA} = \frac{2}{\gamma M_\infty^2}\left[\left(\frac{1 + \frac{\gamma - 1}{2} M_\infty^2}{1 + \frac{\gamma - 1}{2} M_A^2}\right)^{\gamma/(\gamma-1)} - 1\right]$$

From Eq. (9.54), for a given M_∞ the values of local pressure coefficient and local Mach number are uniquely related at any given point A. Now assume as before that point A is the minimum-pressure (hence maximum-velocity) point on the airfoil Furthermore, assume $M_A = 1$. Then, by definition, $M_\infty \equiv M_{cr}$ Also, for this case the value of the pressure coefficient is defined as the critical pressure coefficient $C_{p_{cr}}$. Setting $M_A = 1$, $M_\infty = M_{cr}$, and $C_p \equiv C_{p_{cr}}$ in Eq. (9 54), we obtain

$$\boxed{C_{p_{cr}} = \frac{2}{\gamma M_{cr}^2}\left[\left(\frac{1 + \frac{\gamma - 1}{2} M_{cr}^2}{1 + \frac{\gamma - 1}{2}}\right)^{\gamma/(\gamma-1)} - 1\right]}$$

Note that $C_{p_{cr}}$ is a unique function of M_{cr}; this variation is plotted as curve C in Fig. 9.14

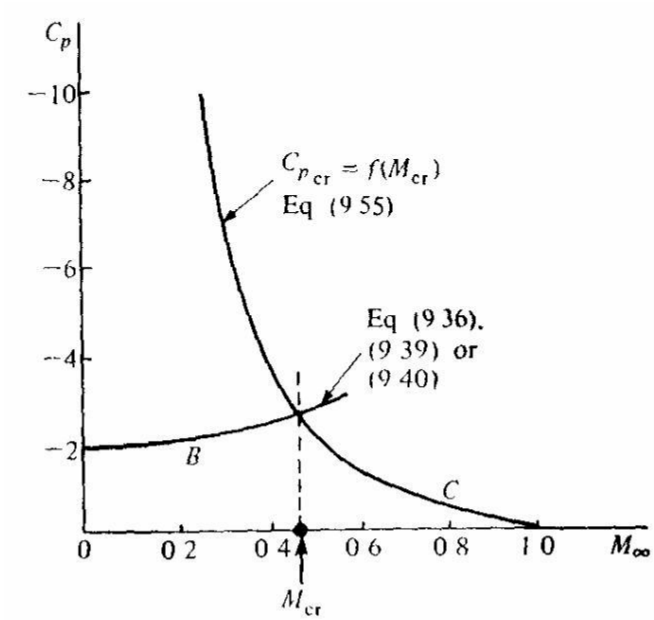

Fig.9.14 Calculation of critical Mach number (For more details Refer: Anderson)

Note in Fig 9.14 that curve C [from eq. for $C_{P_{cr}}$] is a result of the fundamental gas dynamics of the flow; it is unique, and does not depend on the size or shape of the airfoil. In contrast, curve B is different for different airfoils. For example, consider two airfoils, one thin and one thick. For the thin airfoil, the flow experiences only a mild expansion over the top surface, and hence Cp_0 is small. Combined with the chosen compressibility correction, curve B in Fig 9.14 is low on the graph, resulting in a high value of M_{cr}. For the thick airfoil, |Cp| is naturally larger because the flow experiences a stronger expansion over the top surface. Curve B is higher on the graph, resulting in a lower value of M_{cr}. Hence, an airfoil designed for a high critical Mach number must have a thin profile.

When the free-stream Mach number exceeds M_{cr}, a finite region of supersonic flow exists on the top surface of the airfoil. At a high enough subsonic Mach number, this embedded supersonic region will be terminated by a weak shock wave. The total pressure loss associated with the shock will be small, however, the adverse pressure gradient induced by the shock tends to separate the boundary layer on the top surface, causing a large pressure drag. The net result is a dramatic increase in drag. The free-stream Mach number at which the large drag rise begins is defined as the drag-divergence Mach number, it is always slightly larger than M_{cr} The massive increase in drag encountered at the drag-divergence Mach number is the technical base of the "sound barrier" which was viewed with much trepidation before 1947.

Drag divergence Mach number

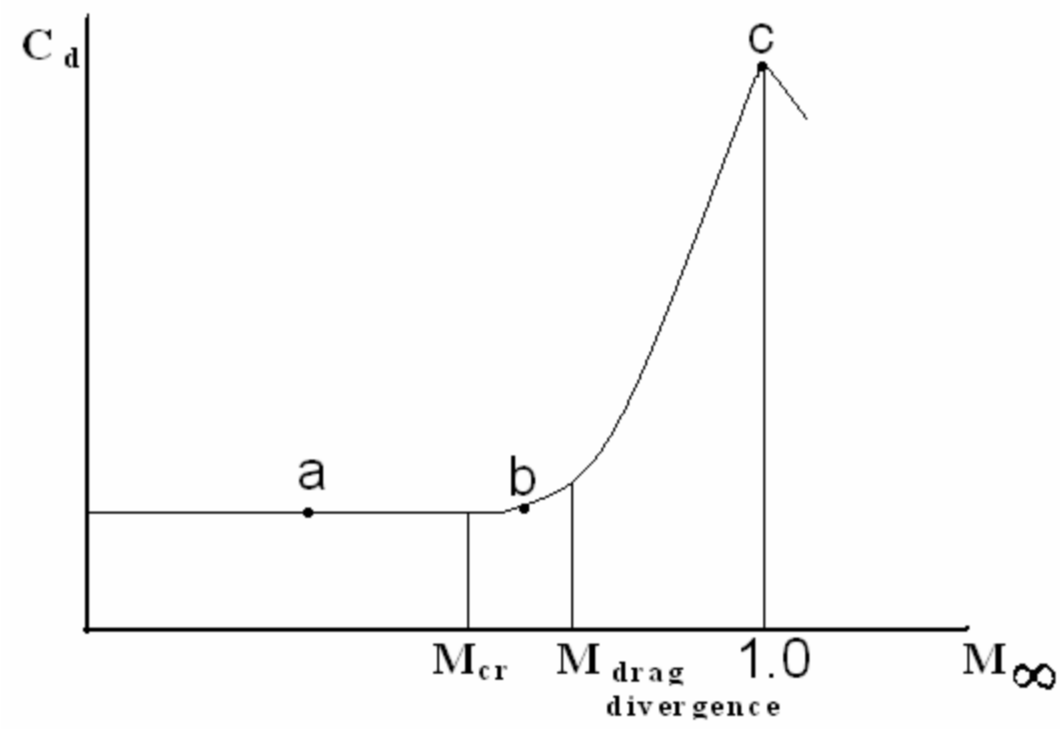

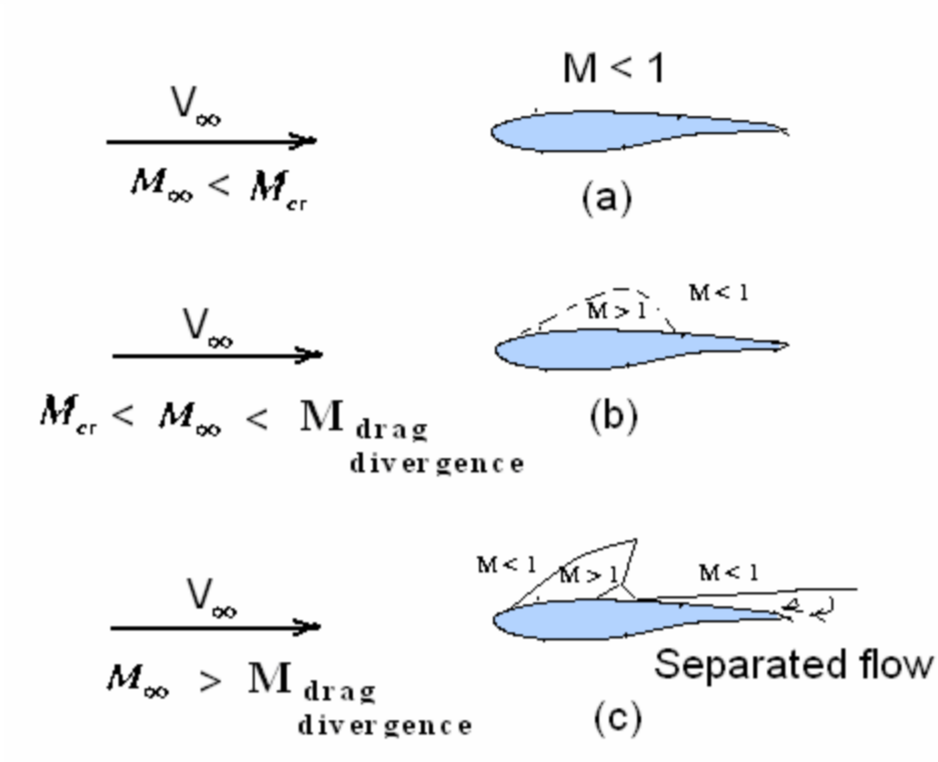

If M_∞ increases slightly above M_{cr}, a bubble of supersonic flow will occur, surrounding the minium pressure point (see above figure (b)). Correspondingly, Cd will still remain reasonably low, as indicated by point b in the above figure. However, if M_∞ is still further increased, a very sudden and dramatic rise in the drag coefficient will be observed as noted by point c in the above figure. The effect of the shock wave on the surface pressure distribution can be seen.

The shock waves themselves are dissipative phenomena, which result in an increase in drag on the airfoil. But in addition, the sharp pressure increase across the shock wave creates a strong adverse gradient, causing the flow to separate from the surface. Such flow separation can create substantial increases in drag. Thus, the sharp increase in Cd shown in the above figure is a combined effect of shock waves and flow separation. The free stream Mach number at which Cd begins to increase rapidly is defined as drag-divergence Mach number.

Note that $M_{cr} < M_{drag\ divergence} < 1.0$

The flow pattern sketched above is characteristic of a flight regime called transonic. When $0.8 \leq M_\infty$

< 1.2, the flow is generally designated as transonic flow, and it is characterized by some complex effects only hinted in the above figure ©.

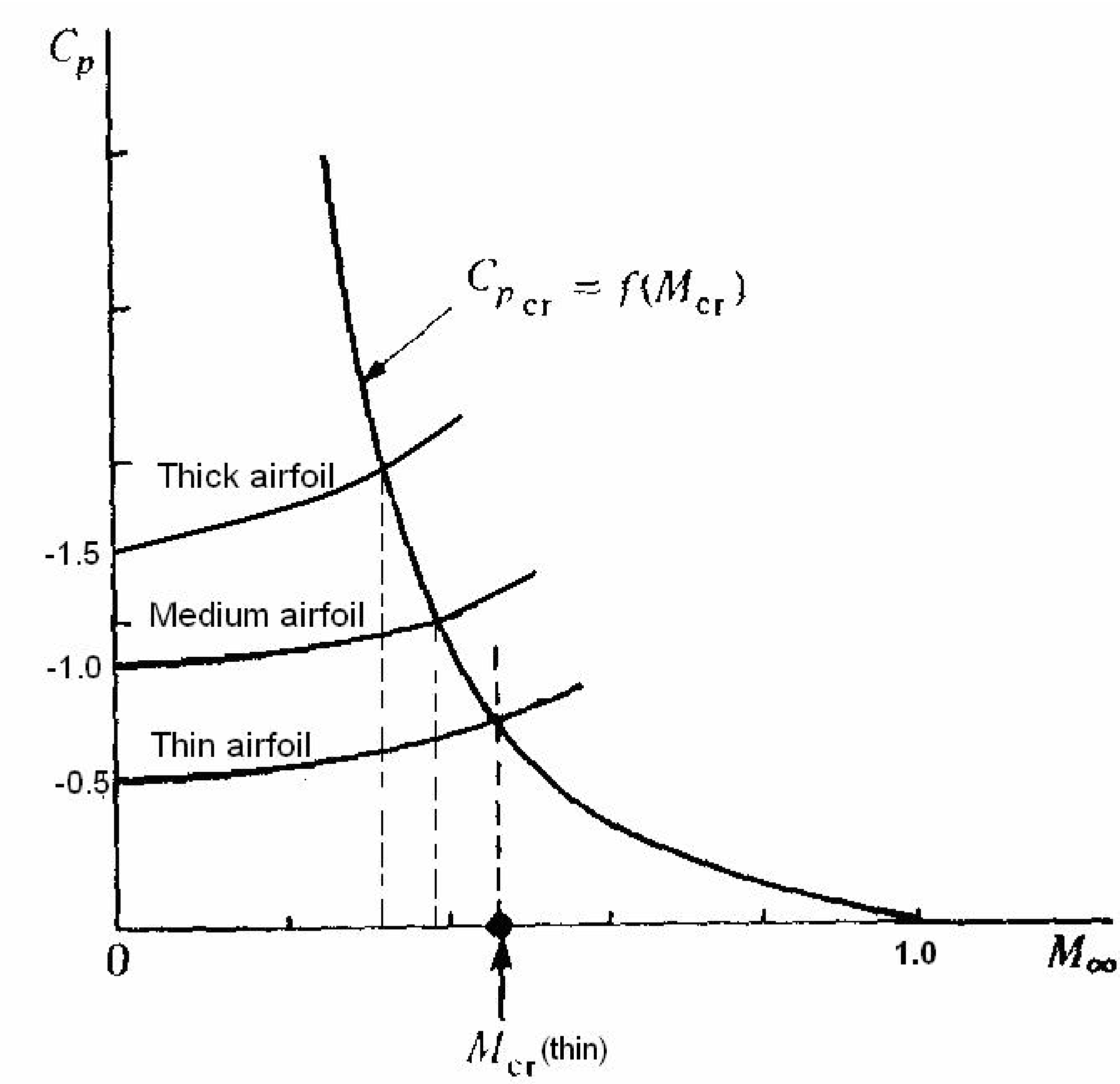

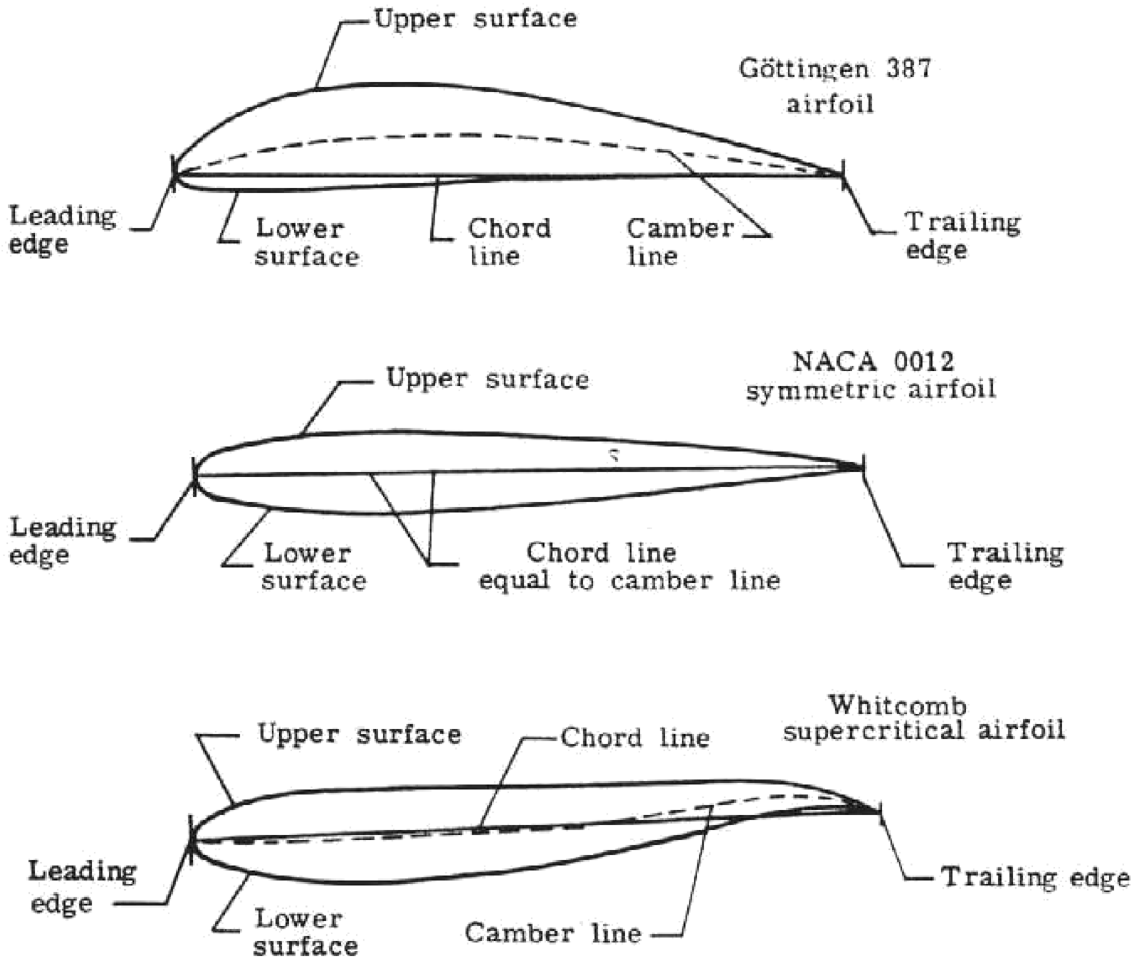
Upper surface
Göttingen 387
airfoil
Leading
edge
Lower
surface
Chord
line
Camber
line
Trailing
edge
Upper surface
NACA 0012
symmetric airfoil
Leading
edge
Lower
surface
Chord line
equal to camber line
Trailing
edge
Whitcomb
supercritical airfoil
Upper surface
Chord line
Leading
edge
Lower
surface
Camber line
Trailing edge

Supercritical airfoil

The supercritical airfoil is a different approach to the increase in drag-divergence Mach number. Here, the shape of the airfoil is designed with a relatively flat top surface as shown in the below figure.

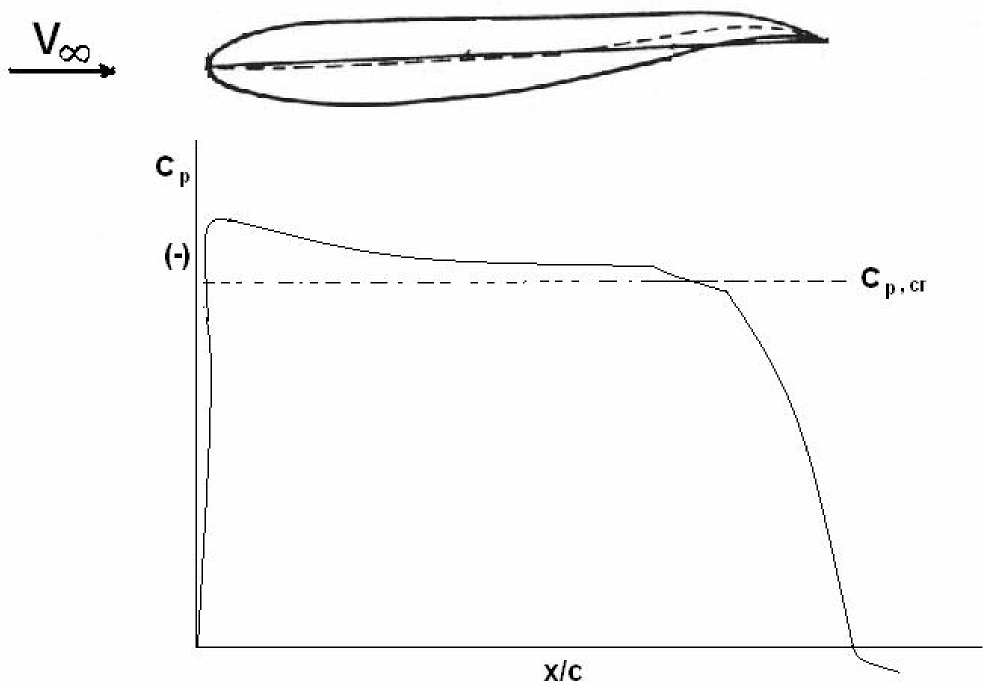

Shape of a typical supercritical airfoil and its pressure coefficient distribution over the top surface

When the free stream Mach number exceeds M_{cr} , a pocket of supersonic flow occurs over the top surface as usual; but because of the top is relatively flat, the local supersonic Mach number is a lower value than would exist in the case of a conventional

airfoil. As a result, the shock wave that terminates the pocket of supersonic flow is weaker. In turn, the super critical airfoil can penetrate closer to Mach 1 before drag divergence occurs. In essence, the increment in Mach number (the "grace period") between M_{cr} and $M_{drag\ divergence}$ is increased by the shape of the supercritical airfoil. One way to think about this is that the supercritical airfoil is "more comfortable" than conventional airfoils in the region above M_{cr}, and it can fly closer to Mach 1 before drag divergence is encountered. Because they are more comfortable in the flight regime above the critical Mach number and because they can penetrate closer to Mach 1 after exceeding M_{cr}

, these airfoils are called supercritical airfoils. They are designed to cruise in the Mach number range above M_{cr}. The pressure coefficient distribution over the top surface of a supercritical airfoil flying above M_{cr} but below $M_{drag\ divergence}$ is sketched in the above figure. After a sharp decrease in pressure around the leading edge, the pressure remains relatively constant over a substantial portion of the top surface. This is in contrast to the pressure coefficient distribution for a conventional airfoil flying above M_{cr} , as shown below (wind

Tunnel data) for NACA 0012 airfoil for M∞ = 0.808, which is above the critical Mach number.

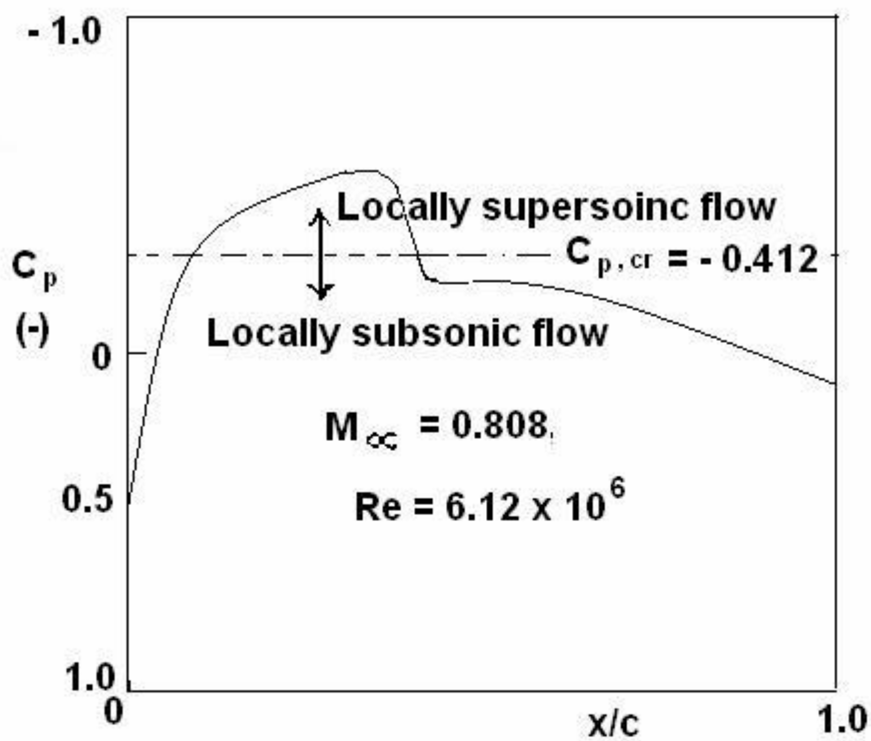

Wind Tunnel measurements of the surface pressure coefficient distribution for the NACA0012 airfoil at zero angle of attack for M_∞ = 0.808, which is above the critical Mach number.

Clearly, the flow over the supercritical airfoil is carefully tailored to achieve the desired result.

The early aerodynamic research on supercritical airfoils was carried out by Whitecomb's an aeronautical engineer at NASA Langly Research Center, during the middle 1960s.

Designers of transonic aircraft can use supercritical airfoils to accomplish one of two objectives:

(1) For a given airfoil thickness, the supercritical airfoil shape allows a higher cruise velocity; or

(2) for a given lower cruise velocity, airfoil thickness can be larger.

The later option has some design advantages. The structural design of a thicker wing is more straightforward and actually results in a more light weight (albeit thicker) wing. Also a thicker wing provides more volume for an increased fuel capacity. Clearly, the use of a supercritical airfoil provides a larger design space for transonic airplanes.

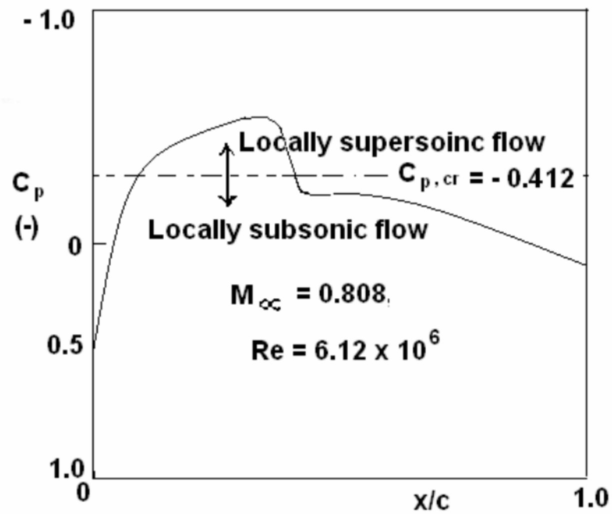

Wind Tunnel measurements of the surface pressure coefficient distribution for the NACA0012 airfoil at zero angle of attack for M_∞ = 0.808, which is above the critical Mach number.

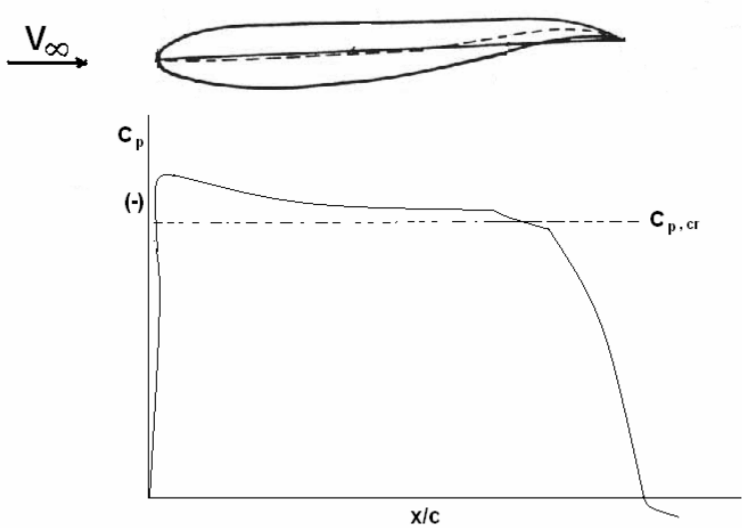

Shape of a typical supercritical airfoil and its pressure coefficient distribution over the top surface

Nature places the maximum velocity at a point that satisfies the physics of the whole flow field not just what is happening in a local region of flow. The point of maximum velocity is dictated by the complete shape of the airfoil, not just by the shape in a local region.

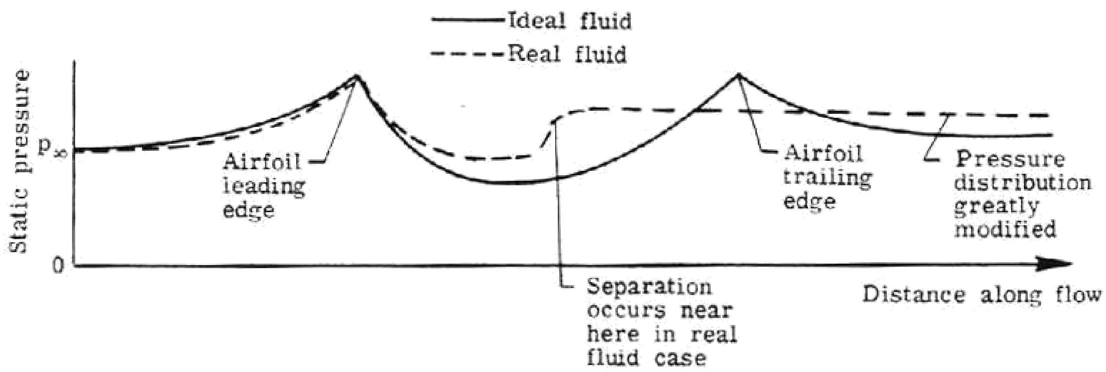

(a) Airfoil upper surface static-pressure distributions.

Wave Drag (At supersonic speeds)

With respect to airfoils (as well as all other aerodynamics bodies), shock waves in supersonic flow create a new source of drag, called wave drag.

Wave drag is an aerodynamics term that refers to a sudden and very powerful form of drag that appears on aircraft and blade tips moving at high-subsonic and supersonic speeds....

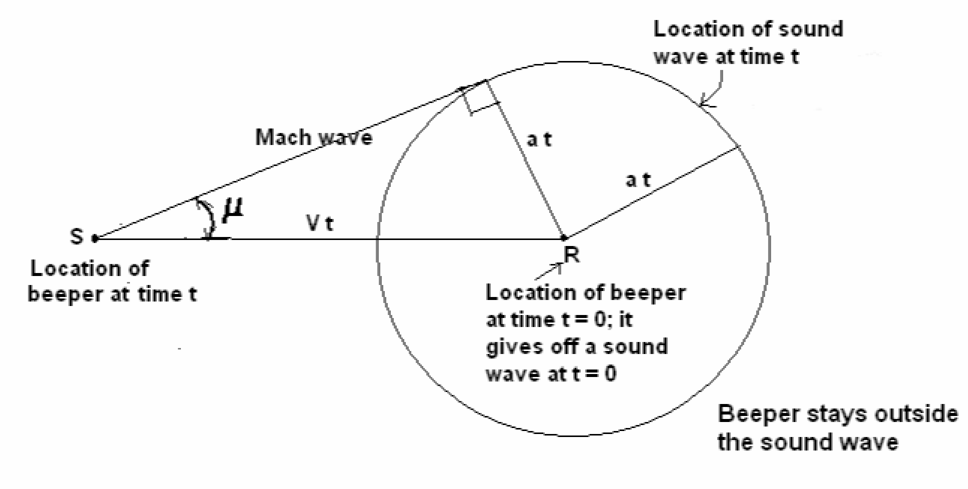

The origin of Mach waves and shock waves.
Beeper is moving faster than the speed of sound

Mach angle

It is defined as μ = arcsin 1/M

Drag divergence Mach number

It is that free-stream Mach number at which the drag coefficient begins to rapidly increase due to occurrence of transonic shock waves. For a given body, the drag divergence Mach number is slightly higher than the critical Mach number.

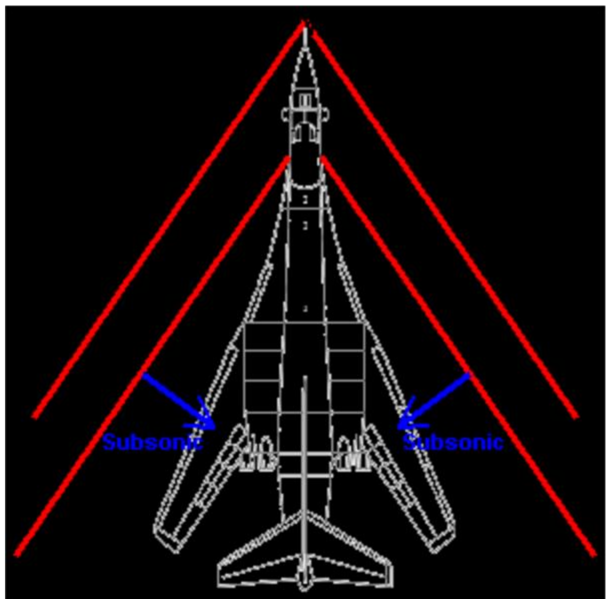

The whole idea of sweeping an aircraft's wing is to delay the drag rise caused by the formation of shock waves. The swept-wing concept had been appreciated by German aerodynamicists since the mid-1930s, and by 1942 a considerable amount of research had gone into it. However, in the United States and Great Britain, the concept of the swept wing remained virtually unknown until the end of the war. Due to the early research in this area, this allowed Germany to successfully introduce the swept wing in the jet fighter **Messerschmitt ME-262** as early as 1941.

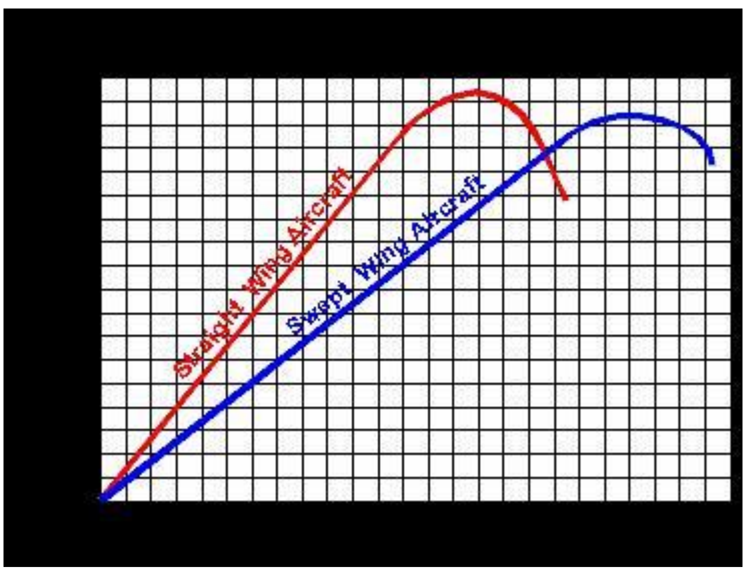

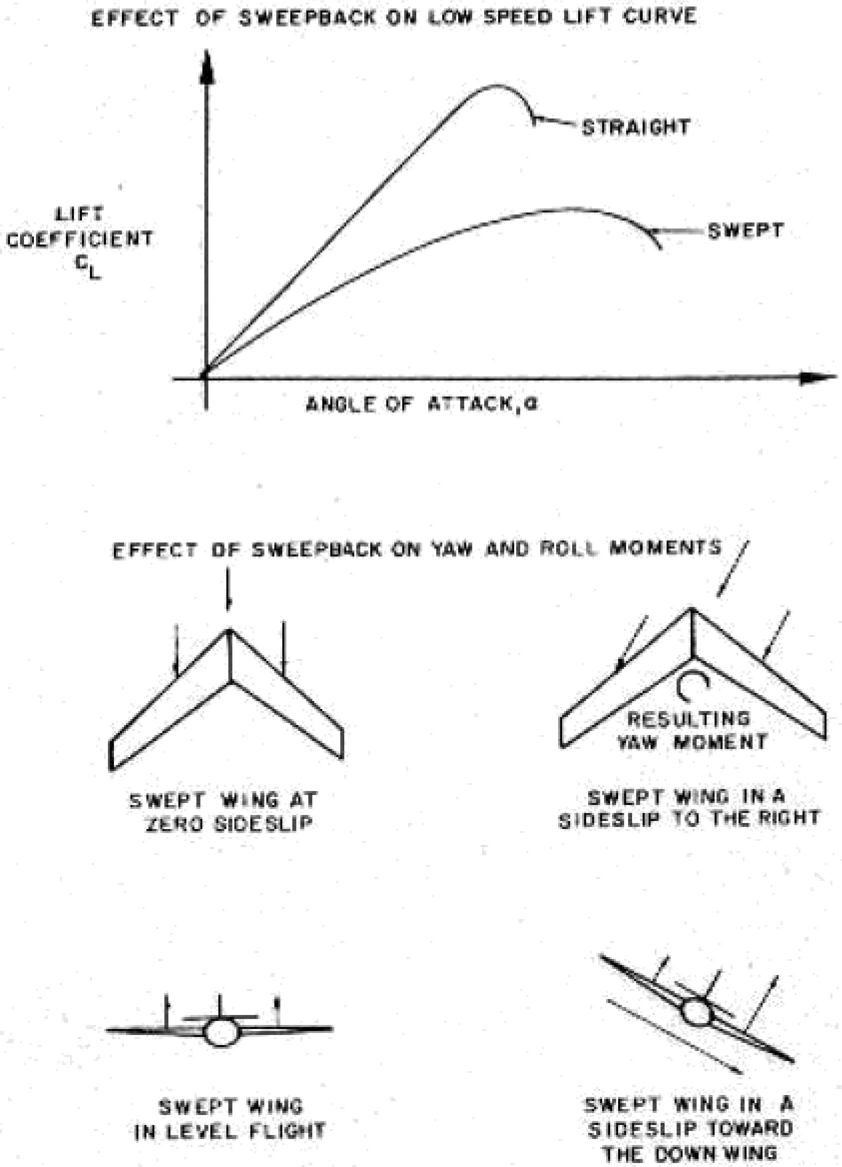

Figure 3.15. Aerodynamic Effects Due to Sweepback

Transonic Area Rule

Within the limitations of small perturbation theory, at a given transonic Mach number, aircraft with the same longitudinal distribution of cross-sectional area, including fuselage, wings and all appendages will, at zero lift, have the same wave drag.

Why: Mach waves under transonic conditions are perpendicular to flow.

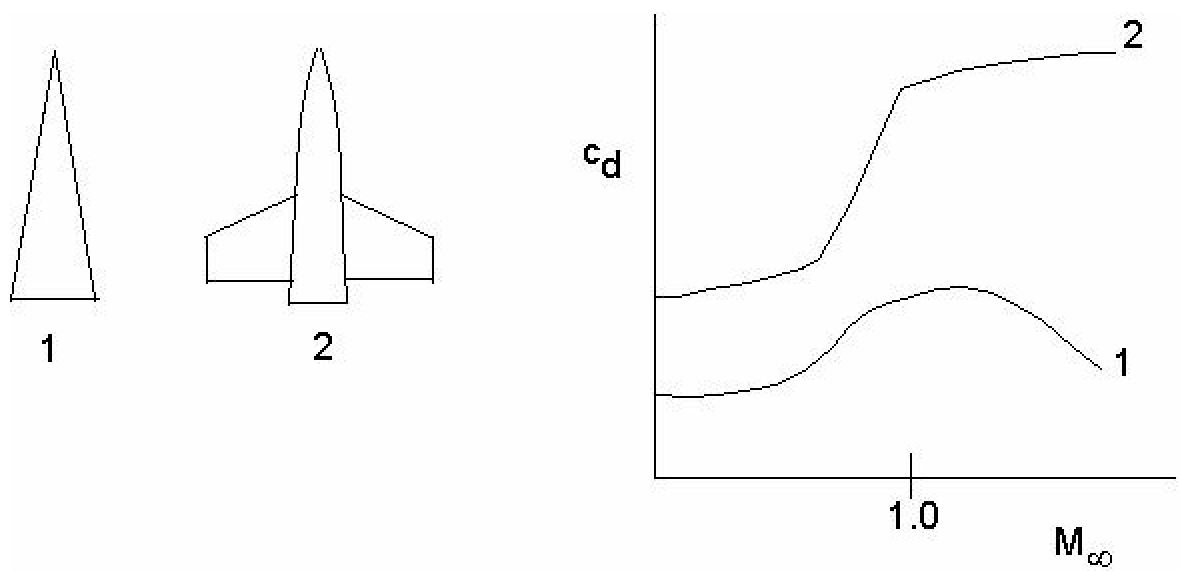

Implication:

Keep area distribution smooth, constant if possible. Else, strong shocks and hence drag result.

Wing-body interaction leading to shock formation:

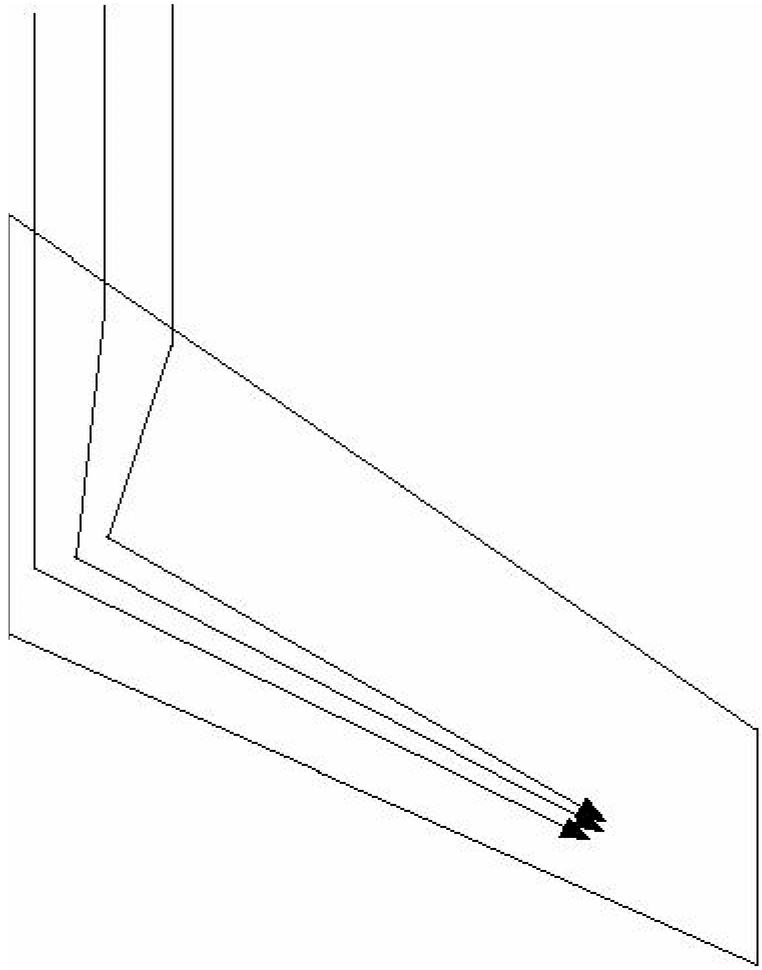

Observed: c_p distributions are such that maximum velocity is reached far aft at root and far forward at tip. Hence, streamlines curves in at the root, compress, shock propagates out.

The **Whitcomb area rule**, also called the **transonic area rule**, is a design technique used to reduce an aircraft's drag at transonic and supersonic speeds, particularly between Mach 0.8 and 1.2. This is the operating speed range of the majority of commercial and military fixed-wing aircraft today.

At high-subsonic flight speeds, supersonic airflow can develop in areas where the flow accelerates around the aircraft body and wings. The speed at which this occurs varies from aircraft to aircraft, and is known as the critical Mach number. The resulting shock waves formed at these points of supersonic flow can bleed away a considerable amount of power, which is experienced by the aircraft as a sudden and very powerful form of drag, called wave drag. To reduce the number and power of these shock waves, an aerodynamic shape should change in cross sectional area as smoothly as possible. This leads to a "perfect" aerodynamic shape known as the **Sears-Haack body**, roughly shaped like a cigar but pointed at both ends.

The area rule says that an airplane designed with the same cross-sectional area as the Sears-Haack body generates the same wave drag as this body, largely independent of the actual shape. As a result, aircraft have to be carefully arranged so that large volumes like wings are positioned at the widest area of the equivalent Sears-Haack body, and that the cockpit, tailplane, intakes and other "bumps" are spread out along the fuselage and or that the rest of the fuselage along these "bumps" is correspondingly thinned.

The area rule also holds true at speeds higher than the speed of sound, but in this case the body arrangement is in respect to the Mach line for the design speed. For instance, at Mach 1.3 the angle of the Mach cone formed off the body of the aircraft will be at about $\mu = \arcsin(1/M) = 50{,}3$ deg (μ is the sweep angle of the Mach cone). In this case the "perfect shape" is biased rearward, which is why aircraft designed for high speed cruise tend to be arranged with the wings at the rear. A classic example of such a design is Concorde.

Anti-shock bodies or **Küchemann carrots** are pods placed at the trailing edge of a transonic aircraft's wings in order to reduce wave drag, thus improving fuel economy, as the aircraft enters the transonic flight regime (Mach 0.8–1.2). Most jet airliners have a cruising speed between Mach 0.8 and 0.85. For aircraft operating in the transonic regime, wave drag can be minimized by having a cross-sectional area which changes smoothly along the length of the aircraft. This is known as the area rule, and is the operating principle behind the design of anti-shock bodies.

On most jet airliners, the mechanisms for deploying the wing flaps are enclosed in fairings, called "flap track fairings", which also serve as anti-shock bodies.

Anti-shock bodies were concurrently developed by Richard Whitcomb at NASA and Dietrich Küchemann, a German aerodynamicist, in the early 1950s. The Handley-Page Victor bomber was particularly well-known for featuring a conspicuous pair of Küchemann carrots, so-called because of their distinctive shape.

Area Rule

The Area Rule was discovered by NASA aerodynamicist Richard Whitcomb in 1950. The rule states that, in order to produce the least amount of drag when approaching supersonic flight, the cross-sectional area of an aircraft body should be consistent throughout the aircraft's length. To compensate for the place on an aircraft where the wings are attached to the fuselage, the fuselage needs to be made narrower so that the cross-section remains the same. This is why aircraft that are designed to fly around the speed of sound have a pinched fuselage where the wings are attached to the body.

Wing Types

Aircraft designers have designed several wing types that have different aerodynamic properties. These have different shapes and attach to the aircraft body at different angles at different points along the fuselage. Not all of these planes have a practical use-some have just been use for research.

The conventional straight wing extends out from the fuselage at approximately right angles. On early biplanes, one wing often was suspended above the fuselage by some sort of bracing supports while the second crossed directly under the fuselage. On monoplanes, designers positioned the wings at different heights depending on the design-some crossed above the fuselage while others were attached at the lower part of the fuselage.

The swept-back wing extends backward from the fuselage at an angle.

The delta wing looks much like a triangle when viewed from above (or the Greek letter "delta" D.) It sweeps sharply back from the fuselage with the angle between the front of the wing (the leading edge) often as high as 60 degrees and the angle between the fuselage and the trailing edge (the back edge of the wing) at around 90 degrees. The tip of a delta wing is often, but not always, cut off.

The forward-swept wing gives an airplane the appearance of flying backward. The wing is angled toward the front of the aircraft and is usually attached to the airplane far back on the fuselage. A small wing called a canard is often attached to the fuselage near the front on this type of aircraft.

A variable-sweep wing can be moved during flight- usually between a swept-back position and a straight position.

The flying wing is an aircraft design where the wing forms virtually the entire airplane and it sweeps back from the center of the aircraft. The fuselage is a very narrow section in the center that joins the wings without any seams.

The term "dihedral" is used to describe wings that are angled upward from the fuselage. Dihedral is the angle at which the wings are slanted upward from the root of the wing (where it is attached to the fuselage) to the wing tip. "Canards" are small wings placed toward the front of the fuselage.

Types of Wings and Transonic Flow

There are a number of ways of delaying the increase in drag encountered when an aircraft travels at high speeds, i.e., the transonic wave drag rise, or of increasing the drag-divergence Mach number (the free-stream Mach number at which drag rises precipitously) so that it is closer to 1. One way is by the use of *thin airfoils*: increase in drag associated with transonic flow is roughly proportional to the square of the thickness-chord ratio (t/c). If a thinner airfoil section is used, the airflow speeds around the airfoil will be less than those for the thicker airfoil. Thus, one may fly at a higher free-stream Mach number before a sonic point appears and before one reaches the drag-divergence Mach number. The disadvantages of using thin wings are that they are less effective (in terms of lift produced) in the subsonic speed range and they can accommodate less structure (wing fuel tanks, structural support members, armament stations, etc.) than a thicker wing.

In 1935, the German aerodynamicist Adolf Busemann proposed that a swept wing might delay and reduce the effects of compressibility. A *swept wing* would delay the formation of the shock waves encountered in transonic flow to a higher Mach number. Additionally, it would reduce the wave drag over all Mach numbers.

A swept wing would have virtually the same effect as a thinner airfoil section (the thickness-cord ratio (t/c) is reduced). The maximum ratio of thickness to chord for a swept wing is less than for a straight wing with the same airflow. One is effectively using a thinner airfoil section as the flow has more time in which to adjust to the high-speed situation. The critical Mach number (at which a sonic point appears) and the drag-divergence Mach number are delayed to higher values; Sweep forward or sweepback will accomplish these desired results. Forward sweep has disadvantages, however, in the stability and handling characteristics at low speeds.

A major disadvantage of swept wings is that there is a spanwise flow along the wing, and the boundary layer will thicken toward the wingtips for sweepback and toward the roots (the part of the wing closest to the fuselage) for sweep-forward. In the case of sweepback, there is an early separation and stall of the wingtip sections and the ailerons lose their roll control effectiveness. The spanwise flow may be reduced by the use of stall fences, which are thin plates parallel to the axis of symmetry of the airplane. In this manner a strong boundary layer buildup over the ailerons is prevented. Wing twist is another possible solution to this spanwise flow condition.

The wing's *aspect ratio* is another parameter that influences the critical Mach number and the transonic drag rise. Substantial increases in the critical Mach number (the subsonic Mach number at which sonic flow occurs at some point on the wing for the first time) occur when using an aspect ratio less than about four. However, low-aspect-ratio wings are at a disadvantage at subsonic speeds because of the higher induced drag.

By bleeding off some of the boundary layer along an airfoil's surface, the drag-divergence Mach number can be increased. This increase results from the reduction or elimination of shock interactions between the subsonic boundary layer and the supersonic flow outside of it.

Vortex generators are small plates, mounted along the surface of a wing and protruding perpendicularly to the surface. They are basically small wings, and by creating a strong tip vortex, the vortex generators feed high-energy air from outside the boundary layer into the slow moving air inside the boundary layer. This condition reduces the adverse pressure gradients and prevents the boundary layer from stalling. A small increase in the drag-divergence Mach number can be achieved. This method is economically beneficial to airplanes designed for cruise at the highest possible drag-divergence Mach number.

A more recent development in transonic technology, and destined to be an important influence on future wing design, is the *supercritical wing* developed by Dr. Richard T. Whitcomb of NASA's Langley Research Center. With the supercritical wing, a substantial rise in the drag-divergence Mach number is realized and the critical Mach number is delayed even up to 0.99. This delay represents a major increase in commercial airplane performance.

The curvature of a wing gives the wing its lift. Because of the flattened upper surface of the supercritical airfoil, lift is reduced. However, to counteract this, the new supercritical wing has increased camber at the trailing edge.

There are two main advantages of the supercritical airfoil. First, by using the same thickness-chord ratio, the supercritical airfoil permits high subsonic cruise near Mach 1 before the transonic drag rise. Alternatively, at lower drag divergence Mach numbers, the supercritical airfoil permits a thicker wing section to be used without a drag penalty. This airfoil reduces structural weight and permits higher lift at lower speeds.

Coupled to supercritical technology is the "area-rule" concept also developed by Dr. Richard T. Whitcomb in the early 1950s for transonic airplanes and later applied to supersonic flight in general.

Basically, the area rule states that minimum transonic and supersonic drag is obtained when the cross-sectional area distribution of the airplane along the longitudinal axis can be projected into a body of revolution that is smooth and shows no abrupt changes in cross section along its length. Or, if a graph is made of the cross-sectional area against body position, the resulting curve is smooth. If it is not a smooth curve, then the cross section is changed accordingly.

The original Convair F-102A was simply a scaled-up version of the XF-92A with a pure delta wing. But early tests indicated that supersonic flight was beyond its capability because of excessive transonic drag and the project was about to be canceled. Area ruling, however, saved the airplane from this fate. In the original YF-102A, the curve of the cross-sectional area plotted against body station was not very smooth as there was a large increase in cross-sectional area when the wings were attached. The redesigned F-102A had a "coke-bottle"-waist-shaped fuselage and bulges added aft of the wing on each side of the tail to give a better area-rule distribution. The F-102A could then reach supersonic speeds because of the greatly reduced drag and entered military service in great numbers.

Later, the area-rule concept was applied to design of a near-sonic transport capable of cruising at Mach numbers around 0.99. In addition to area ruling, a supercritical wing was used.

Transonic is an aeronautics term referring to a range of velocities just below and above the speed of sound. It is defined as the range of speeds between the critical mach, when some parts of the airflow over an aircraft become supersonic, and a higher speed, typically near Mach number, when all of the airflow is supersonic....

speed range. Supercritical airfoils are characterized by their flattened upper surface, highly cambered (curved) aft section, and greater leading edge

The **leading edge** is a line connecting the forward-most points of a wing's profile. In other words, it's the front edge of the wing. When an aircraft is moving forward, the leading edge is that part of the wing that first contacts the air....

Geometric and aerodynamic twist

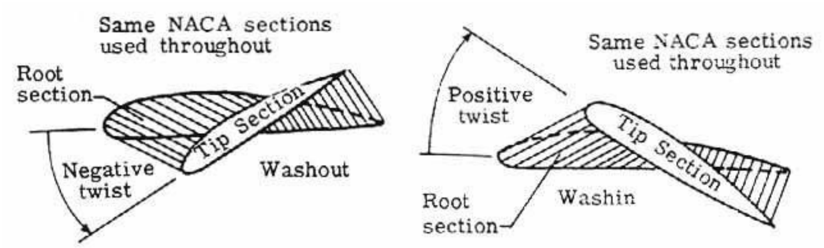

(a) Geometric twist.

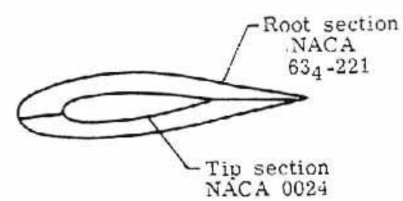

(b) Aerodynamic twist.

Wings are given twist so that the angle of attack varies along the span. A decrease in angle of attack toward the wing tip is called washout whereas an increase in angle of attack toward the wing tip is called washin. Geometric twist (fig. (a)) represents a geometric method of changing the lift distribution, whereas aerodynamic twist, by using different airfoil sections along the span represents an aerodynamic method of changing the lift distribution in a spanwise manner (fig. (b)). To give minimum induced drag it was demonstrated that the spanwise efficiency factor e should be as close to 1 as possible. This is the case of an elliptic spanwise lift distribution. A number of methods are available to modify the spanwise distribution of lift.

Vortex flow effects

Note that upwash and downwash are due to both the bound vortex and the tip vortices

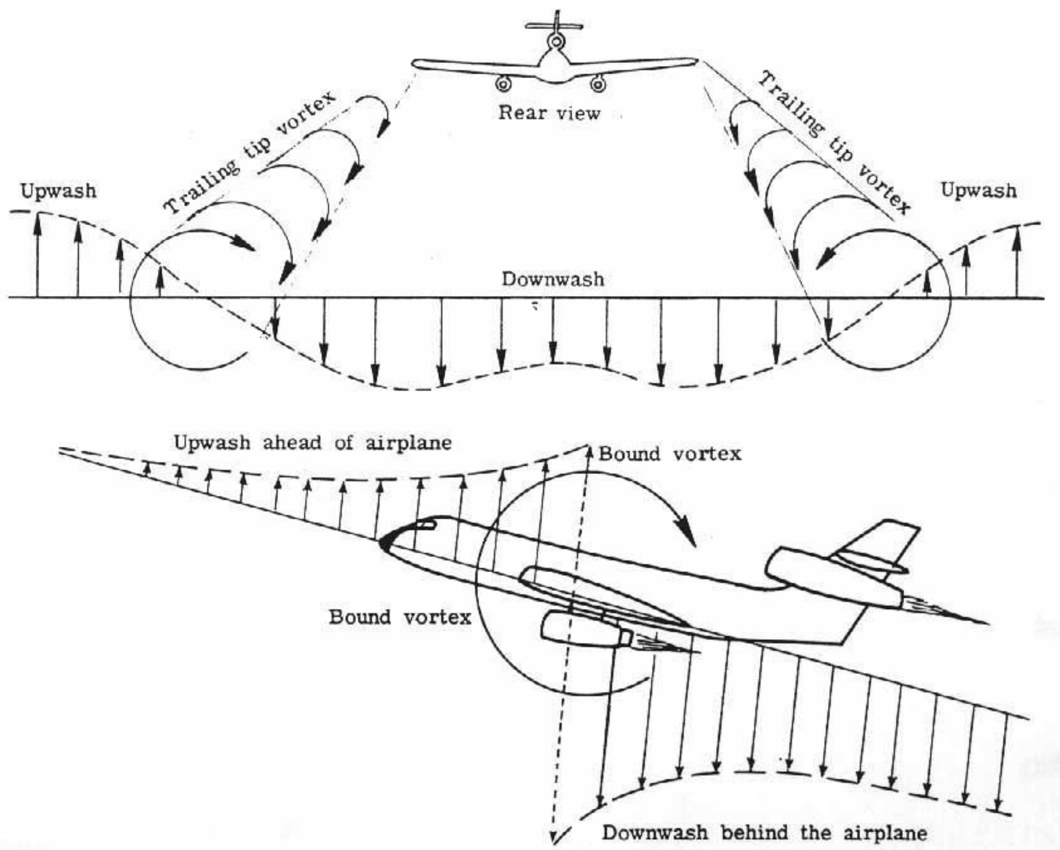

The important effects of the vortex system are shown in figure. Indicated are the directions of air movement due to the vortex system. The left-tip vortex rotates clockwise, the right-tip vortex rotates counterclockwise (when viewed from behind), and the bound vortex rotates clockwise (when viewed from the left side). The bound vortex is directly related to the lift on the wing as in the dimensional case.

Upwash and downwash fields around an airplane

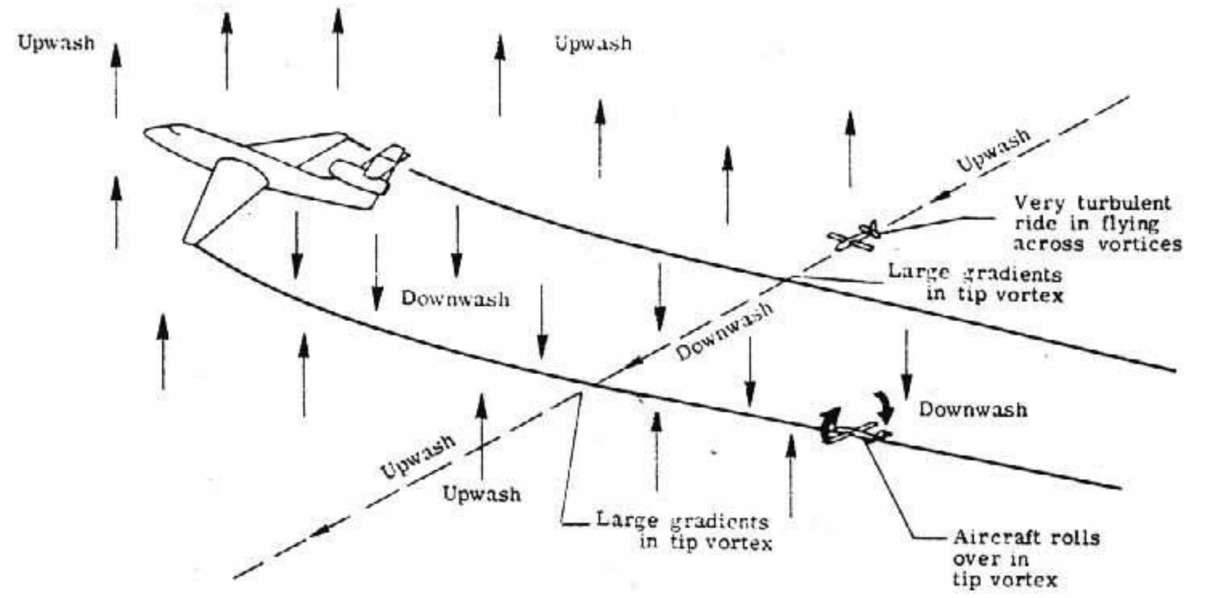

In both the 2D and 3D cases the upflow (or upwash) in front of the wing balanced the downflow (or downwash) in back of the wing caused by the bound vortex. But, in the finite-wing case one must also take into account the Lip vortices (assuming that the influence of the starting vortex is negligible). The tip vortices cause additional down... wash behind the wing within the wing span. One can see that, for an observer fixed in the air (fig. 55) all the air within the vortex system is moving downwards (this is called downwash) whereas all the air outside the vortex system is moving upwards (this is called upwash). Note that an aircraft flying perpendicular to the flight path of the airplane creating the vortex pattern will encounter upwash, downwash, and upwash in that order. The gradient, or change of downwash to upwash, can become very large at the tip vortices and cause extreme motions in the airplane flying through it. Also shown is an airplane flying into a tip vortex. Note that there is a large tendency for the airplane to roll over. If the control surfaces of the airplane are not effective enough to counteract the airplane roll tendency, the pilot may lose control or in a violent case experience structural failure.

The problems of severe tip vortices are compounded by the take-off and landings of the new generation of jumbo jets. During these times the speed of the airplane is low and the airplane is operating at high lift coefficients to maintain night. The Federal Aviation Agency has shown that for a 0.27 MN (600 000 lb) plane, the tip...

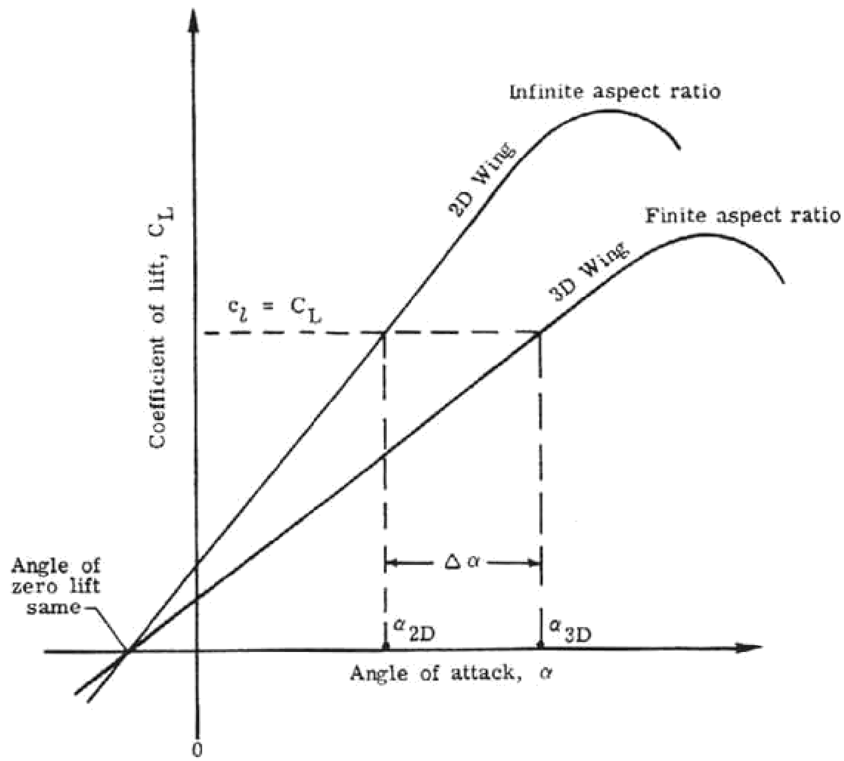

Effect of aspect ratio on coefficient of lift

Figure shows the coefficient of lift curves ('lift curves") obtained for both wings by experiment. Readily evident is the effect that the tip vortices have in creating the additional downwash w at the wing; the lift curve is flattened out so that at the same angle of attack less lift is obtained for the smaller aspect ratio wing. This is not a beneficial effect.